A PARAMETRIC STUDY ON THE INFLUENCE OF BOUNDARY FRAME FLEXIBILITY IN STEEL PLATE SHEAR WALLS

A Thesis

by

Shaghayegh Sadeghzadeh Benam

Submitted to the

Graduate School of Sciences and Engineering
In Partial Fulfillment of the Requirements for
the Degree of

Master of Science

in the
Department of Civil Engineering

Özyeğin University
January 2020

i

A PARAMETRIC STUDY ON THE INFLUENCE OF BOUNDARY FRAME FLEXIBILITY IN STEEL PLATE SHEAR WALLS

Approved by:

_____
Assistant Professor Ahmet Yiğit
Özçelik, Advisor,
Department of Civil Engineering
Özyeğin University

_____
Professor Gülay Altay
Department of Civil Engineering
Özyeğin University

_____
Assistant Professor Ziya Müderrisoğlu
Department of Civil Engineering
Beykent University

Date Approved:

To My Family,

ABSTRACT

Steel plate shear walls (SPSWs) are known to be a reliable lateral force-resisting system, particularly attractive for high-seismic regions, due to their high lateral strength and stiffness and stable hysteretic behavior. SPSWs comprise thin infill plates that are connected to the beams and columns of the surrounding boundary frame on all four edges. Being the primary element resisting the lateral load, thin infill plates buckle almost immediately when the SPSW is loaded laterally. Despite shear buckling of thin infill plates, thin infill plates exhibit substantial post-buckling strength and stiffness due to a mechanism called tension field action. To take advantage of tension field, the surrounding boundary frame is required to anchor thin infill plates by resisting the diagonal tension forces exerted by thin infill plates due to the formation of tension field and by limiting the inward deflection of thin infill plates to enable them to yield in tension. Pursuant to this goal, it is necessary to capacity-design the boundary frame to ensure thin infill plates yield prior to hinging in the boundary frame. In addition to the capacity design requirement, a stiffness limit for the boundary frame, based on elastic behavior, is provided by design codes to minimize pull-in of boundary frame. Furthermore, for preventing excessive plastic deformation in the horizontal boundary elements (HBEs) a limit for plastic section modulus of HBEs is provided. In this study, a parametric study is undertaken to quantify the effect of boundary frame flexibility (or stiffness) on the development of diagonal tension and the variation of tension stresses in thin infill plates of SPSWs. The web plate thicknesses are chosen, and relevant boundary frame elements are designed according to the forces applied by web plate without considering seismic actions. 27 one story one bay SPSWs with 3 different aspect ratios (ratio between width and length) and 9 different plate thickness using lightest sections for beams and columns

are designed following the capacity design principles. Later for each design, 2 additional bigger column sections are assigned while beam sections remained constant. In total, 81 designs are provided. In addition to the capacity design requirements, these designs also fulfill the stiffness requirement given for boundary frame in design codes. Nonlinear pushover analyses are performed using a simplified model known as strip model (validated against experimental data available in literature) representing the cyclic behavior of thin infill plates. It is observed that column stiffness does not affect the distribution of the stresses in the web plates. Additionally, in pushover analysis it is observed that the capacity design method underestimates the shear forces. Results showed that the accumulation of plastic deformation at the mid- span of the HBE is critical for designs with aspect ratios of 1 and web plates with thickness less than 1.3 mm. Finally, the closed-form expression for uniformity of the stresses in the web plates is also obtained as a function of flexibility of beams and columns, aspect ratios and drifts.

ÖZETÇE

Çelik perde duvarlı çerçeveler yanal yükler etkisi altında güvenilir sistemler olarak tanınmış, bilhassa da deprem bölgelerinde yüksek yanal yük gerilimi, rijitlik ve kararlı histerik davranış özelliklerinden ötürü birçok yerde kullanılmıştır. Çelik perde duvarlı çerçeveler ince bir levhanın dört bir yanını saran kolon ve kirişlerden oluşmaktadır. Bu ince levha, yanal yüklerin etkisi altında dayanım gösteren ilk elemanlardan biri olup; yanal yükler etkisi altında burkulur. Kesme kuvvetinin oluşturduğu burkulmaya rağmen, ince levha önemli ölçüde burkulma sonrası dayanım ve rijitlik göstermektedir. Bunun temel nedeni ise çekme alanı mekanizması oluşumudur. Çekme alanının oluşabilmesi için çelik levha etrafını saran çerçevenin ince çelik levhaya sabitlenmesi, çekme alanı oluşumdan dolayı meydana gelen eksenel çekme kuvvetlerine dayanması gerekir ve ince levhanın içeriye doğru eğrilmesini engelleyerek levhanın çekme kuvvetinden dolayı akmasını sağlamalıdır. Bütün bunları sağlayabilmek için levhayı saran çerçevenin mafsallaşma oluşmadan ince levhanın akmasını sağlayacak şekilde tasarlanması gerekmektedir. Bununla birlikte, çerçevenin tasarımında belirtilen rijitlik sınırları kolon ve kirişler için belirlenip, çerçevenin yükler etkisi altında içe çekilmesi engellenmelidir. Bu çalışmada, parametrik bir yaklaşım ele alınmış olup levha çerçevesinin rijitliğinin ince levhada eksenel çekme alanı üzerindeki etkisi incelenmiştir. 27 tane tek katlı ve tek açıklıklı çelik perde duvarlar 3 farklı en boy oranı ve 9 farklı levha kalınlığı, olabilecek en küçük kiriş ve kolon kesit ölçüleri kullanılarak tasarlanmıştır. Bu tasarımlara ek olarak, aynı en boy oranları ve levha kalınlıkları ile 2 ek kolon kesiti kiriş kesitleri sabit kalacak şekilde tasarıma eklenmiştir. Sonuç olarak 81 tane tasarım sunulmuştur. Bu tasarımlar, tasarım yönetmenliğinde belirtilmiş olan levha çerçevesi rijitlikleri göz önünde bulundurularak oluşturulmuştur. Doğrusal olmayan itme analizleri,

çubuk model tekniği ile yapılmış olup ince levhanın yapısal davranışları incelenmiştir. Yapılan analizler sonucunda kolon rijitliklerinin levha üzerindeki yük dağılımda etkili olmadığı gözlenmiştir. İtme analizleri, uygulanan tasarım metodunda bulunan kesme kuvvetlerinin normalden daha az bir değere sahip olduğunu gözler önüne sermiştir. Sonuçlar, kirişlerin orta kısmında oluşan plastik sekil değiştirmelerinin en boy oranının 1'e ve levha kalınlığının 1.3 mm'den az olduğu tasarımlarda gözlendiğini vurgulamıştır. Sonuç olarak, levhalar üzerindeki gerilme dağılımı kiriş ve kolonların esnekliği, en boy oranı ve ötelemeye bağlı olarak ifade edildi.

ACKNOWLEDGMENT

importantly, for his unending support and for pushing me farther than I thought I could go.

TABLE OF CONTENTS

LIST OF TABLES

LIST OF FIGURES

ABBREVIATIONS

A_b : Sectional Area of the Horizontal Boundary Element

A_c : Sectional Area of the Vertical Boundary Element

A_s : Cross-Sectional Area of the Strips

B_1 : Moment magnification factor

C_m : Equivalent uniform moment Factor

C_{pr} : Strain Hardening Factor

E : Modulus of Elasticity

F_u : Ultimate Tensile Strength

F_y : Yield Strength of Beams and Columns

$F_{y\ HBE}$: Yield Stress of the Horizontal Boundary Element

F_{yp} : Yield Strength for Web Plate

h : Distance Between Vertical Boundary Element Centerlines

HBE   : Horizontal Boundary Element

H_p : Clear Height of the Web Plate

I_b : Moment of Inertia of a Horizontal Boundary Element Taken Perpendicular to the Direction of the Web-Plane Line

I_c : Moment of Inertia of a Vertical Boundary Element Taken Perpendicular to the Direction of the Web-Plane Line

I_{HBE} : Moment of inertia of Horizontal Boundary elements

I_{VBE} : Moment of inertia of Vertical Boundary elements

K : Effective Length

L : Distance Between Vertical Boundary Element Centerlines

L_p : Clear Length of the Web Plate

LRFD	: Load Resistance Factor Design
LRFS	: Lateral Force Resisting Systems
M_{pr}	: Reduced Flexural Strength of Beam
$M_{r(HBE)}$	: Required Second Order Flexural Strength in the Horizontal Boundary Elements
$M_{r(VBE)}$	: Required Second Order Flexural Strength in the Vertical Boundary Elements
n_s	: Number of the Strips
P_{e1}	: Elastic Critical Buckling Strength
P_{e1}	: Elastic critical buckling strength of the member in the plane of bending
P_u	: Required Strength
P_y	: Available Axial Yield Strength
R_y	: Ratio of expected Yield Stress to the Specified Minimum Yield Stress for the Boundary Element
R_yF_y	: Expected Yield Strength of the W-Shaped Section of the Boundary Element
$R_yF_{y\ HBE}$	: Expected Yield Stress of the Web Plate Material
R_{yp}	: Ratio of expected Yield Stress to the Specified Minimum Yield Stress for the Web Plate
$R_{yp}F_{yp}$	: Expected Yield Strength of the Web Plate
S_h	: Distance from Center of the Plastic Hinge to the Center of the Vertical Boundary Element
SPSW	: Steel Plate Shear Wall
t_w	: Thickness of Web Plate

$t_{w\,HBE}$	: Thickness of the Horizontal Boundary Element Web
VBE	: Vertical Boundary Element
$Z_{AISC341}$	: Calculated Plastic Section Modulus for Horizontal Boundary Element Suggested by AISC 341-16
$Z_{database}$	: Plastic Section Modulus Obtained from AISC Shape Database
σt_w	: Distributed Load by the Web Plate to the HBE
ϕ_c	: Resistance Factor for Compression Based on Load Resistance Factor Design Method

CHAPTER I

INTRODUCTION

1.1. Background

Structures in contemporary construction world must be resist lateral loads such as earthquake and wind load in addition to vertical loads such as gravity loads. There are various types of LRFS that can be used in high seismic regions such as steel moment frame, concrete shear walls, braced frames, and steel plate shear walls.

Steel plate shear walls (SPSW) are one of the lateral load resisting systems and an innovative way to provide lateral stiffness and strength to structures. Since 1970's SPSWs have been used in great number of buildings either in mid-rise or high-rise in Japan, Canada and United States. In Japan, these walls were used in new buildings while in U.S. they were used for upgrading the seismic behavior of structures and also, for retrofitting existing buildings (Mörel, 2004).

 SPSWs provide supreme ductility, stable hysteretic behavior, high resistance to strength degradation under cyclic loading, great initial stiffness, high post-buckling strength and capable of dissipating significant amount of energy. Compared to concrete shear walls, SPSWs provide more flexibility in the plan area usage of the buildings, supply more light weight structure, reduce both gravity and seismic loads transition to the foundation which leads to a considerable decrement in foundation and construction cost (Sabelli and Bruneau, 2007).

SPSWs consist of thin infill steel plates referred to as web plates connected to the surrounding boundary frame, namely, beams and columns, that are known as the horizontal boundary elements (HBE) and vertical boundary elements (VBE), respectively. The beam-to-column connections of the boundary frame can be either simple or rigid connections; however, moment-resisting connections are typically adopted to take advantage of the moment-frame action. A conventional SPSW configuration is demonstrated in Figure 1.1.

Figure 1.1. A conventional SPSW configuration adopted from Alavi and Nateghi (2013)

SPSWs can be used in various configuration such as, stiffened steel plate and un-stiffened thin steel plate based on the design philosophy. Application of the stiffened SPSW with horizontal and vertical elements and un-stiffened SPSW are demonstrated in Figure 1.2 and 1.3 respectively. Generally, SPSWs with stiffened plate are not used since

Astaneasl (2001) indicated that these systems are not only economical but also, not recommended.

Figure 1.2. Stiffened SPSW with horizontal elements adopted from Ismaeil and
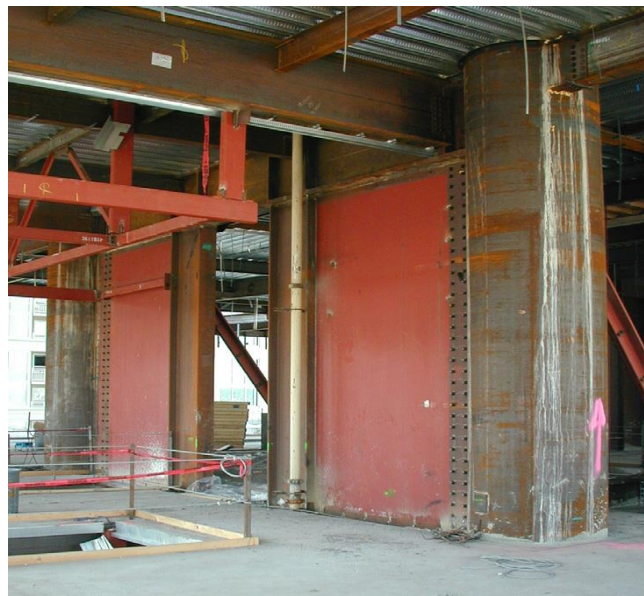
Hassaballa (2013)

Figure 1.3. Un-stiffened SPSW adopted from Ismaeil and Hassaballa (2013)

On the other hand, un-stiffened thin web plates that is connected to the surrounding boundary frame have a post-buckling strength several times greater that the elastic buckling strength of the web plate (Elgaaly et al., 1993). Lateral load resisting system of the web plate is dominated by tension filed mechanism. Detailed information related to the tension field mechanism development in SPSWs with thin web plate will be explained in section 1.1.1.

1.1.1. Tension field Action and Inclination Angle

In aerospace engineering it is recognized by Wagner (1931) that the post-buckling strength of the unstiffened shear plate can be considerable. Unlike column buckling, buckling of unstiffened plate is not equivalent to the failure. In the following years, researchers realized that in the steel building construction, post-buckling strength and ductility of the slender web plate could be substantial and later on, this behavior is allowed in AISC 341-05, Seismic Provision for Structural Steel Buildings, AISC (2005).

When the web plate is thin, shear buckling occur at low levels of lateral loading (Driver, 1997) and web plate experience early shear buckling. At post-buckling stage lateral load resisting mechanism of the SPSW changes from in plane shear to an inclined tension field mechanism. Inclined tension field generates fold lines in the un-stiffened thin plate as it is illustrated in Figure 1.4. At this point, lateral loads transferred through the plate by the principle tension stresses. Tensile stresses in web plate are so large in comparison with compressive stresses that the compressive stresses can be neglected entirely.

Formation of the tension field action mechanism is the primary concept of the steel plate shear wall which is desired to be achieved. The concept of the consideration of the post-buckling strength is adopted from AISC manual for design of plate girders

based largely on the work of Basler (1961). Idealized tension field action in one-story one-bay SPSW is illustrated in figure 1.5.

Figure 1.4. Tension field mechanism (Webster, 2013)
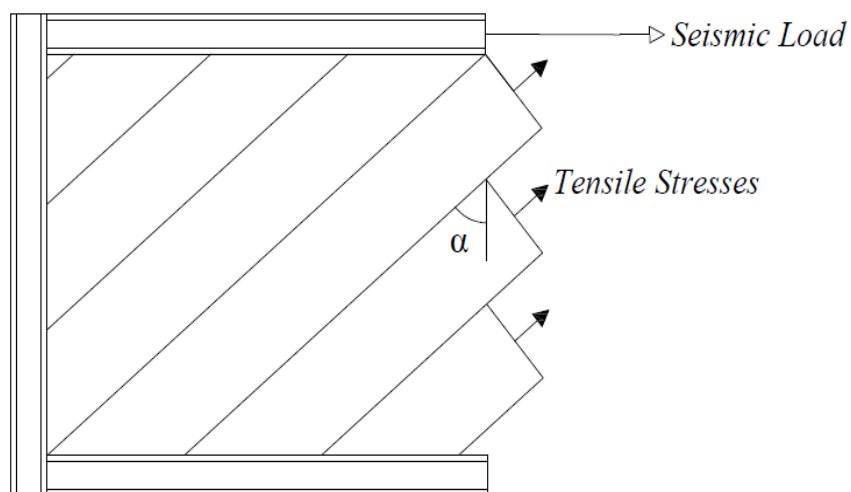
Figure 1.5. Idealized tension field action in one-bay one-story SPSW

The inclination angle of tension field forces (α), which is shown in figure 1.4 is the angle between the column and the line of action of the inclined tensile forces. Based on the elastic strain energy formulation, Timler (1998) derived Equation 1.1 for the

inclination angle of tension field. In this equation it is considered that the slender web plate has no compression strength and the tension field forces is assumed to be distributed with the same stress among the entire web plate with a constant angle which can be calculated with Equation 1.2.

$$\tan^4 \alpha = \frac{1 + \dfrac{t_w L}{2A_c}}{1 + t_w h \left[\dfrac{1}{A_b} + \dfrac{h^3}{360 I_c L} \right]}$$

Eq (1.1)

$$V_n = 0.5 F_{yp} t_w L_p \sin(2\alpha)$$

Eq (1.2)

1.1.2. Stiffness and Strength Requirement for Boundary Frame Elements

Generally, web plates work almost entirely in tension while the tension acts along the length of the boundary elements. Reliant on the stiffness of HBE and VBE, web plate of the SPSWs entirely yield in tension at the design story drift. As such, large inward forces exerted on the boundary elements. VBEs and HBEs of SPSWs should provide sufficient stiffness to allow the web plate to develop full tension strength. Additionally, for preventing excessive accumulation of plastic deformation in the mid-span of HBEs, proper plastic section modulus for the HBE should be provided.

Based on the AISC 341-16, Seismic Provisions for Structural Steel Buildings, (AISC, 2016a), stiffness limits for VBE and HBE to ensure the web plate full yielding in tension are presented in Equations 1.3 and 1.4.

$$I_b \leq \frac{0.0031 L^4 tw}{h}$$

Eq (1.3)

$$I_c \leq \frac{0.0031 h^4 tw}{L}$$

Eq (1.4)

1.2. *Aim and Objectives*

In this thesis, a parametric study has undertaken on one-story SPSWs with different plate thicknesses and different aspect ratios with moment resistant beam-to-column connections. The objectives of this study are;

1. To determine the effect of boundary frame stiffness on the variation of the tensile stresses in web plates

2. To determine the effects of the given flexural stiffness requirements in equations 1.3 and 1.4 for beams and columns on the distribution of the stresses in the web plate and formation of plastic hinges in horizontal and vertical boundary elements

3. To evaluate the proper plastic section modulus values for the horizontal boundary elements to reduce the accumulation of plastic deformation at mid-span

4. To determine the correlation between the flexibility of the beams and columns and uniformity of tension field stresses in the web plate

1.3. *Organization of Thesis*

This thesis includes six chapters, "Chapter I" provides general information about SPSW and "Chapter II" covers a literature review on the topic. "Chapter III" includes the validation of the numerical model used in this study against experimental data. In "Chapter lV" capacity design procedure of the vertical and horizontal boundary elements is explained. "Chapter V" includes the parametric study undertaken to quantify the effect of boundary frame flexibility on the variation of the tension stresses in the web plate of SPSWs. Ultimately, "Chapter Vl" covers the summary and conclusions of the study.

CHAPTER II

LITERATURE REVIEW

2.1. Studies on Inclination Angle of Tension Field

2.1.1. Study of Thorburn, Kulak and Montogomery (1983)

In the early to mid-1980s Thorburn et al. (1983) was conducted a study to review the existing steel plate shear walls system which were designed as stiffened plates to observe the development of less shear stresses in the panel than the critical shear buckling. However, the theoretical approach revealed intrinsic post-buckling strength in a steel plate.

As a result of this, Thorburn et al. (1983) developed complementary method of analysis for steel plate shear wall. An analytical model was developed to study the resistance of story shear provided by buckled web functioning as tension field in a real sized plate. Modeling of the tension zone developed in a buckled shear wall could be accessible analytically by dividing the panel into the series of inclined truss members that orients as a series of pin ended tension only truss members which is represented in Figure (2.1). All of the trusses have the equal width and they were adjusted with the same angle of inclination. With considering this model, equation 2.1 for the angle of inclination was proposed by Thorburn et al. (1983). Resulting stress distribution in the thin steel plate orients at the same inclination as the diagonal tension stress.

$$\tan^4 \alpha = \frac{1 + \dfrac{\left(L_p \times t_w\right)}{2A_c}}{1 + \dfrac{\left(H_p \times t_w\right)}{A_b}} \qquad\qquad \text{Eq (2.1)}$$
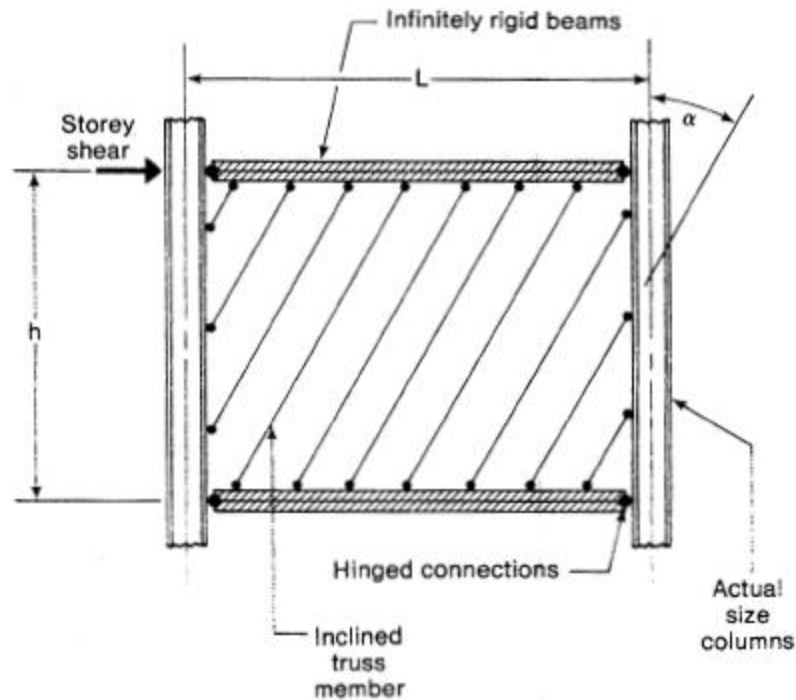
Figure 2.1. Typical one story strip model represented by Thorburn et al. (1983)

2.1.2. Study of Timler and Kulak (1983)

Timler and Kulak (1983) aimed to validate the proposed analytical model of Thorburn et al. (1983) with physical testing of the system in order to examine the adequacy of the proposed post buckling model.

A frame with the scale of actual building and one-story height with aspect ratio equals to one was tested under both cyclic loading to the serviceability limit and loading to the failure. All the beam to column connection of the frame were connected by pin joints. Specimen was loaded in an incremental way. Initially, the specimen was subjected

to cyclic loading three times up to the permissible deflection limit in each direction. A final test was conducted until the test frame reached its ultimate capacity.

As a result, it has been observed that the load deflection response of the actual test frame is similar to the results obtained from the analytical model. Good agreement was obtained in comparing the predicted stresses in the strips by Thorburn et al. (1983) with actual stresses emerged in the web plate. From the final results of analyzing single story panel with the aspect ratio equals to one , it was concluded that simplified analytical method for thin steel plate shear wall offered by Thorburn et al. (1983) was a satisfactory approach.

In sequence, Timler and Kulak (1983) observed some shortcoming in the inclination angle of tension field, equation 2.1 developed by Thorburn et al. (1983). They identified that the bending effect of the horizontal component of the tension field force acts on the column. Consequently, they proposed a modification for the equation 2.1 which includes column stiffness (I_c) to make it more accurate. Timler and Kulak (1983) proposed equation 1.1 for calculating the inclination angle of tension field.

2.2. *Studies on Stiffness and Characteristic of the Boundary Elements*

2.2.1. Study of Thorburn, Kulak and Montogomery (1983)

Using strip model proposed by Thorburn et al. (1983) which was shown in figure 2.1, parametric studies were undertaken to examine the effects of the column stiffness, web thickness, panel dimensions, on the strength and stiffness characteristic of the shear wall.

The results depicted that column stiffness influences the strength and the characteristic of the steel plate shear wall. For very rigid columns, thin steel plate of the wall gets stiffer. For the flexible column, variation of the tensile forces across the web plate increase and consequently, compressive stresses enhance in the corners of the plates which lead to the reduction in the effectiveness of the web. Normally, maximum stresses should occur at the middle part of the steel plate and it decreases toward the edge of the plate. For the single-story plate, the load carrying capacity of the steel plate increases as the thickness of web utilized increases. As the plate height increases, lateral stiffness reduces and similarly, increment in length increases the stiffness of plate.

2.2.2. Study of Caccese, Elgaaly, Chen (1993)

Caccese et al. (1993) was investigated the seismic behavior of unstiffened thin steel plate shear wall under lateral loading induced to a structure by earthquake or wind. The objection of the study is to evaluate the seismic performance of the thin steel plate shear wall. In this study, two major parameters of beam to column connection and steel plate slenderness ratio were considered.

Experimentally, cyclic tests were undertaken to five, three-story ¼ scale specimens that include three specimens with varying plate thickness such as 0.76 mm, 1.9 mm and 2.66 mm with moment resisting beam to column connection and two specimens with shear beam to column connections with plate thickness equal to 0.76 mm and 1.9 mm. Lateral loading was applied to the top of the third story of the specimen to a maximum displacement of 2% drift. At this point if the specimen was intact, it is pushed monotonically to the maximum displacement limit of the actuator.

It was concluded that utilizing slender plate in shear wall increased the stiffness, load carrying capacity and energy absorption in the system. Inelastic behavior of the

system commenced by yielding of the unstiffened plate and plastic hinge formation in the columns governed the system strength. Be that as it may, with the thick plate failure mode of the system governed by column instability before the development of yield strength in the plate. Therefore, only negligible increase in system strength was achieved. They were also concluded that with thin plate the system elastically responds to a minor seismic event. Final remarks of this study emphasized the importance of using slenderer plates since they allow sufficient energy absorption and safer approach compared to previous model.

2.2.3. Study of Elgaaly, Caccese, Du (1993)

Elgaaly et al. (1993) used finite elements methods to verify the experimental results that achieved by Caccese et al. (1993) and determined the behavior of the steel plate shear wall up to their ultimate capacity. In the analyses, both material and geometry nonlinearities were considered. The model consists of replacing the plate by diagonal tension members as same as the strip model proposed by Timler and Kulak (1983).

It is found that the wall with thicker plate was not specifically stronger because of the governing of the column yielding. In the finite element modeling, shell element was used to model the web plate. Deformed shape of the three-story which is loaded from the top and pushed monotonically is shown in Figure 2.2.
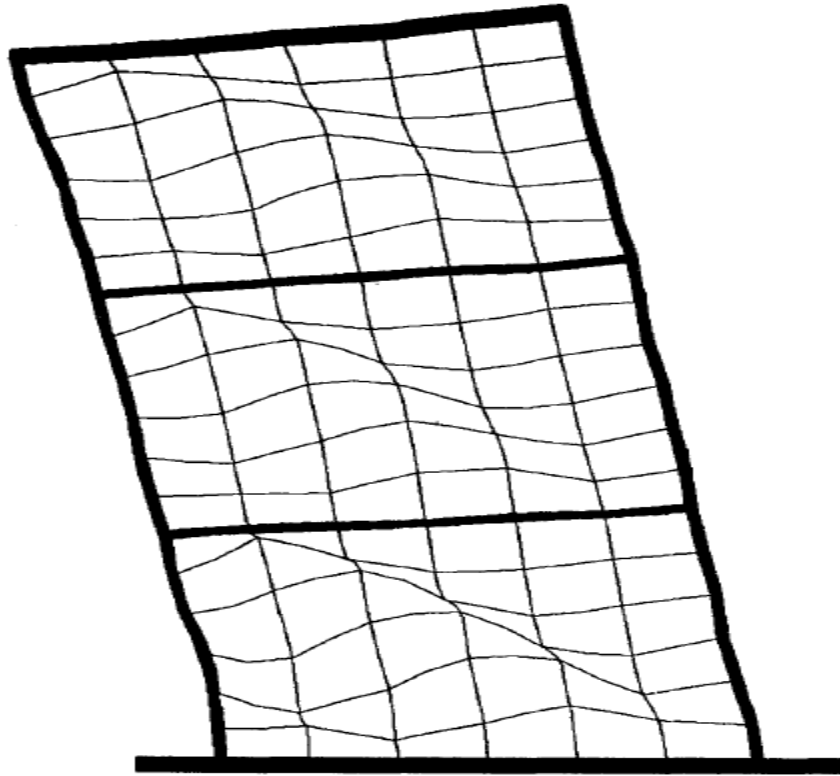
Figure 2.2. Deformed shape of the specimen with three-story (Elgaaly et al., 1993)

It has been seen that the finite element method over-predicted the capacity and stiffness of the system compared with the experimental results. Over-prediction of the capacity and stiffness by finite element modeling was due to the difficulties in modeling the initial imperfection and the inability to model out of plane deformation of the frame members. On the other hand, thin plates that adequately anchored to the surrounding boundary frame provided post-buckling strength several times greater than the elastic buckling strength. The results were in a good agreement with the experimental results with respect to initial stiffness, ultimate strength, and displacement at the ultimate strength.

2.2.4. Study of Berman and Bruneau (2003)

Berman and Bruneau (2003) proposed a revised design procedure for the steel plate shear wall using strip model due to the unconservative designs with lower ultimate

capacity of resisting lateral loads than expected. While doing plastic analysis of the strip model as an alternative, equation 2.2 was derived to obtain the appropriate plate thickness for infill steel plate. Equation 2.2 could have been beneficial for controlling the failure mechanism and structural over-strength. In equation 2.2, V_s is the design story shear and Ω_s is the overstrength of the system.

$$ t = \frac{2V_s\Omega_s}{F_{yp}L\sin 2\alpha} \qquad\qquad \text{Eq (2.2)} $$

Single story and multistory steel plate shear walls were designed with simple and rigid beam-to-column connection with respect to the fundamental plastic collapse mechanism. Ultimate strength predicted from the collapse mechanism analogized with the experimental result. The experimental results given for multistory specimens were either those for the first story shear in the case of Driver (1998) and total base shear in cases where loading was applied to the top story only in the work of Caccese et al. (1993) and Elgaaly (1998).

Lastly, for single and multistory steel plate shear wall with simple and rigid beam to column connections, failure mechanisms have been investigated. It was reported that fundamental plastic collapse mechanism is proper for investigating the ultimate capacity in comparison with the experimental results were in a reasonable agreement.

2.2.5. Study of Lopez Garcia and Bruneau (2006)

Lopez-Garcia and Bruneau (2006) aimed to investigate the seismic behavior of the intermediate beams other than those at the roof and foundation level in a multi-story steel plate shear wall. Primary issue was to determine the sufficient strength to avoid the formation of in-span plastic hinges.

Linear and nonlinear analysis were performed for analyzing the intermediate beams of the four SPSWs with four stories. All four infill plates of SPSWs located at the central part of the frames with three bays. Their intermediate beams were designed to resist three kinds of forces: (I) Forces imposed by gravity forces only; (II) forces determined by the ASCE7, American Society of Civil Engineers load combination (ASCE, 2005) and (III) forces imposed by fully yielded plates. A schematic view of the considered SPSW is illustrated in figure 2.3.

It was concluded from the analyses results that the intermediate beams designed based on the criteria I and II tended to subject to plastic deformation and plastic hinging. SPSWs designed with the forces imposed by fully yielded plates exhibited inelastic deformation only at the ends of the beams and in the infill plate even the occurrence of plastic collapse mechanism.
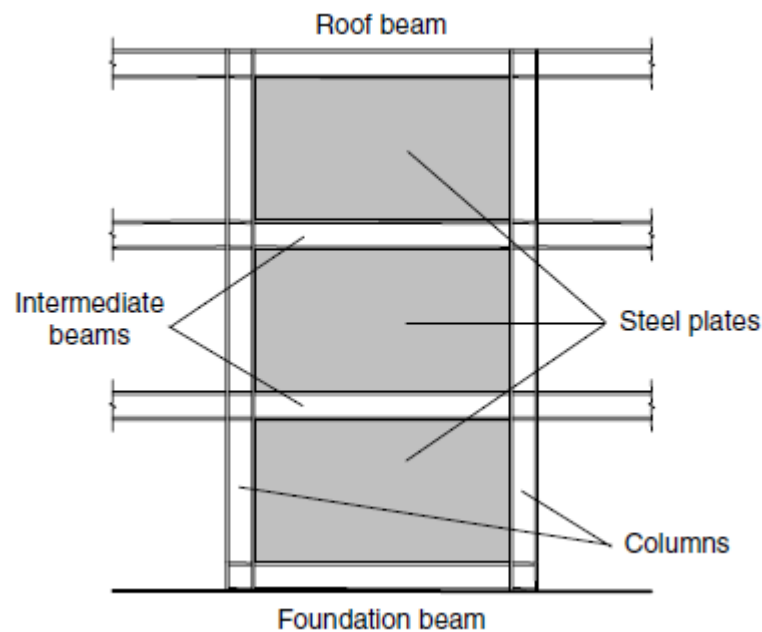
Figure 2.3. Schematic of SPSW considered by (Lopez-Garcia and Bruneau, 2006)

2.2.6. Study of Berman and Bruneau (2008)

Berman and Bruneau (2008) reviewed the current approaches presented in AISC 341-05 which is commentary for determination of capacity design loads for the VBEs of SPSWs. Afterwards, new procedure was proposed that uses fundamental plastic collapse mechanism and linear beam analysis to approximate the design actions for VBEs of SPSWs for given web plates and horizontal boundary elements sizes. To make it practical, proposed procedure did not include nonlinear analysis.

Two four-story SPSWs configuration were considered nominally known as SPSW-V with minimum plate thickness required for the design story shear forces variable at each story and SPSW-C with minimum available plate thickness constant all over four story. SPSW-C and SPSW-V is shown in Figure 2.4.
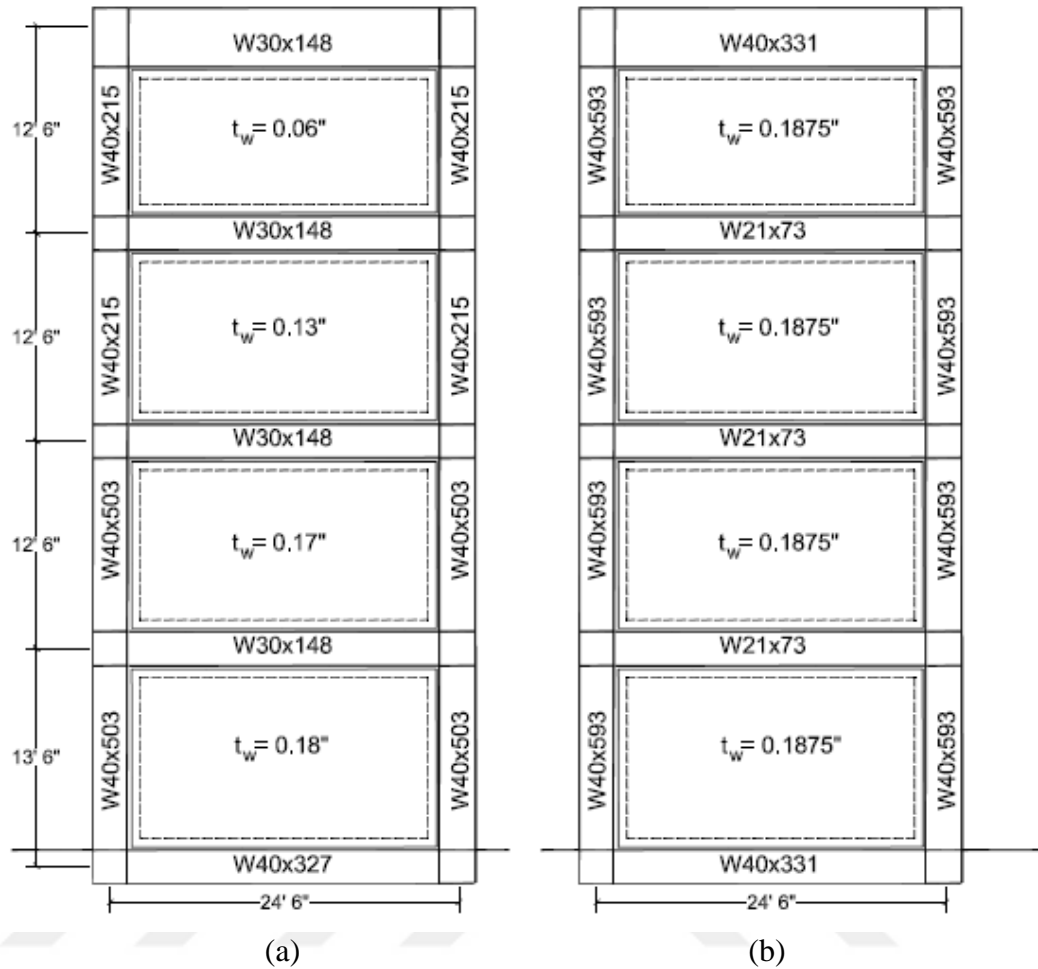
Figure 2.4. Four story (a) SPSW-V and (b) SPSW-C retrieved from Berman and

Bruneau (2008)

The resulting VBE design loads estimated using both current and proposed design

procedures compared with the loads determined by nonlinear pushover analysis.

Nevertheless, these methods did not necessarily exhibit desirable VBE capacity design

while nonlinear static analysis includes more accurate results which can be tedious for

broad use in design. Accordingly, for estimating VBE design loads combined with linear

elastic beam model was proposed to investigate the axial forces in the HBEs with uniform

plastic collapse mechanism. Estimated lateral seismic loads leaded to full web plate

yielding and formed plastic hinging at HBEs end. For this method, it was sufficient to

involve only linear computer analyses without development of the strip model and should

involve strength demands for hinging of the HBE ends. Conclusively, moment and axial force diagrams of the proposed uniformed plastic collapse mechanism and linear model of one of the vertical boundary elements were compared. It has seen that from the moment and axial force diagrams of pushover analyses, both SPSW-V and SPSW-C are in a good agreement.

2.2.7. Study of Bing Que and Bruneau (2010)

In this research analytical works were conducted to evaluate the adequacy of flexibility limit factor (C_2) specified for VBE by Qu and Bruneau (2010). Based on the AISC 341-05, for preventing undesirable behavior of the columns minimum moment of inertia was required for the vertical boundary elements in steel plate shear walls.

For conceptual understanding of behavior of the vertical boundary elements in a SPSW, Wagner (1931) described SPSW as a system similar to the cantilever vertical plate girder. In sequence, by the analytical work done by Wagner (1931) and Kuhn et al. (1952) an equation has been derived (equation 2.3) that limited the columns flexibility in a plate girder theory based on elastic behavior. In this equation σ_{max} and σ_{mean} represent the maximum and average of web plate tension force.

$$\sigma_{max} = (1 + C_2)\sigma_{mean} \qquad \text{Eq (2.3)}$$

By the time passing, they made it clear that between the behavior of the SPSW and plate girder there were many significant differences.

To check the shear yielding of the VBEs some experimentally tested SPSWs were selected and strip model for conducting analytical model was developed. All the

specimens were modeled with 20 strips as infill plates and corresponding maximum VBE shear obtained from the pushover analysis using SAP2000.

As a result, it was revealed that undesirable pull-in deformation of the VBE were principally caused by the VBE shear yielding and literally not correlated to the flexibility factor. Continuously, energy method was undertaken to determine the approximate values of the critical out of plane buckling strength of VBE. It was seen that the flexibility limit (ω_t) was uncorrelated with the satisfactory of the in plane and out of plane buckling performance of the VBE.

CHAPTER III

FINITE ELEMENT MODEL AND MODEL VALIDATION

3.1. *Strip Model*

Modeling of the web plate of SPSW could be conducted with two different approaches, namely, the continuum model and the strip model. In the continuum model, web plates are modeled using shell elements with a specified initial imperfection so that the out-of-plane buckling behavior of web plates is explicitly simulated. Strip model is a simplified model used to simulate the post-buckling behavior of the web plate under lateral loading and the tensile yielding of the web plate at the calculated inclination angle of tension field, α. In this method, series of parallel evenly spaced diagonal tension-only truss elements with the same sectional area connected to the surrounding beams and columns represent the inclined tension field fold lines in the web plate. The cross-sectional area of a strip is given in equation 3.1. Typical strip model is depicted in figure 3.1(a). It should be noted that in figure 3.1(a) for the sake of clarity, strips in one direction have been depicted.

$$A_S = \frac{\left[L_p \cos(\alpha) + h_p \sin(\alpha)\right] t_w}{n_s} \qquad \text{Eq (3.1)}$$

In this study, strip model selected and modeled in OpenSEES (McKenna et al., 2000) in order to represent the post-buckling behavior of the web plate. Two dimensional SPSW that is modeled for this study is illustrated with strips in two directions in figure 3.1(b) schematically.
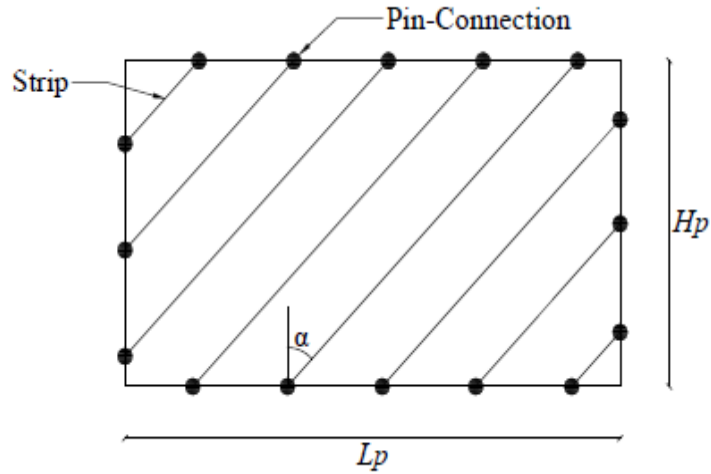
Figure 3.1(a). Strip model with strips in one direction
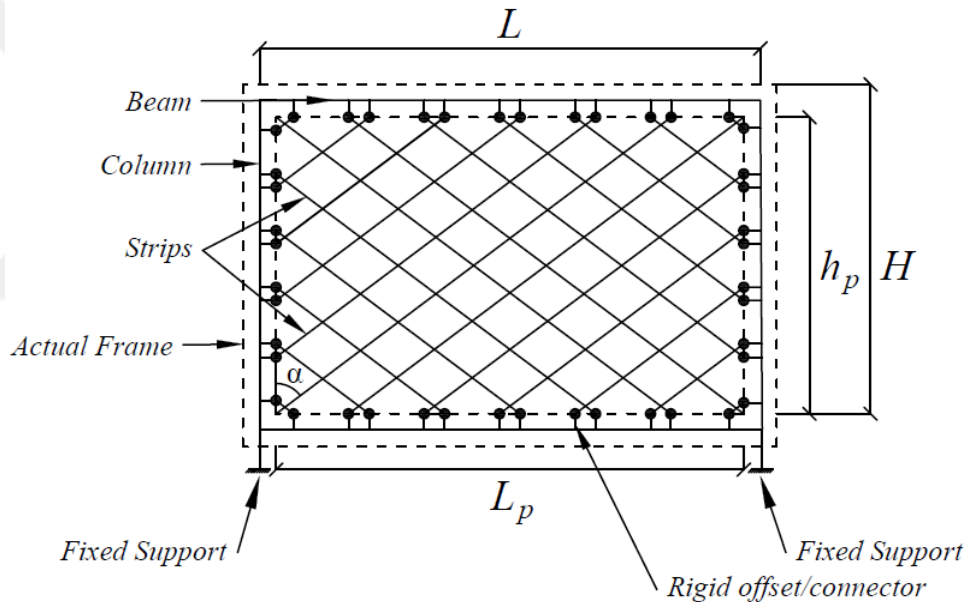
Figure 3.1(b). Two-dimensional modeling of the SPSW

As a material for the web plate, "hysteretic" material is adopted which is available in the OpenSEES material library. Hysteretic material is used to construct with an insignificant compressive strength and uniaxial bilinear response under tension with pinching of force and deformation. Tension-only behavior of the web plate presented in figure 3.2. Since, when unloaded after an incursion into the inelastic range (point a), a

strip exhibits residual deformations (point b), tensile stresses will not develop in the next cycle in the same direction until point 'b' is reached. This hysteretic behavior caused pinching effect (Sabelli and Bruneau, 2007). For representing the web plate as a series of strips, co-rotational truss elements are used to simulate the web plate behavior.
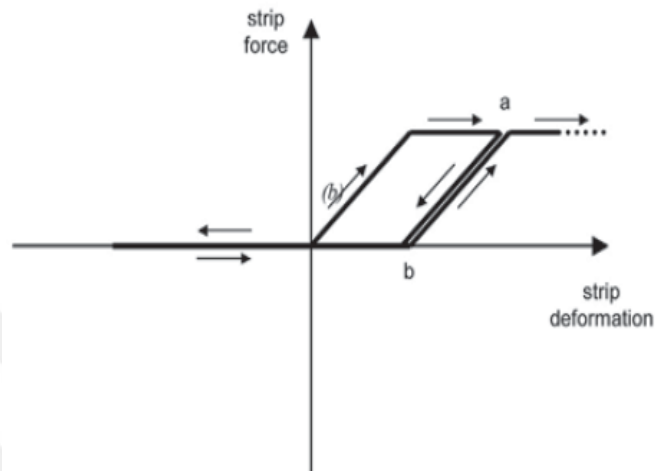
Figure 3.2. Tension-only Behavior of the Web Plate (McKenna et al., 2000)

Subsequently, for the VBEs and HBEs "steel02" is used as a material with an isotropic hardening. Behavior of the "steel02" is represented in Figure 3.3. For modeling beams and columns in OpenSEES nonlinear force-based beam-column elements which consider the distributed plasticity along the elements is used for boundary elements.
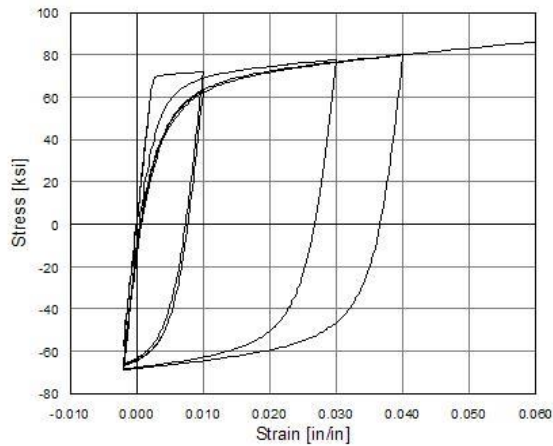
Figure 3.3. Hysteresis Behavior of the Boundary Elements of SPSW (McKenna et al., 2000)

As it can be seen in figure 3.1(b) all of the strips are connected to the surrounding boundary frame with rigid links to represent the end offsets. As an element, Elastic beam to column elements is used. For constructing the rigid links, elements with considerable sectional area is considered to simulate the very stiff behavior of these elements.

3.2. *Validation of the Strip Model*

To validate the strip model, a SPSW specimen tested by Lubell et al. (2000) was chosen and was modeled in OpenSEES (McKenna et al., 2000). Chosen SPSW is one story height with one bay width designated as SPSW2 in Lubell et al. (2000). The test conducted in both elastic and inelastic response regions of the specimens under fully reversed cyclic quasi-static loading. The one-story test specimen stood for one bay of a steel- framed office building core that is quarter scale. Unstiffened web plate had width to height aspect ratio (L/H) of 1:1 with a column-to-column centerline spacing of 900 mm. For the beams and columns, the wide flange section S75X8 was used with the continuous columns through the height of the building. For preventing the out of plane displacement of the frame and anchoring the internal panel forces to the top beam of the

SPSW2, an additional wide flange section S75X8 welded along adjoining flange was integrated. A schematic of single panel SPSW2 is shown in figure 3.4. Material of boundary frame had a yield stress of 380 MPa. For providing full moment connections at all beam column joints, entire beam section continuously fillet welded to the column flanges. Thickness of the infill panel was 1.5 mm (16 gauge) hot rolled steel plate and the material had a yield strength of 320 MPa.
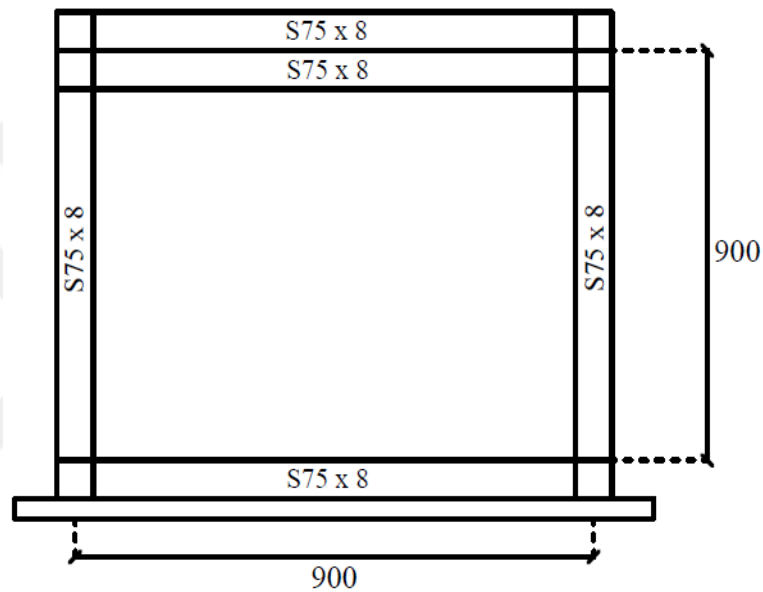
Figure 3.4. Schematic view of SPSW2

The specimen was tested according to procedures as recommended in ATC-24 (1992), Guidelines for cyclic seismic testing of component of steel structures protocol. A cyclic quasi-static analysis was undertaken in a force-controlled manner until to a point in which displacement was achieved to significant yielding. SPSW2 subjected to three cycle at each load level with a global yield corresponding to 190 kN base shear with a 6-mm story displacement. At 6X6-mm story displacement system failure occurred due to the column fracture. Formation of plastic hinges at the bottom and top of the columns occurred due to inward deformation of the SPSW2 and in consequences taking on an

hourglass shape. Deformation and yielding pattern of specimen SPSW2 after the completion of three cycles at 6X6-mm is illustrated in Figure 3.5.
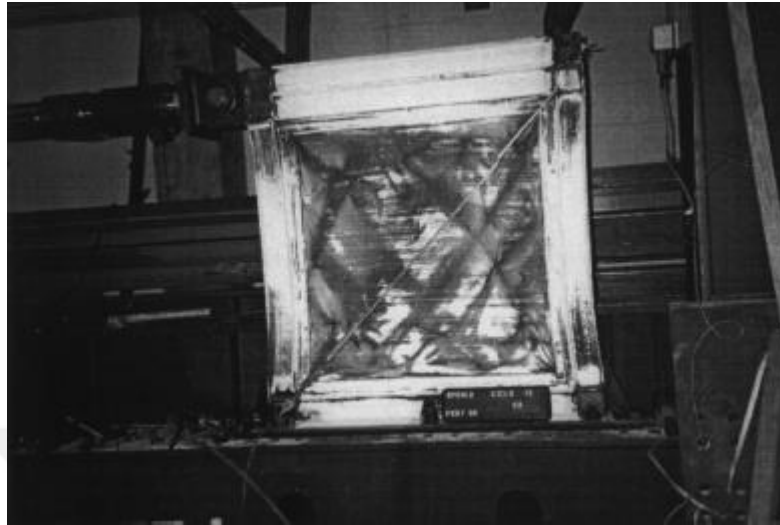
Figure 3.5. Deformation and yield pattern of SPSW2 at 6x6-mm retrieved from Lubell et al. (2000)

According to the section 3.1, SPSW2 of Lubell et al. (2000) is modeled in OpenSEES as a strip model. Analogous to the experimental model 320 MPa is designated as a yield stress to the web plate with a modulus of elasticity of 200 GPa and with a strain hardening ratio of 0.5%. The yield stress of vertical and horizontal boundary elements is 380 MPa and strain hardening ratio is 0.5%. For modeling the web plate, 10 strips are used with an inclination angle calculated based on equation 1.1 in both directions. All 10 strips are connected to the surrounding boundary frame with rigid links to represent the end offsets. Bottom beam of the SPSW was anchored to the ground along its length and columns bases are assumed to be fixed.

The base shear vs. horizontal displacement response of the numerical analysis is given in Figure 3.6 and compared with the experiment of Lubell et al. (2000). As it can be seen from OpenSEES results in the Figure 3.6, strip model is capable of predicting the base shear during the loading accurately. However, the strip model does not accurately

anticipate the lateral stiffness and overestimates it at small displacement levels almost less than 4.5 mm (0.5% drift). From this observation, it is supposed that overestimation of the elastic stiffness is associated with the fact that the panel zones were assumed to be rigid in the model. In addition, the strip model does not capture the unloading strength of the specimen, which is due to the web plates that are modeled with tension-only strips. However, web plate has a certain compressive strength (Webster, 2013) which is neglected in the OpenSEES model. For this study, adequacy of the assumed strip model is proved since one-directional pushover will apply for investigating the influence of the boundary frame stiffness on distribution of the stresses in the web plate. Therefore, matching the base shear versus horizontal displacement of the loading part of the experimental results with the OpenSEES results is essential in this study case.
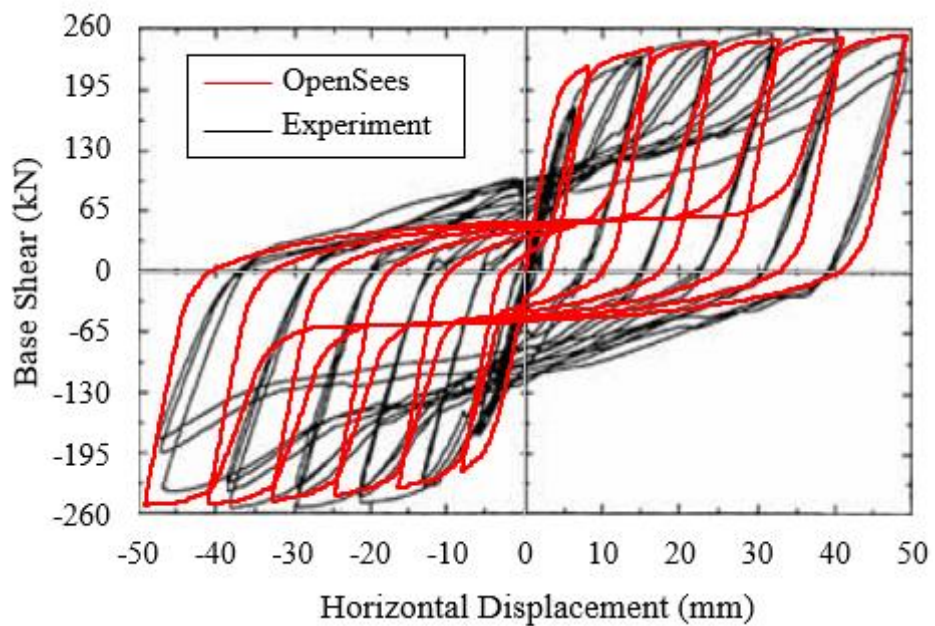
Figure 3.6. Base shear vs. displacement of the experiment [adapted from Lubell et al. (2000)] and the OpenSEES model.

CHAPTER IV

STEEL PLATE SHEAR WALL DESIGNS

4.1. Design Procedure

In this section, design procedures of SPSWs are explained and necessary requirement for ductility of the system are addressed. Incidentally, some general demands for designing SPSWs was taken from AISC341-16 and AISC360-16, Specification for Structural Steel Buildings (AISC, 2016c). Design of SPSW is intended to ensure ductile performance based on the tension yielding of the web plate. VBEs and HBEs were designed based on the forces corresponding to the web plate strength with referring to AISC Design Guide 20 for Steel Plate Shear Walls by Sabelli and Bruneau (2007).

For high seismic regions, boundary elements of SPSWs are designed to permit the web plate develop significant diagonal tension and allow web plate to reach its expected yield strength across the entire web plate. Desired performance is aimed to prevent yielding of the VBEs and HBEs prior to the yielding of the web plate. In the case of small transverse stiffness of the VBE, uniform tension field cannot be developed across the entire web plate and the strength of the system significantly reduced. VBEs and HBEs are both designed to resist web plate tension forces acting inward on the SPSW through the flexure at a derived inclination angle with equation 1.1, based on the geometry of the frame and section properties of the beams and columns. Moreover, figure 4.1 demonstrates that the HBE at the top and bottom of the VBEs resist significant compression induced by the inward flexure forces of the VBE in addition to the flexural forces exerted by tension in the web plate. It demonstrates that the compression under the

right VBE ($P_{VBE(right)}$) is stabilized by the tension under the left VBE ($P_{VBE(left)}$) and tension stresses in the web plate (σt_w) (Sabelli and Bruneau, 2007).
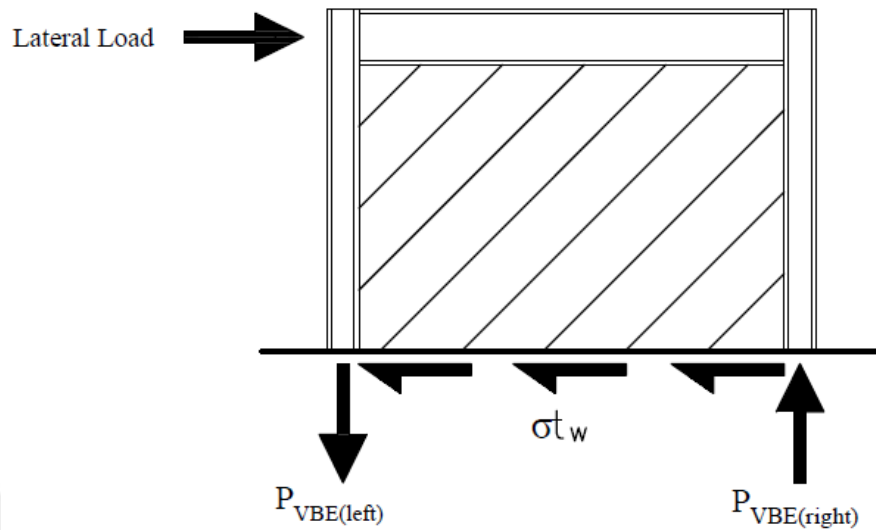
Figure 4.1. Idealized behavior of the SPSW retrieved from Sabelli and Bruneau (2007)

4.2. Design of HBE

For designing HBEs of SPSWs suggested procedure by Sabelli and Bruneau (2007) is undertaken and it is shown in figure 4.2. Detailed information about the steps of procedures are provided in the following sections.
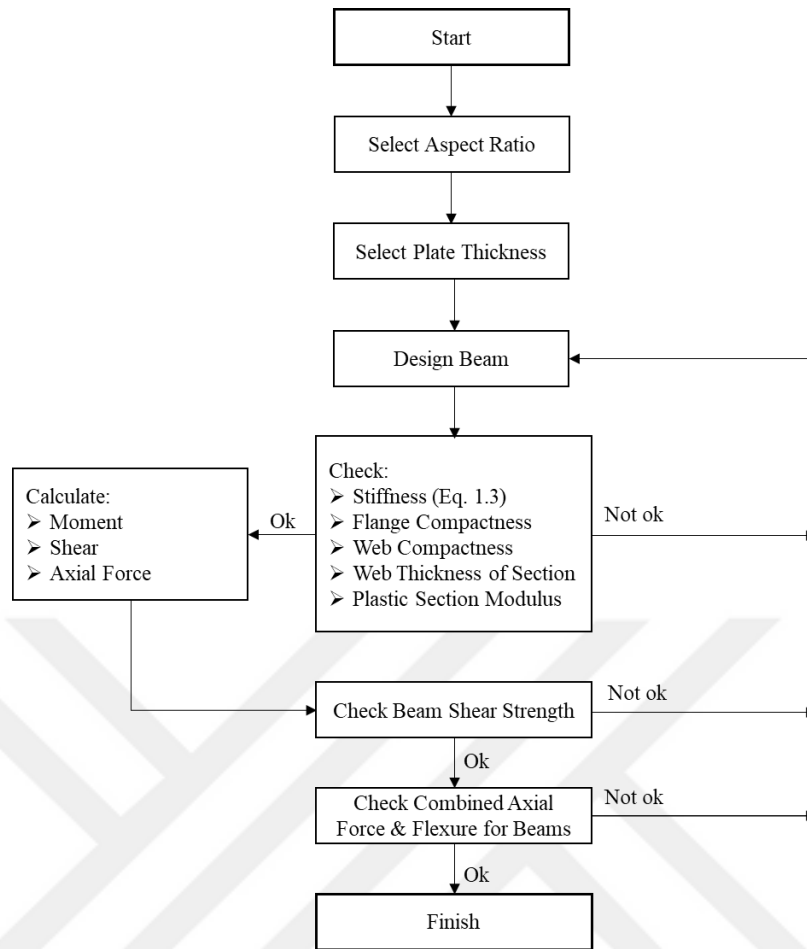
Figure 4.2. Design process of the HBE

It is worth to mention that compactness of the web and flange of the W-shaped section is satisfied based on the limits suggested by AISC 341-16 for compression elements for highly ductile members.

4.2.1. Web Thickness Limit of the W-section for the HBE

Based on the effects of stresses of web-plate tension yielding on the boundary elements, major axial force inserted to the HBE. In addition, required flexural forces at the top and bottom HBEs is quite large. For the ductile system behavior, it is preferable to choose a section for HBE which is at least as strong as the expected strength of the web-plate. Recommendation for the minimum web thickness of the HBE in the SPSW

for the sections with different material grade is mentioned in equation 4.1 (Sabelli and Bruneau, 2007).

$$t_{wHBE} \geq \frac{t_w R_{yp} F_{yp}}{F_{yHBE}}$$
<div align="right">Eq (4.1)</div>

4.2.2. Plastic Section Modulus Limit of HBE

Excessive accumulation of the plastic deformation on the HBE could cause by the plastic hinging within the span of the HBE. This incremental plastic deformation prevents full yielding of the web plate and tolerates lower global plastic strength (Purba and Bruneau, 2011, 2014). AISC 341-16 suggests two approaches for prevention of in-span plastic hinging in the HBE with either choosing a section for HBE which has plastic section modulus equal or greater than the value derived by equation 4.2 ($Z_{AISC341}$) and designing the HBE to resist the moment twice more the exact value.

$$Z_{AISC341} = \frac{\omega_{yb} L_p^2}{4 F_{yHBE}}$$
<div align="right">Eq (4.2)</div>

In equation 4.2, ω_{yb} is the vertical component of infill plate stress which is shown in figure 4.3 and calculated with Equation 4.3.

$$\omega_{yb} = R_{yp} F_{yp} t_w \cos^2 \alpha$$
<div align="right">Eq (4.3)</div>
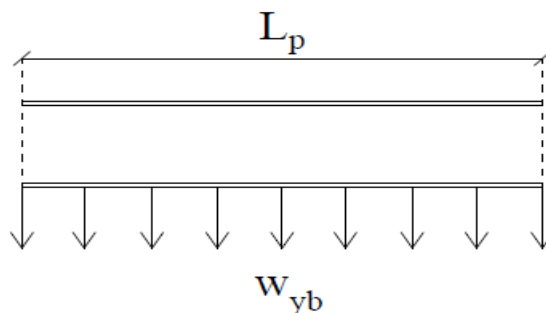
Figure 4.3. Vertical component of the distributed load exerted by infill plate on beam

4.2.3. Shear Strength of Web Plate

Based on the angle of inclination from equation 1.1, ϕV_n is derived corresponding to AISC 341-16 in accordance with the limit state of shear yielding in Equation 4.4.

$$\phi V_n = 0.90(0.42)F_{yp}t_w L_p \sin(2\alpha) \qquad \text{Eq (4.4)}$$

4.2.4. Axial Force in the HBE

Axial force in the HBE has two sources, firstly VBEs reactions due to the inward forces from the web plate, equation 4.5 and secondly, effects of the web on the HBEs are imposed by equations 4.5 and 4.6 respectively.

$$P_{HBE(web)} = \frac{1}{2}R_{yp}F_{yp}\sin(2\alpha)t_w L_p \qquad \text{Eq (4.5)}$$

$$P_{HBE(VBE)} = \frac{1}{2}R_{yp}F_{yp}\sin^2(\alpha)t_w h_p \qquad \text{Eq (4.6)}$$

Half of the forces from equations 4.5 and 4.6 are considered for estimating the axial force of the HBE based on the assumption by Sabelli and Bruneau (2007). For instance, inward forces of the VBE calculated by equation 4.6 divided equally between the top and bottom of the VBE and likewise, half of the forces from equation 4.5 imposed on either side of the HBE. As a consequence, total axial forces on the HBE at the left side and right side calculated with equation 4.7. Figure 4.4 schematically presents the total axial force in the HBE.

$$P_{uHBE} = \frac{1}{2}P_{HBE(VBE)} \pm \frac{1}{2}P_{HBE(web)} \qquad \text{Eq (4.7)}$$
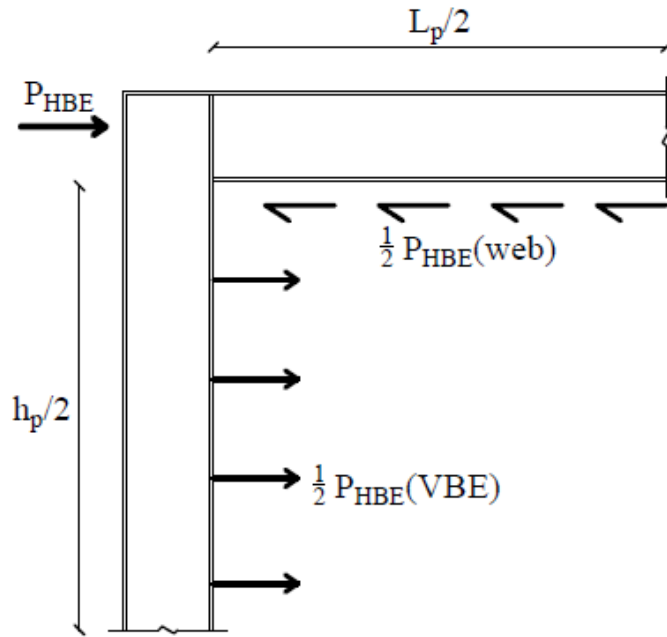
Figure 4.4. Total Axial Force (P_{uHBE}) in the HBE

4.2.5. Flexural Forces of the HBE

Required flexural forces of the HBE can be significantly large at the top and bottom of the SPSW. Formation of the plastic hinges could be assumed that caused by the same flexural forces at the ends of the beams. Accordingly, HBEs are assumed to be strong enough and are designed to resist web plate tension by assuming them as a simply supported beam. Required flexural forces of the HBE calculated from the loading defined by equation 4.8. In this study gravity loads were not considered.

$$M_{u(HBE)} = \frac{\omega_{yb} L_p^{\,2}}{8}$$
Eq (4.8)

For imposing the second order effect (P-δ) for each member subjected to compression and flexure, based on the AISC360-16, B1 is used to find $M_{r(HBE)}$ with equation 4. 9. In this study calculation of P-Δ effect is ignored since the SPSWs are capacity designed with referring to assumption considered by Sabelli and Bruneau (2007).

$$M_{r(HBE)} = B_1 M_{u(HBE)}$$
<div align="right">Eq (4.9)</div>

Where;

$$B_1 = \frac{C_m}{1 - \dfrac{P_{uHBE}}{P_{e1}}}$$
<div align="right">Eq (4.10)</div>

In which, C_m is conservatively taken as 1.0 and P_{e1} is calculated by equation 4.11.

$$P_{e1} = \frac{\pi^2 EI_{HBE}}{L^2}$$
<div align="right">Eq (4.11)</div>

Besides, the shear developed by web plate tension should be considered. Total shear in the left and right side of the HBE is given in equations 4.12 and 4.13 and the maximum absolute value has chosen to be the required shear strength of the HBE.

$$V_{uLeft} = \frac{M_{pr(Left)} + M_{pr(Right)}}{L_p} + \frac{\omega_u}{2} L_p$$
<div align="right">Eq (4.12)</div>

$$V_{uRight} = \frac{M_{pr(Left)} + M_{pr(Right)}}{L_p} - \frac{\omega_u}{2} L_p$$
<div align="right">Eq (4.13)</div>

In this study, presence of the axial forces at HBE-to-VBE connections cause a reduction in flexural strength (Mpr) of the beams which is calculated with equation 4.14 at the plastic hinges location, thus, lower shear strength is required for the connections.

$$M_{pr} = C_{pr} R_y F_y Z_x$$
<div align="right">Eq (4.14)</div>

Reduction of the flexural strength can be calculated by adopting the interaction equation available in AISC360-16. Reduced flexural strength (M_{pr}^*) at the left side and right side of the HBE is:

When;

$P_{u(HBE)}$ (Left/Right)/P_y <0.2

$$M^*_{pr} = M_{pr}\left[1 - \frac{1}{2}\left(\frac{P_{uHBE}}{P_y}\right)\right]$$

Eq (4.15)

And otherwise;

$$M^*_{pr} = \frac{9}{8}M_{pr}\left[1 - \frac{P_{uHBE}}{P_y}\right]$$

Eq (4.16)

In equations 4.15 and 4.16, P_y is axial yield strength of the HBE and can be calculated by multiplying the A_b and F_{yHBE}. Furthermore, C_{pr} adopted from AISC358-16, Prequalified Connections for Special and Intermediate Steel Moment Frame for Seismic Applications (AISC, 2016b) and can be expressed as following equation 4.17.

$$C_{pr} = \frac{F_y + F_u}{2F_y} \le 1.2$$

Eq (4.17)

Consequently, calculated required shear strength for HBEs should be higher than the design shear strength of the HBEs and combined axial forces and flexure for HBE should be satisfied. It should be noted that the lateral torsional buckling did not considered in HBE design since presence of the slabs in each floor elevation prevents the lateral torsional buckling in beams and therefore compression strength is governed by major axis (x axis) buckling. In this study K is taken conservatively as 1.

4.3. *Design of VBE*

In high-seismic design of the SPSWs, the failure of the VBE under overturning forces should be prevented at the forces corresponding to yielding of the web plate. For achieving this, it is sufficient to design the VBEs for the sum of the shear strength of the shear strengths of the connected web plates (Sabelli and Bruneau, 2007).

Design procedure of the VBE is undertaken based on the steps mentioned in figure 4.5. It should be mention that the web and flange compactness of the VBEs should satisfy the limits for compression elements in highly ductile members suggested in AISC341-16.
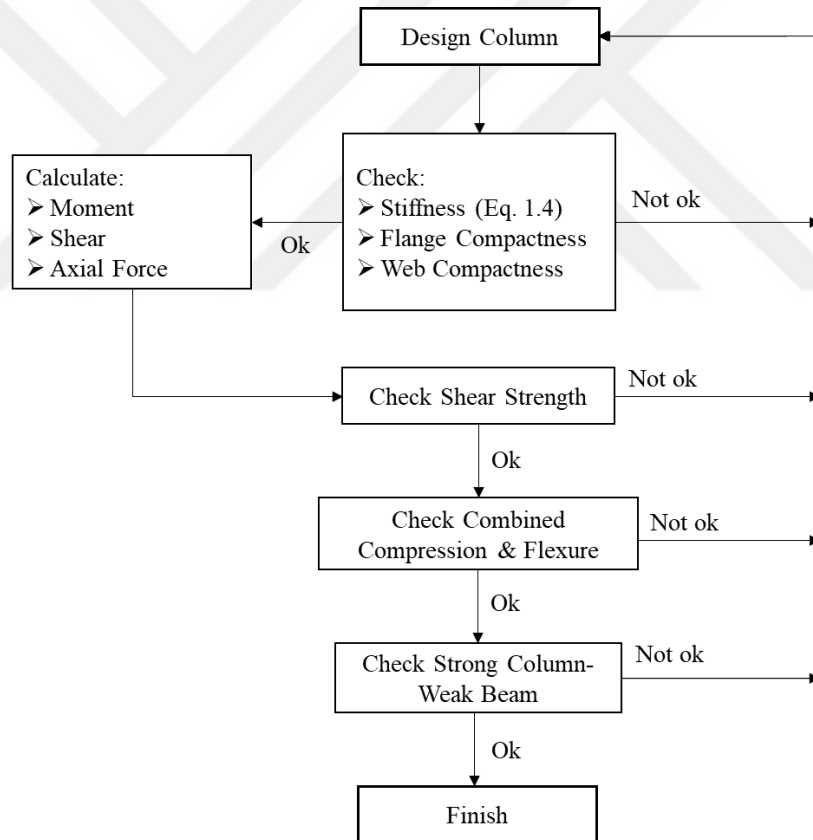
Figure 4.5. design process of the VBE

4.3.1. Axial Force in VBE

The axial compressive strength of the VBE can be calculated by the sum of the web plate strength with the addition of the sum of the HBE shears, equation 4.18.

$$P_{u(Compression)} = \sum \frac{1}{2} R_{yp} F_{yp} \sin(2\alpha) t_w h_p + \sum V_u \qquad \text{Eq (4.18)}$$

Due to the division of the seismic tension forces between the web plate and HBE, tensile forces in the VBE are significantly lower than the corresponding compressive seismic forces of the opposite VBE. For estimating the seismic axial tension force in VBE, sum of the beam shear forces separating into two parts: (a) beam shear due to plastic hinge formation which acts upward and (b) web plate tension forces on the HBE which acts downward. The expression is as following:

$$P_{u(Tension)} = \sum \frac{1}{2} R_{yp} F_{yp} \sin(2\alpha) t_w h_p + \sum \left[\frac{M_{pr(Left)} + M_{pr(Right)}}{L_p} - \frac{\omega_{yb}}{2} L_p \right] \qquad \text{Eq (4.19)}$$

4.3.2. Flexural Forces of the VBE

Flexural forces of the VBEs can be calculated by assuming the fix ends for both VBEs. Total flexural forces of the VBEs includes the contribution of the web plate tension and forces from HBE plastic hinging and it can be estimated separately and then combined.

The moment induced by the web plate tension ($M_{VBE\,(web)}$) at the connection is:

$$M_{VBE(web)} = \frac{R_{yp} F_{yp} \sin^2(\alpha) t_w h_c^2}{12} \qquad \text{Eq (4.20)}$$

Based on the flexural strength of the beams which is reduced by the presence of the axial force, the moment from HBE plastic hinging is calculated. The flexural force at the connection of the VBE *($M_{VBE(HBE)}$)*, is considered conservatively equal to one-half of the moment at the HBE due to the plastic hinging, *(M_{pb})*.

$$M_{VBE(HBE)} = \frac{1}{2} \sum M_{pb}$$
Eq (4.21)

Where,

$$M_{pb} = M_{pr} + V_u s_h$$
Eq (4.22)

In equation 4.22, $V_u s_h$ is the additional moment due to the beam shear from the location of the plastic hinge to the column centerline and s_h is the distance from center of the plastic hinge to the center of the VBE according to AISC358-16. In this study it is assumed that hinges formed at the end of the HBE, therefore, s_h is equal to one-half of the VBE depth.
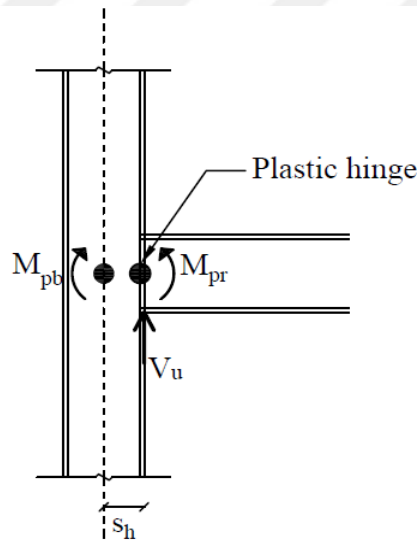
Figure 4.6. Flexural force exerted to the column due to the shear at the plastic hinge location retrieved from Sabelli and Bruneau (2007)

Subsequently, total flexural force in the VBE is calculated with Equation 4.23 with considering the P-δ effect. In this study calculation of P-Δ effect is ignored since the SPSWs are capacity designed with referring to assumption considered by Sabelli and Bruneau (2007).

$$M_{u(VBE)} = M_{VBE(web)} + M_{VBE(HBE)}$$
Eq (4.23)

For implementing the P-δ effect following procedure is undertaken.

$$M_{r(VBE)} = B_1 M_{u(VBE)}$$
<div align="right">Eq (4.24)</div>

Where;

$$B_1 = \frac{C_m}{1 - \dfrac{P_{u(Compression)}}{P_{e1}}}$$
<div align="right">Eq (4.25)</div>

In which, C_m is conservatively taken as 1.0 and P_{e1} is calculated with equation 4.26.

$$P_{e1} = \frac{\pi^2 E I_{VBE}}{h^2}$$
<div align="right">Eq (4.26)</div>

4.3.3. Shear Force in the VBE

Shear in the VBE formed as a consequences of web plate tension and the part of the shear in the HBE which is not resisted by the web plate.

The shear due to the web plate tension is:

$$V_{VBE(web)} = \frac{1}{2} R_{yp} F_{yp} \sin^2(\alpha) t_w h_p$$
<div align="right">Eq (4.27)</div>

And the shear due to hinging of the HBE is estimated by equation 4.29 as follows:

$$V_{VBE(HBE)} = \sum \frac{1}{2} \left(\frac{M_{pc}}{h_p} \right)$$
<div align="right">Eq (4.28)</div>

where, M_{pc} is plastic bending moment of the column and it is equal to expected flexural strength of the beams at plastic hinge location. In sequence, total shear force of the VBE is equivalent to:

<div align="center">38</div>

$$V_u = V_{VBE(HBE)} + V_{VBE(web)}$$ Eq (4.29)

It should be stated that lateral torsional buckling in the VBEs and bending of the section about the major axis are considered.

4.4. Strong-Column/Weak-Beam Check

Strong-column/weak-beam requirement should be satisfied in conformance with AIS341-16. In this section the aim is to prevent the significant inelastic deformation capacity of the HBEs through flexural yielding and design VBEs stronger than the fully yielded or strain-hardened beams. For performing the strong-column/weak-beam checking requirement. Following equation 4.30, specified relationship should be satisfied at beam-to-column connections.

$$\frac{M^*_{pc}}{M^*_{pb}} \geq 1.0$$ Eq (4.30)

In the above equation, M^*_{pb} is sum of the projection of the expected flexural strengths of the beams at the plastic hinge locations to the column centerline. M^*_{pb} can be calculated as follows.

$$M^*_{pb(Left/Right)} = \sum \left(M_{pr} + V_{u(Left/Right)} s_h \right)$$ Eq (4.31)

And total value of expected flexural forces at the beam plastic hinge location M^*_{pb}

is equal to:

$$M^*_{pb} = M^*_{pb(Left)} + M^*_{pb(Right)}$$ Eq (4.32)

M^*_{pc} is sum of the projection of the nominal flexural strength of the columns above and below the joint to the beam centerline and it is reduced by the axial force in the column. The expected axial force is calculated based on the strength of the web plate and the beam above. For the VBE in compression:

$$\sum M^*_{pcC} = 2\left(F_y - P_{u(Compression)} / A_{gVBE}\right)Z_x \qquad \text{Eq (4.33)}$$

And for the VBE in tension:

$$\sum M^*_{pcT} = 2\left(F_y - E_{m(Tension)} / A_g\right)Z_x \qquad \text{Eq (4.33)}$$

Ultimately, total M^*_{pc} is equal to:

$$M^*_{pc} = M^*_{pcC} + M^*_{pcT} \qquad \text{Eq (4.34)}$$

4.5. SPSW Designs

Table 4.2 shows the 27 SPSWs designed for this study. The aim is to determine the effect of increasing column stiffness on the distribution of the stresses in the web plate. Pursuant to this goal, additional SPSWs are designed with the same plate thickness, same aspect ratio, same beam section with changing column sections. There are 9 plate thickness and 3 aspect ratios which is shown in table 4.1. Totally 81 SPSWs designed based on the mentioned design procedure for VBE and HBE in the sections 4.1 and 4.2. All of the 81 SPSWs tabulated in table 4.2. Additionally, naming method of the SPSW designs are illustrated in the table 4.1. In this table x, y and z are the variables designated for the aspect ratio values (L_p /H_p), different plate thickness and design options, respectively. Design options indicates the stiffness of the column section. Design option of 1 has the less stiff column section while the design option of 3 has the stiffest column

section. For instance, if the aspect ratio is equal to 1, plate thickness is equal to 0.55 mm and design option 1 is chosen, then the name of the design appears to be as D 1-1-1 with respect to the numbers designated under x, y and z as shown below.

Table 4.1 Naming scheme of SPSW designs

Name of Design	x	Aspect Ratio	y	Plate Thickness (mm)	z	Design Option
D-x-y-z	1	1	1	0.55	1	1
			2	0.79		
			3	0.95		
	2	1.5	4	1.27	2	2
			5	1.98		
			6	2.38		
	3	2	7	3.17	3	3
			8	3.57		
			9	4.36		

Table 4.2 SPSW designs

L=4000mm, h=4000mm				L=5500 mm, h=4000mm				L=6500 mm, h=4000mm			
Name	tw	Beam	Column	Name	tw	Beam	Column	Name	tw	Beam	Column
D-1-1-1	0.55	W16X31	W14X68	D-2-1-1	0.55	W21X57	W14X132	D-3-1-1	0.55	W24X84	W14X159
D-1-1-2			W14X74	D-2-1-2			W14X145	D-3-1-2			W14X176
D-1-1-3			W14X82	D-2-1-3			W14X159	D-3-1-3			W14X193
D-1-2-1	0.79	W16X45	W14X82	D-2-2-1	0.79	W24X76	W14X159	D-3-2-1	0.79	W27X94	W14X193
D-1-2-2			W14X132	D-2-2-2			W14X176	D-3-2-2			W14X211
D-1-2-3			W14X145	D-2-2-3			W14X193	D-3-2-3			W14X233
D-1-3-1	0.95	W18X46	W14X132	D-2-3-1	0.95	W24X84	W14X176	D-3-3-1	0.95	W30X108	W14X233
D-1-3-2			W14X145	D-2-3-2			W14X193	D-3-3-2			W14X257
D-1-3-3			W14X159	D-2-3-3			W14X211	D-3-3-3			W14X283
D-1-4-1	1.27	W21X57	W14X132	D-2-4-1	1.27	W27X102	W14X233	D-3-4-1	1.27	W33X130	W14X311
D-1-4-2			W14X145	D-2-4-2			W14X257	D-3-4-2			W14X342
D-1-4-3			W14X159	D-2-4-3			W14X283	D-3-4-3			W14X398
D-1-5-1	1.98	W30X108	W14X233	D-2-5-1	1.98	W33X141	W14X342	D-3-5-1	1.98	W36X170	W14X426
D-1-5-2			W14X257	D-2-5-2			W14X398	D-3-5-2			W14X455
D-1-5-3			W14X283	D-2-5-3			W14X426	D-3-5-3			W14X500
D-1-6-1	2.38	W18X211	W14X257	D-2-6-1	2.38	W36X210	W14X550	D-3-6-1	2.38	W36X194	W14X500
D-1-6-2			W14X283	D-2-6-2			W14X605	D-3-6-2			W14X550
D-1-6-3			W14X311	D-2-6-3			W14X665	D-3-6-3			W14X605

L=4000mm, h=4000mm				L=5500 mm, h=4000mm				L=6500 mm, h=4000mm			
Name	tw	Beam	Column	Name	tw	Beam	Column	Name	tw	Beam	Column
D-1-7-1	3.17	W12X252	W14X311	D-2-7-1	3.17	W24X306	W14X605	D-3-7-1	3.17	W36X256	W14X605
D-1-7-2			W14X342	D-2-7-2			W14X665	D-3-7-2			W14X665
D-1-7-3			W14X398	D-2-7-3			W14X730	D-3-7-3			W14X730
D-1-8-1	3.57	W12X279	W14X342	D-2-8-1	3.57	W24X335	W14X665	D-3-8-1	3.57	W40X278	W14X730
D-1-8-2			W14X398	D-2-8-2			W14X730	D-3-8-2			W14X808
D-1-8-3			W14X426	D-2-8-3			W14X808	D-3-8-3			W14X873
D-1-9-1	4.36	W14X665	W14X730	D-2-9-1	4.36	W14X550	W14X730	D-3-9-1	4.36	W40X327	W14X730
D-1-9-2			W14X808	D-2-9-2			W14X808	D-3-9-2			W14X808
D-1-9-3			W14X873	D-2-9-3			W14X873	D-3-9-3			W14X873

CHAPTER V

PARAMETRIC STUDY OF SPSW AND RESULTS

5.1. Details of SPSW Design

As a material, for the web plate ASTM A36 steel with F_{yp} equal to 250 MPa is used. Besides, for the beams and columns ASTM A992 with F_y and F_u equal to 345 MPa and 450 MPa are used respectively with modulus of elasticity of 200 GPa. Additionally, based on the material used, R_{yp} and R_y values are taken from AISC341-16 and considered to be 1.3 and 1.1 for web plate and beams, columns respectively. 0.5% and 1% strain hardening ratio are considered for the web plate, beam and columns respectively. Moment resistant connections are used for all HBE-to-VBE connections. The column bases are assumed to be fixed connection while the bottom beam is not anchored to the foundation.

Later on, nonlinear pushover analyses are conducted in OpenSEES, and each model is pushed monotonically from left to right up to a drift ratio of 5.0% to ensure the full yielding of the web plate in a deformation-controlled manner. In this study gravity loading is ignored. The aim of this parametric study is to observe the effect of boundary frame stiffness on the development and variation of tension field stresses in the web plate.

5.2. Analysis Results of SPSWs

5.2.1. Implemented Plastic Section Modulus Limit

As it is stated in section 4.2.2, for preventing the excessive accumulation of the plastic deformation on the HBE, $Z_{database}$ which is the section properties of shapes taken from AISC Steel Construction Manual (AISC, 2015), should be either equal or greater

than the $Z_{AISC341}$ calculated with equation 4.2. In all of eighty-one designed boundary elements for SPSWs with wide flange sections, higher value for plastic section modulus is chosen. In figures 5.1, 5.2 and 5.3 normalized $Z_{AISC341}$ with respect to $Z_{database}$ and aspect ratios of 1, 1.5 and 2 are illustrated respectively.

As it can be seen in figures 5.1, 5.2 and 5.3, it is realized that in this case of study, designed one-story SPSWs with the bottom beam not connected to the ground, $Z_{AISC341}$ values suggested by AISC341-16 only control the design of the beams in D-1-1, D-1-2, D-1-3 and D-1-4. For the rest of SPSW designs with the considered plate thicknesses and aspect ratios, $Z_{database}$ of the beam sections have greater plastic section modulus values. From here it can be concluded that in the SPSWs similar to this case of study, $Z_{database}$ for SPSWs with aspect ratio of 1 and plate thickness more than 1.3mm and also in SPSWs with aspect ratio of 1.5 and 2, are reasonable.
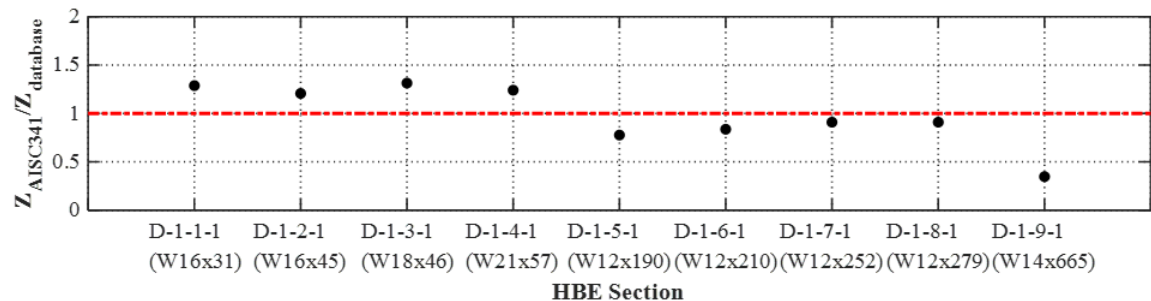
Figure 5.1. Normalized plastic section modulus in SPSWs with aspect ratio of 1
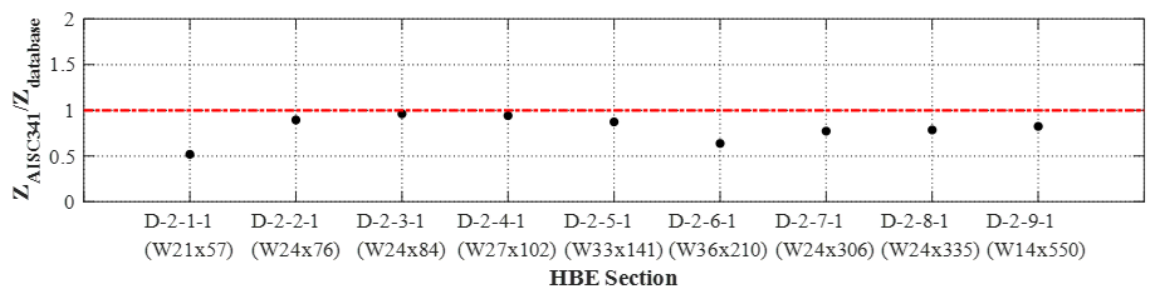
Figure 5.2. Normalized plastic section modulus in SPSWs with aspect ratio of 1.5
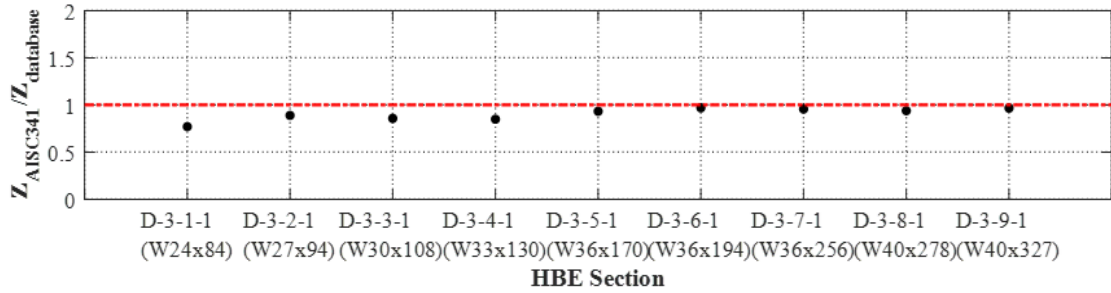
Figure 5.3. Normalized plastic section modulus in SPSWs with aspect ratio of 2

5.2.2. Stiffness Limit Implementation for Boundary Frame

All of the designed beams and columns are satisfied the stiffness requirements given in equations 1.3 and 1.4. In figure 5.4, Normalized stiffness of the HBE is ratio of the required stiffness of the HBE (equation 1.4) to the moment of inertia of the chosen section. Similarly, in figure 5.5, Normalized stiffness of the VBE is the ratio of the required stiffness of the VBE (equation 1.3) to the moment of inertia of the chosen section.

It can be seen in figure 5.4 that SPSWs with aspect ratio of 1, shear forces in the beams become critical as the web plate is getting thicker. For instance, for the web plates with 2mm plate thickness and more, shear force dominates in the beam mostly while PM interaction is more critical in the columns in all of the designs (figure 5.5). Due to the high shear force in the HBE with thick plates, stiffer columns are required with high weight which results in increase in the weight of the building.

It is worth to mention that, once the aspect ratio is more than 2 such as 2.5, for this case of study, it is unattainable to design boundary elements for thick web plate (more than $\cong$ 3mm) with the available W-shaped sections in AISC Shape Database (v15.0) (Manual, 2005) since they do not satisfy the stiffness requirements for beams and columns.

In addition, for aspect ratios lower than 2, with the considered plates with different thickness in this study, beams and columns mostly satisfies the stiffness limits due to the fact that the chosen W-shaped sections already have the moment of inertia higher than the estimated value by equations 1.3 and 1.4. Moreover, as it can be seen in figure 5.5 stiffness requirement for the columns in this case of study with single story and one-bay SPSW is not necessary since PM ratio is more critical in the system.
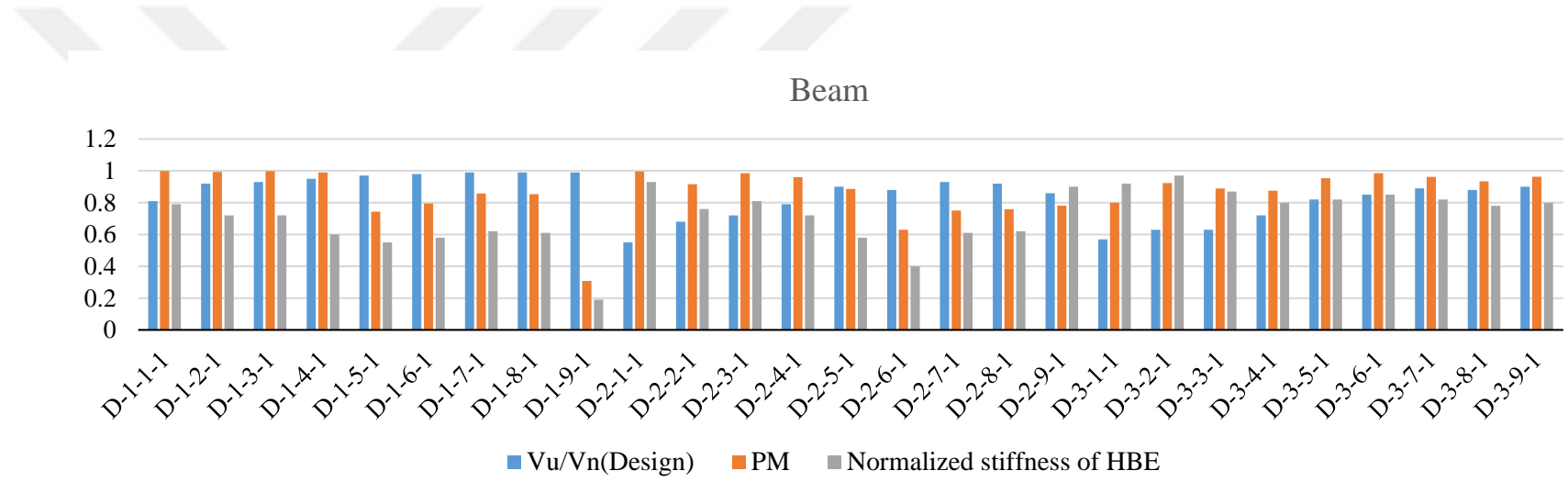
Figure 5.4. Comparison of the design forces and HBE stiffness ratio in beams
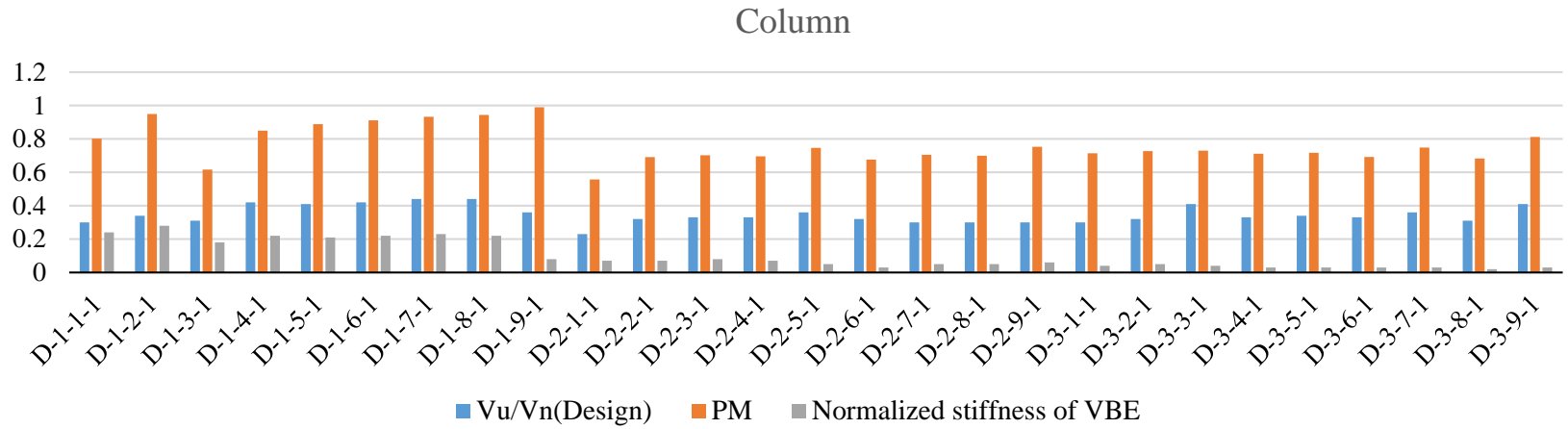
Figure 5.5. Comparison of the design forces and VBE stiffness ratio in columns

5.3. SPSW Pushover Analysis Results

5.3.1. Adequacy of Calculated Shear Forces in Columns and Beams According to Sabelli and Bruneau (2007)

From the calculation of the total forces in the VBE and HBE according to the capacity design procedure undertaken in chapter 4, it is concluded that the suggested procedure was underestimated the ultimate shear force in the VBEs based on the values derived from nonlinear pushover analysis of SPSWs performed in OpenSEES.

In figure 5.6, normalized shear force for beams and columns are illustrated. It should be mention that required shear strength derived from pushover analysis in OpenSEES normalized with required shear strength from design. As it can be seen in figure 5.6, It is concluded that for this case of study, Design Guide underestimates the required shear forces in the VBEs since the required shear forces from pushover analysis are approximately doubles the estimated value per Sabelli and Bruneau (2007). In other words, the closed-form equations provided in the Design Guide, significantly underestimates the shear force demands in VBEs. Since in most of the VBEs shear strength does not dominated, underestimation is not critical, but it should not be ignored. On the other hand, predicted shear forces in the HBEs are much accurate. For instance, in the designs with aspect ratio of 1, estimated shear forces in the HBE are approximately between 0% to 20% more than the shear forces from pushover analysis. Additionally, in designs with aspect ratio equal to 1.5 and 2, required shear strengths estimated in capacity design are between 0% to 10% less than the required shear forces from pushover analysis. It should be mention that, underestimation of the required shear forces in capacity design of the HBE might be critical because, require shear forces from structural analysis could be more than 1. In the mentioned critical cases, design of beams should be repeated, and

stiffer section should be assigned. This results stems from the fact that the closed-form equations do not consider the depth of the boundary frame elements; however, the horizontal component of the web plate stress acting along the boundary frame elements due to the offset from the centerline of the boundary frame elements. As the aspect ratio increases, deeper beams are needed; consequently, these secondary forces become prominent. It is recommended the boundary frame depth be considered in design, especially for high aspect ratio SPSWs.
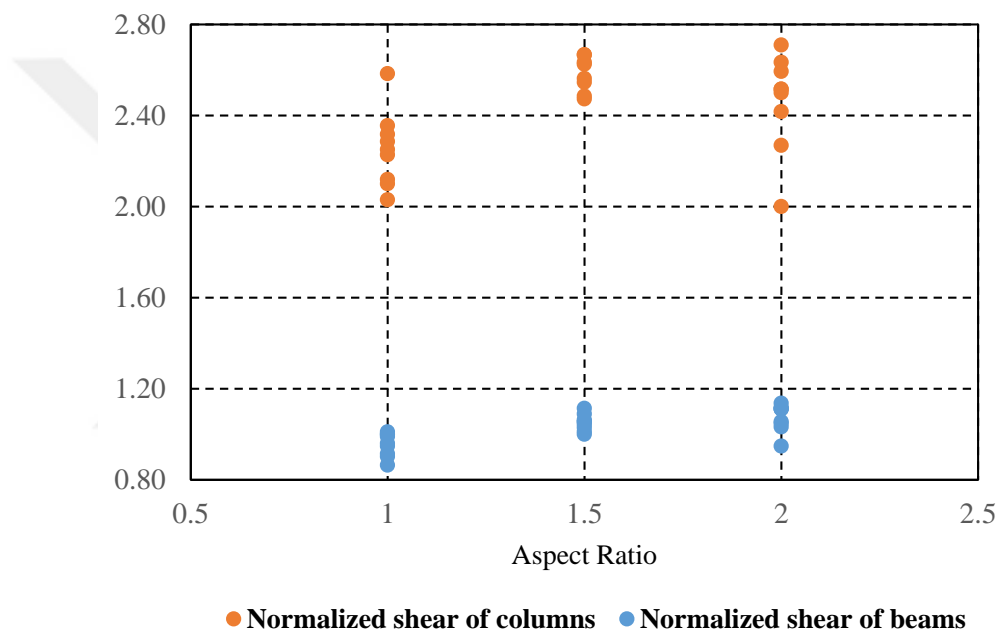
Figure 5.6. Normalized shear forces in columns and beams

5.3.2. Effect of Boundary Frame Flexibility on Stress Distribution in the Web Plate

Subsequent to nonlinear pushover analysis of 81 SPSWs, normalized base shear versus drift of SPSWs with plate thicknesses of $t_w = 0.55$ and $t_w = 4.36$ and aspect ratios of 1, 1.5 and 2 are illustrated in figure 5.7. In these figures base shear at the columns end normalized with respect to the design shear strength of the web plates. For instance, as

shown in figure 5.7, for one set of design such as D-1-1-1, D-1-1-2 and D-1-1-3, with aspect ratio of 1 and 0.55 mm plate thickness, normalized capacity curve of SPSWs are demonstrated in one figure. As it is mentioned before all of the SPSWs in one set are designed with constant beam section and increasing column section such that the third designs option in all sets have the stiffest column section among two others.

The observation can be done from the normalized base shear for all designs presented in figure 5.7 and figures A.1, A.2 and A.3 in appendix A. From figure 5.7 and figures A.1, A.2 and A.3, it is concluded that in all of the design sets stiffest columns have higher lateral stiffness in the elastic range. It should be mention that, for the drift ratio over 1%, column stiffness affect the lateral stiffness and lateral strength as expected while the web plate yield and plastic hinges formed at the both end of the top beam and at the base of the left and right columns. In post-yield region boundary frame provides full tension yielding in the web plate.

Additionally, in designing D-1-2-2, due to the compactness requirement of W-shaped sections for highly ductile members, W14x132 replaced with the W14x99 in columns and approximately, 25% increment in stiffness is observed by referring to the figure A.1.
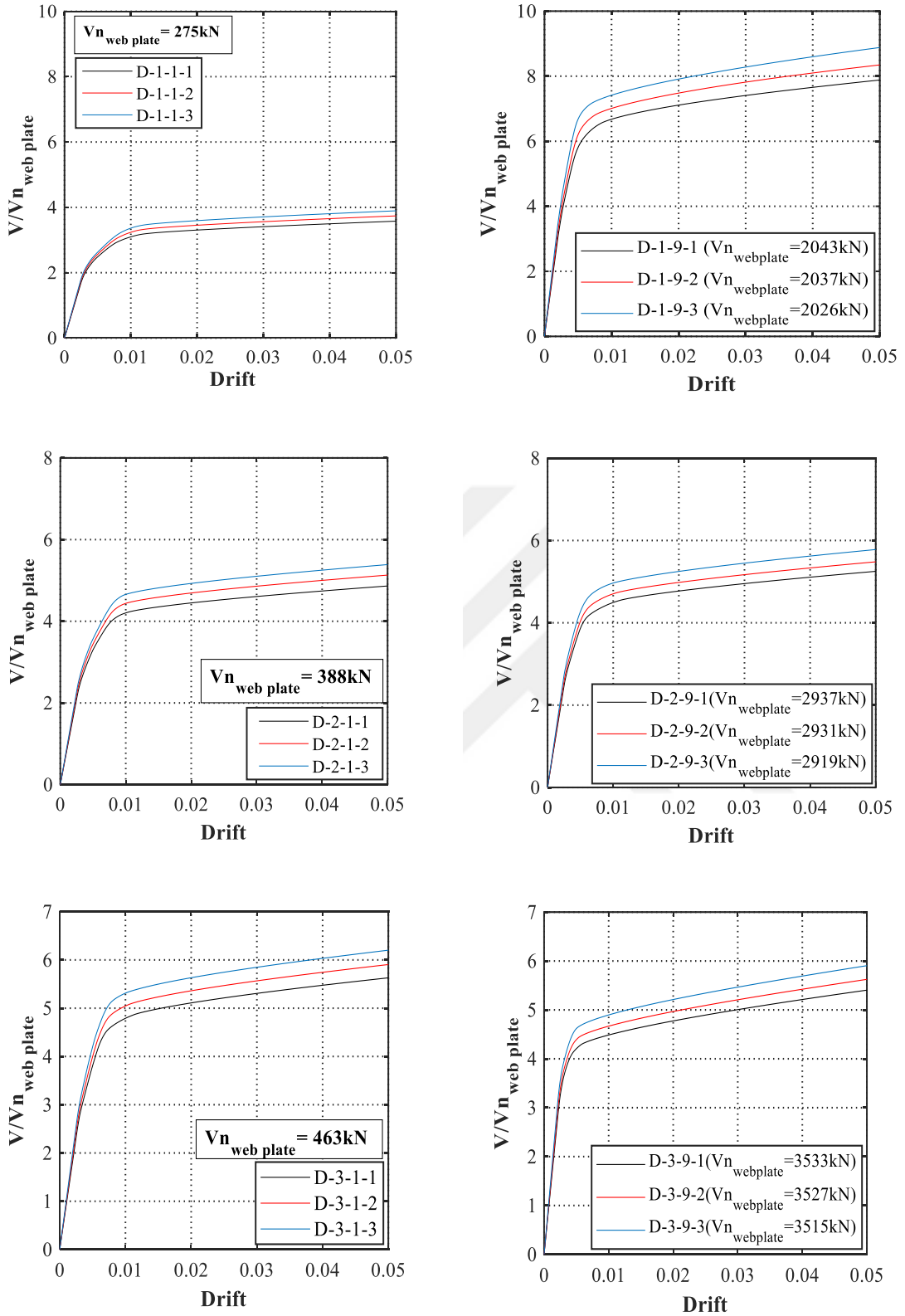
Figure 5.7. Normalized base shear versus drift of proposed design with t_w=0.55

and t_w=4.36

Figure 5.8 shows the distribution of the web plate stress acting on the boundary frame along the beams and columns at drift ratio of 0.2% with plate thickness of 0.55 and 4.36 and aspect ratio of 1. Also, figure 5.9 shows the σavg of the 50 strips connected to the boundary frame elements at 0.2% drift. As seen in the figure 5.9, at 0.2% drift, with considering stress in all 50 strips, σ_{avg} of the strips connected to the bottom beam and right column are approximately equal to 150 MPa and 200 MPa for 0.55 mm plate thickness and 4.36 mm plate thickness respectively. This mentioned values for the web plate stresses are lower than the σ_{avg} of the strips connected to the top beam which are between 190-197 MPa and 269-278 MPa and σ_{avg} of strips connected to the left column which are between 183-191 MPa and 269-278 MPa for the 0.55mm and 4.36 mm plate thickness respectively. From these values for all plate thickness, it can be concluded that in frames with aspect ratio of 1, anchorage of the web plate provided by the top beam and left column is higher than the bottom beam and specially the right column regardless of the high flexural stiffness of the columns.

Figure 5.8. Web plate stress distribution along the boundary frame at 0.2% drift with

L/H=1

Figure 5.9. σ_{avg} of the strips connected to the surrounding boundary frame elements for all designs at 0.2% drift with L/H=1

Figures 5.10, 5.11 show the σ_{max} and σ_{min} both normalized with the expected yield stress of the web plate for the designs with aspect ratio of 1. As it can be seen in figures 5.9, 5.10 and 5.11, with the increasing column stiffness, σ_{avg} in the strips increase which imply that increasing column stiffness provides better restraining to the web plate with reduction in the deflection. Also, at this drift, σ_{min} and σ_{max} of the web plate are affected slightly by the increasing stiffness in the column section.
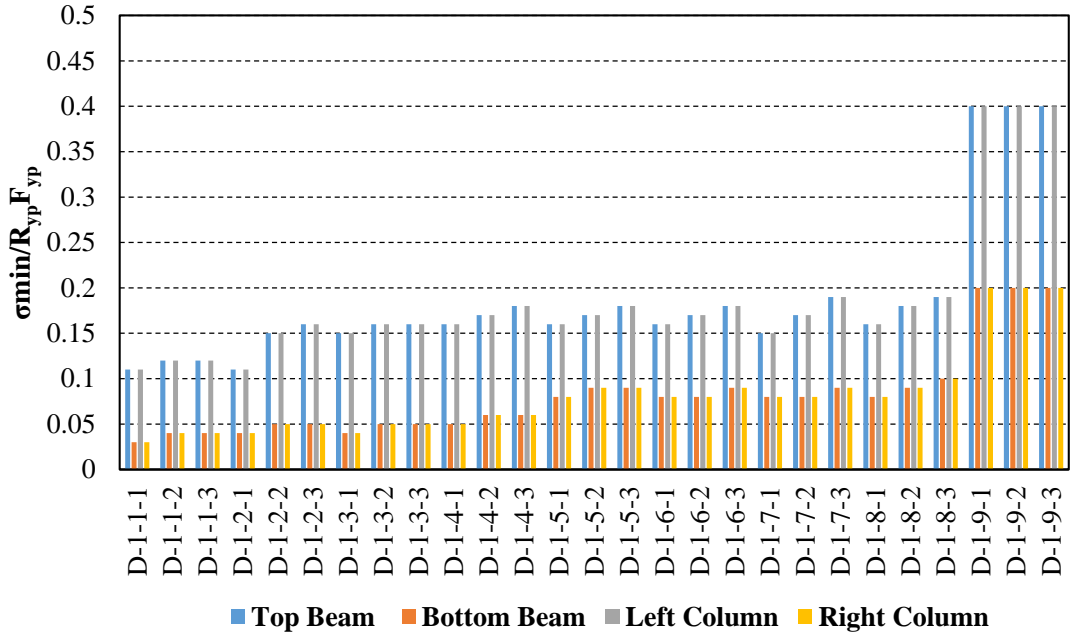
Figure 5.10. Normalized σ_{min} of the web plate in SPSWs with L/H=1 at 0.2% drift
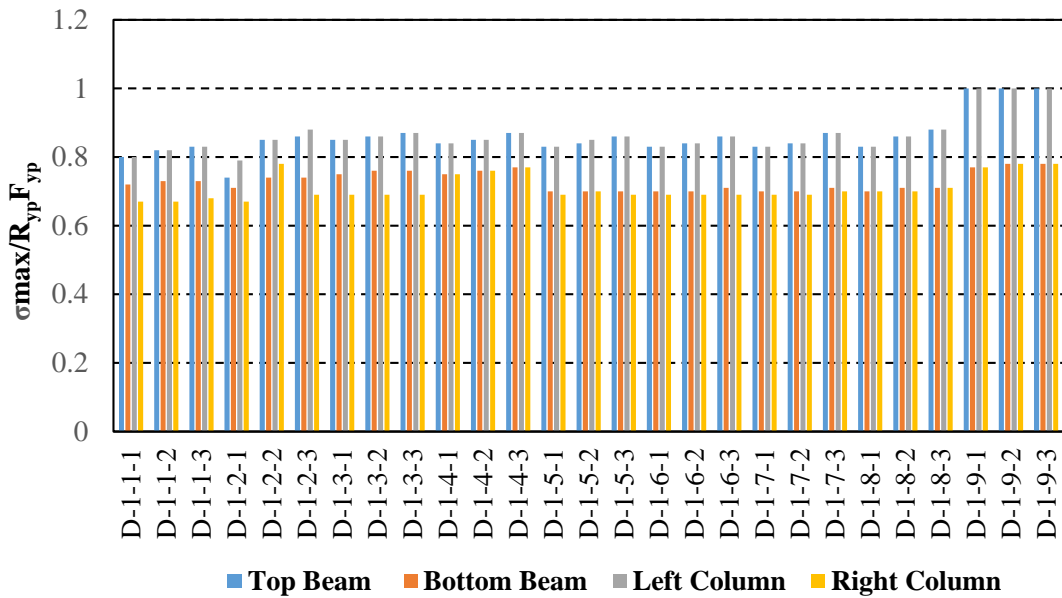
Figure 5.11. Normalized σ_{max} of the web plate in SPSWs with L/H=1 at 0.2% drift

From $\sigma_{max}/R_{yp}F_{yp}$ in the figure 5.11, it can be assumed that the maximum stress in the web plate provide by strips which is connected to the top beam in one end and the left column in the other end and σ_{max} and σ_{min} in these strips affected more by increasing stiffness of the columns. Additionally, figure 5.8 is the approval to the observation that

the maximum stress is occur adjacent to the right end of the top beam and bottom end of the left column, respectively. In other words, strips which are closer to the top left and right bottom beam to column connection carry less tensile stress. Figure 5.12 schematically depicted the strips with maximum stress in SPSWs with aspect ratio of 1.
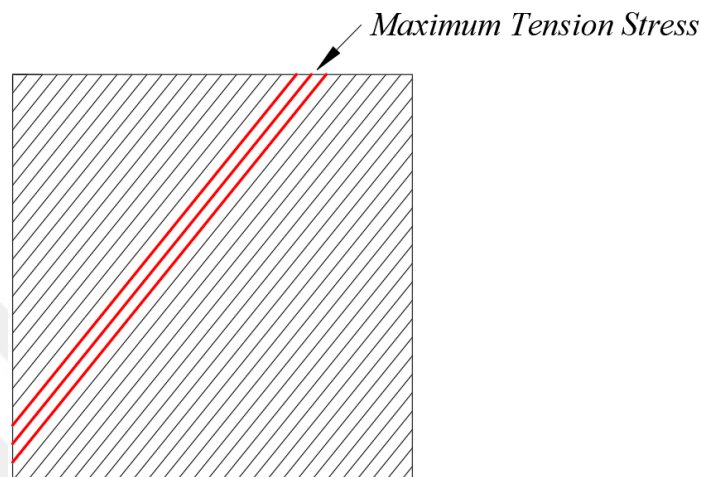
Figure 5.12. Schematic location of maximum stress in the strips in SPSWs with L/H=1

Figure 5.13 shows the stress distribution of the web plate along the boundary frame and figure 5.14 shows the average stresses in the strips, it can be understood that, at 2% drift, the entire web plate yield in tension and increasing column stiffness does not have any effect on the distribution of the web plate stress as long as the boundary frame capacity designed. In SPSWs with aspect ratio of 1, at both left and right columns bases and at both ends of the top beam plastic hinges formed while bottom beam remains essentially elastic in all of the designs.

Figure 5.13. Web plate stress distribution along the boundary frame at 2% drift with

L/H=1

Figure 5.14. σ_{avg} of the strips connected to the surronding boundary frame elements for all designs at 2% drift with L/H=1

In figure 5.15 distribution of the web plate stress acting along the beams and columns at drifts of 0.2% with chosen 0.55 mm and 4.36 mm plate thicknesses and aspect ratio of 1.5 is depicted. Figures 5.17 shows the σ_{avg} of the 50 strips connected to the surrounding beams and columns of all designs at 0.2% drift with aspect ratios of 1.5.

From figures 5.15 and 5.16, at 0.2% drift, it can be seen that the σ_{avg} of the strips connected to top beam and bottom beam with 0.55 mm plate thickness and aspect ratio of 1.5 are between 198-203 MPa and 180 MPa respectively. Similarly, web plate with 4.36 mm plate thickness has the σ_{avg} values between 212-219 MPa and 190 MPa for the strips connected to top and bottom beam respectively. On the other hand, σ_{avg} values are for strips connected to the left column and right column with aspect ratio of 1.5 are between 174-179 MPa and 143-141 MPa for 0.55mm plate thickness and between 196-204 MPa and 163 MPa for 4.36 mm plate thickness. From the results it can be concluded that in SPSWs with aspect ratio of 1.5, and thin web plate anchorage provided by the top

beam and bottom beam is more than the left and right column. As the web plate get thicker anchorage provided by the left column and top beam is increasing.
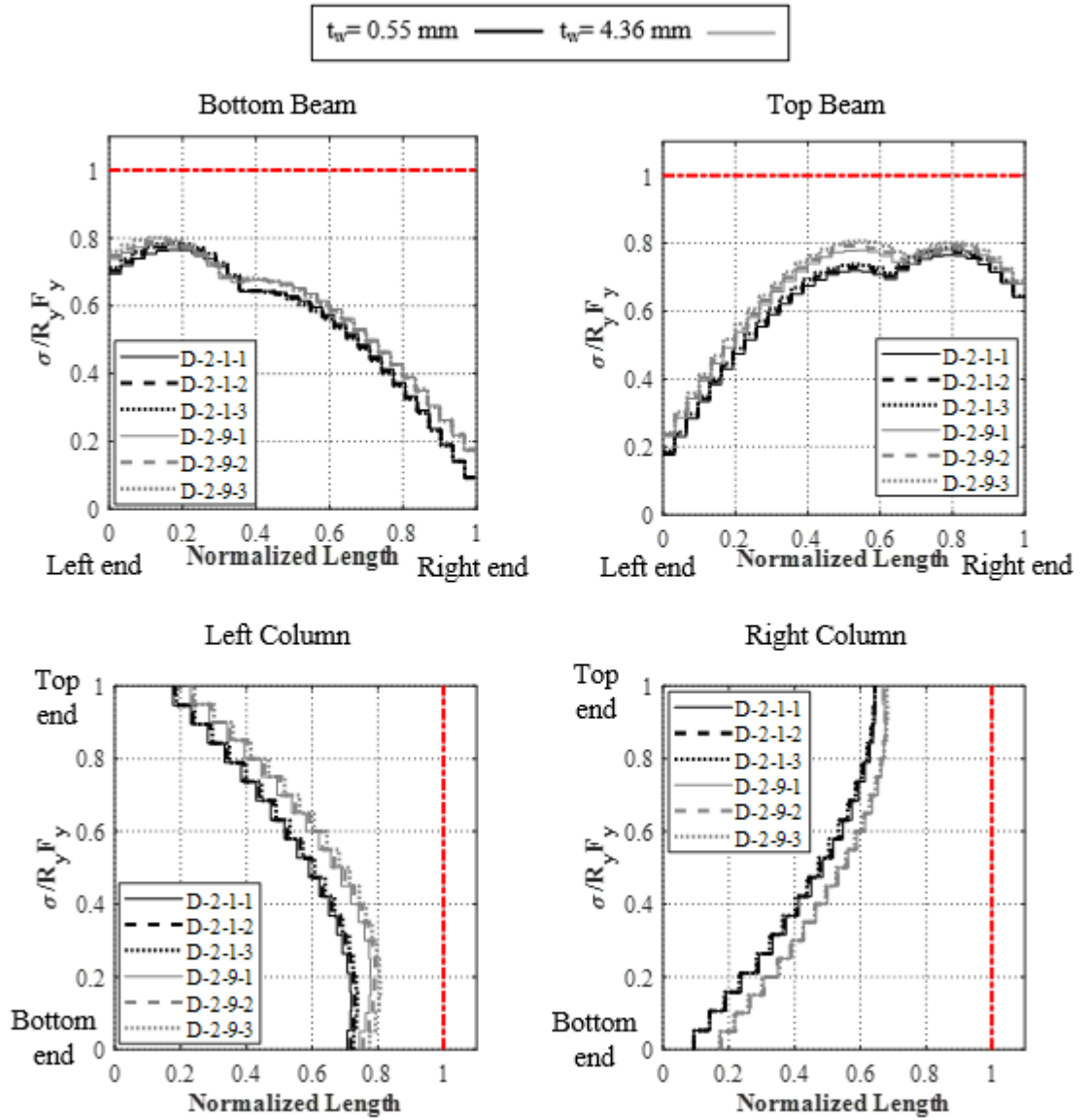
Figure 5.15. Web plate stress distribution along the boundary frame at 0.2% drift with
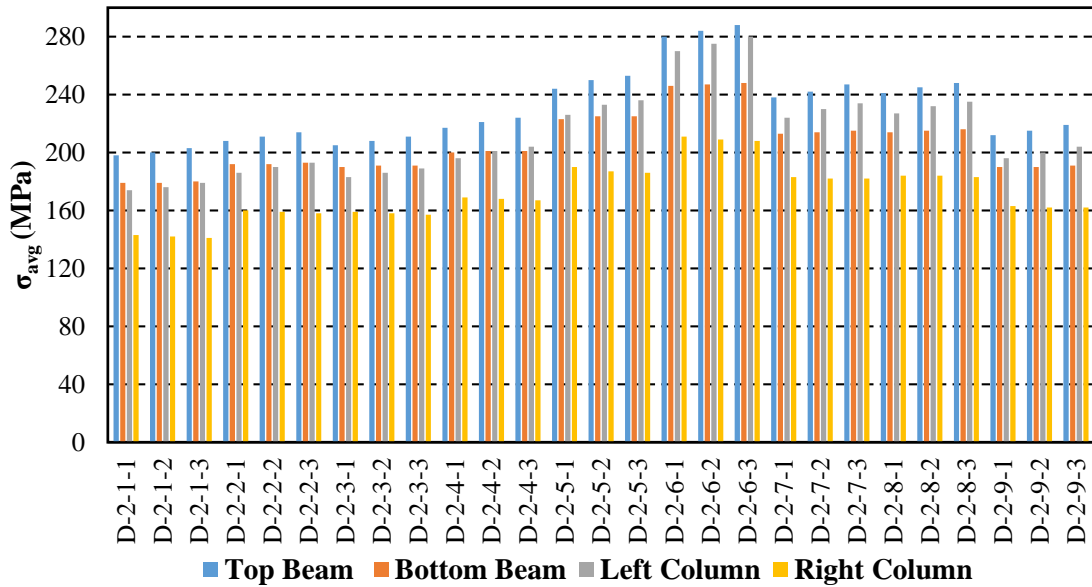
L/H=1.5

Figure 5.16. σavg of the strips connected to the surrounding boundary frame elements

for all designs at 0.2% drift with L/H=1.5

Likewise, in figure 5.17 distribution of the web plate stress acting along the beams

and columns at drifts of 0.2% with chosen 0.55 mm and 4.36 mm plate thicknesses and

aspect ratio of 2 is depicted. Figures 5.18 shows the σavg of the 50 strips connected to

the surrounding beams and columns of all designs at 0.2% drift with aspect ratios of 2. It

could be observed in figures 5.17 and 5.18 that, at 0.2% drift, the σavg of the strips

connected to top beam and bottom beam are between 199-204 MPa and 193-195 MPa for

0.55mm plate thickness and aspect ratio of 2. In sequence, σavg values are between 255-

263 MPa and 245-248 MPa for the 4.36 mm plate thickness with aspect ratio of 2 for the

strips connected to top and bottom beam, respectively. In this aspect ratio, σavg of the

strips connected to the left and right columns are between 170-175 MPa and 160-156

MPa for 0.55 mm plate thickness and between 230-236 MPa and 208-204 MPa for 4.36
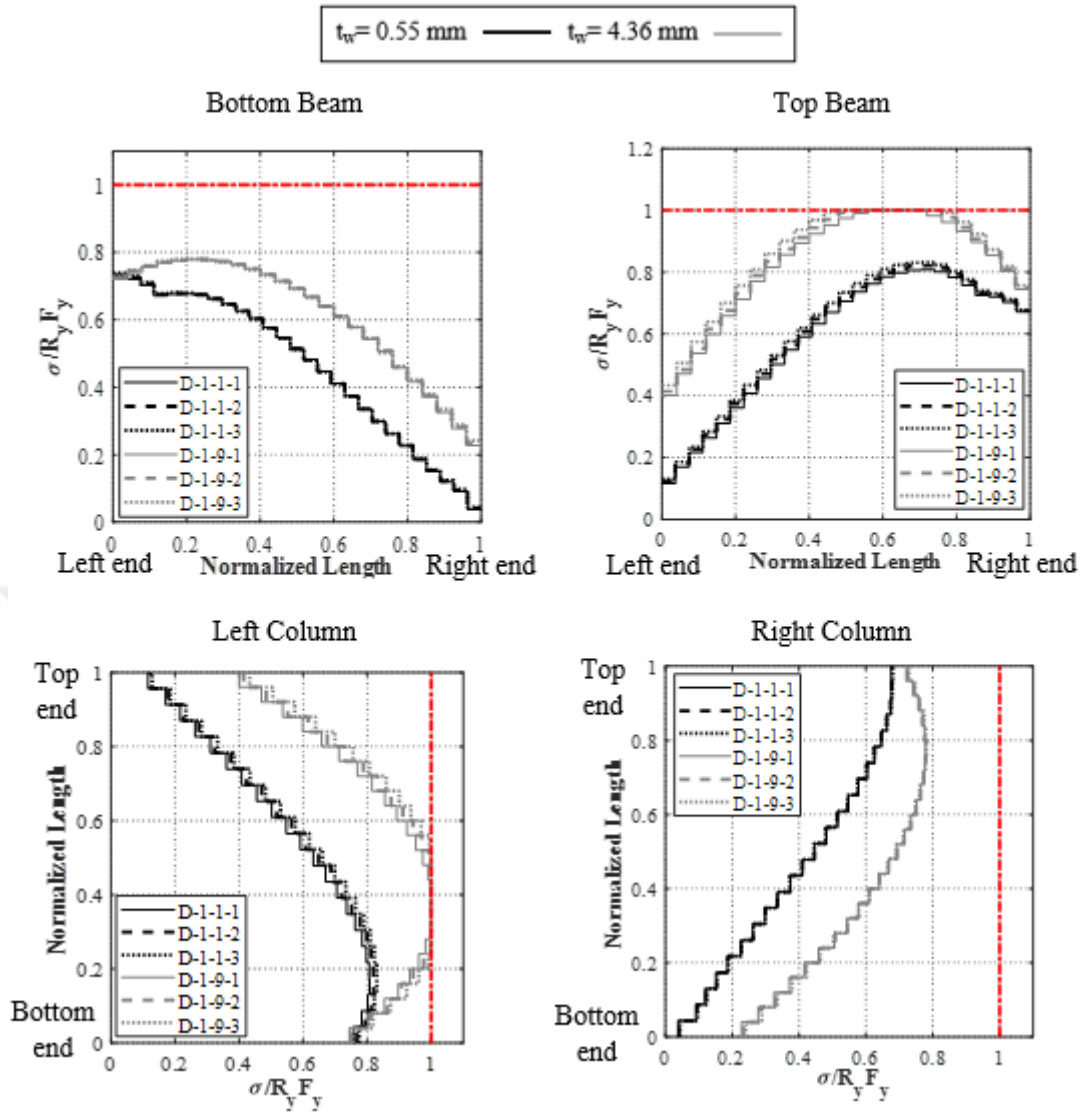
mm plate thickness respectively.
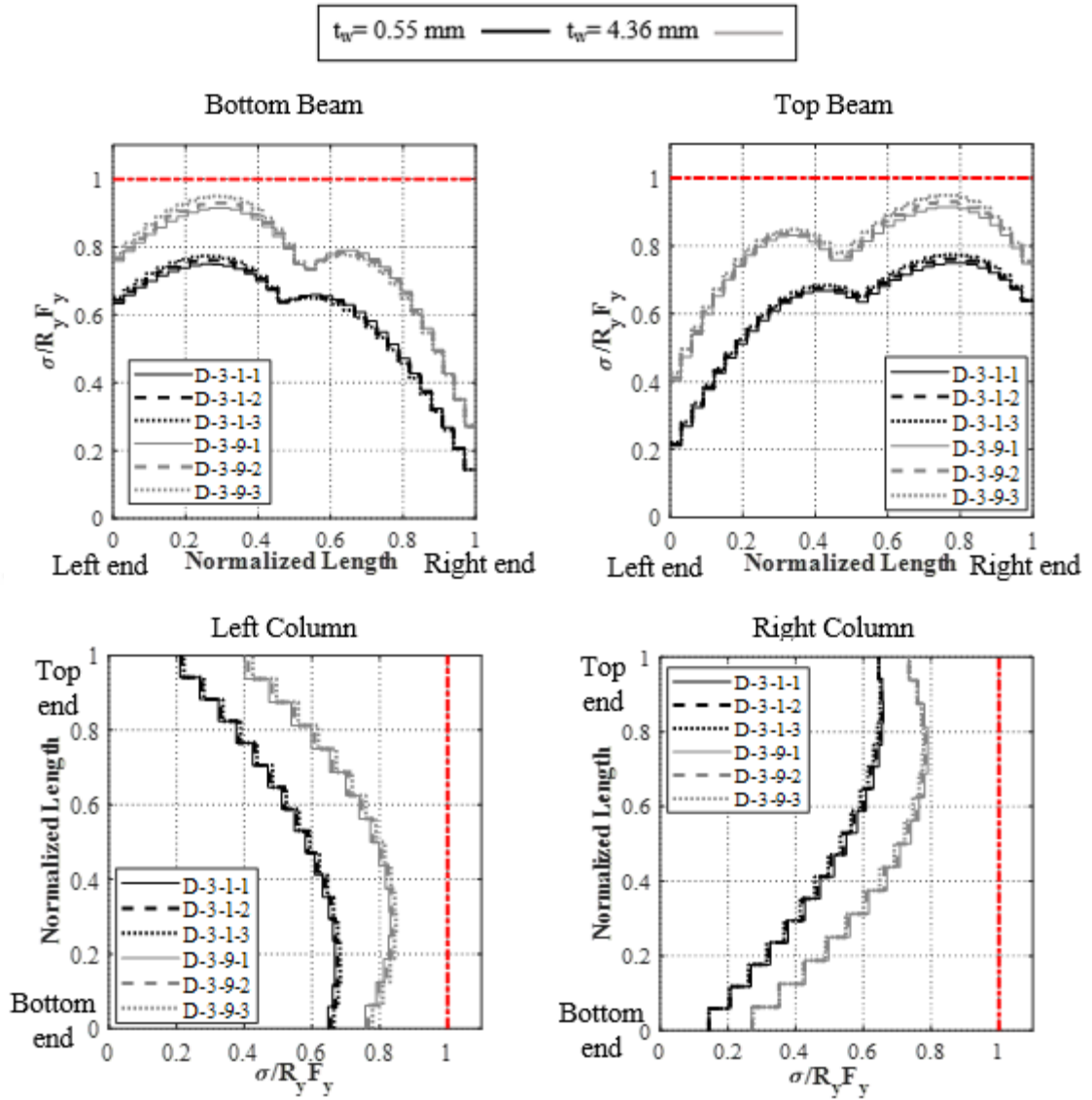
Figure 5.17. Web plate stress distribution along the boundary frame at 0.2% drift with
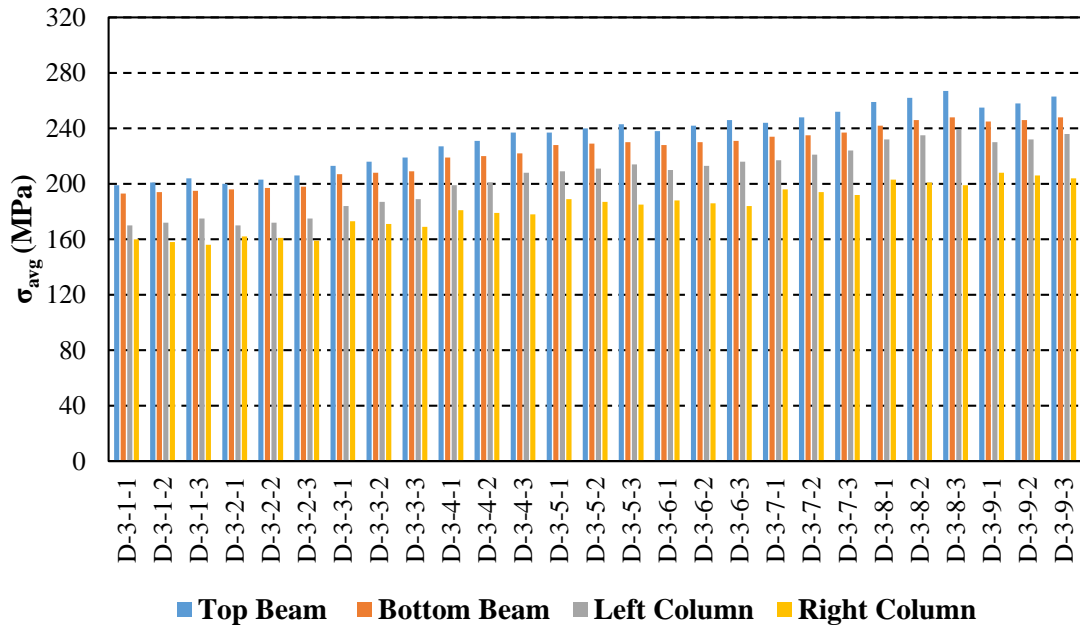
L/H=2

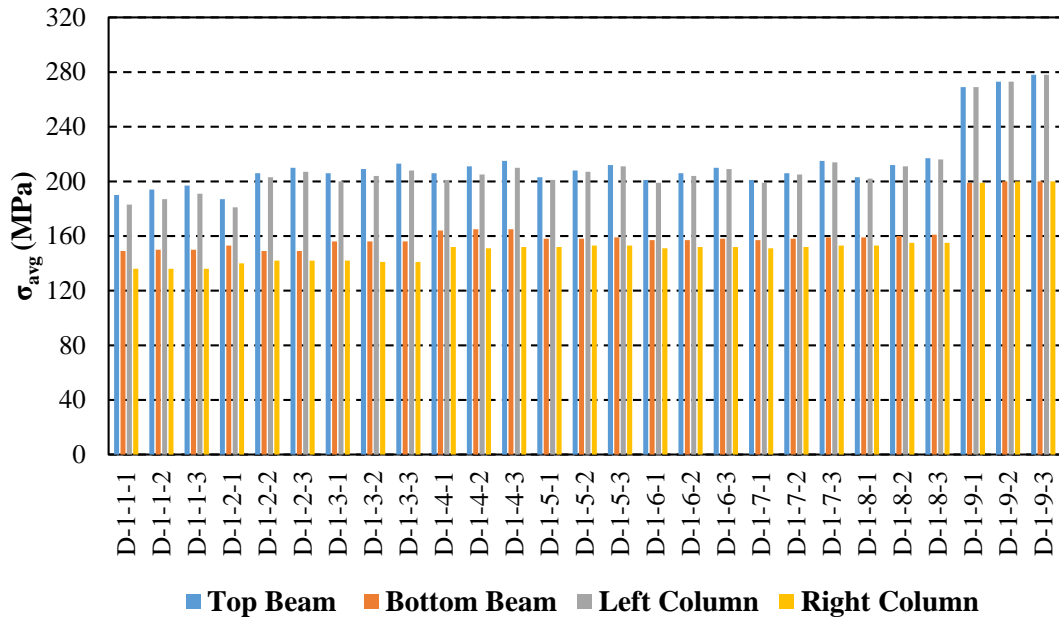**Figure 5.18.** σ_{avg} of the strips connected to the surrounding boundary frame elements for all designs at 0.2% drift with L/H=2

From the average stresses of web plates of the SPSWs with aspect ratio of 2 (figure 5.18), it can be concluded that in SPSWs with higher aspect ratios, top and bottom beam provide better anchorage for the web plate even though in capacity designing of the SPSWs, columns with high flexural stiffness are assigned. However, in aspect ratios equal to 1.5 and 2 with the increasing column stiffness, σ_{avg} of the strips that are connected to top beams and bottom beams on both side and the strips connected to the top beams in one side and the left column on the other side increase. This means that increasing column stiffness provides better restraining by beams and left column of the SPSWs. On the other hand, in these aspect ratios, by increasing columns stiffness, average stress imposed by the strips to the right columns decreased. These phenomena refer to the fact that better restraining provides by the beams which leads the SPSW to the smaller deflection.

Additionally, figures 5.19 to 5.22 show normalized σmax and σmin with respect to the web plate yield strength at drifts of 0.2% and aspect ratios of 1.5 and 2 respectively.

Similar to the SPSWs with aspect ratio of 1, at 0.2 % drift, σmin and σmax of the beams and column with aspect ratio of 1.5 and 2 are not affected by the increasing column flexural stiffness considerably.
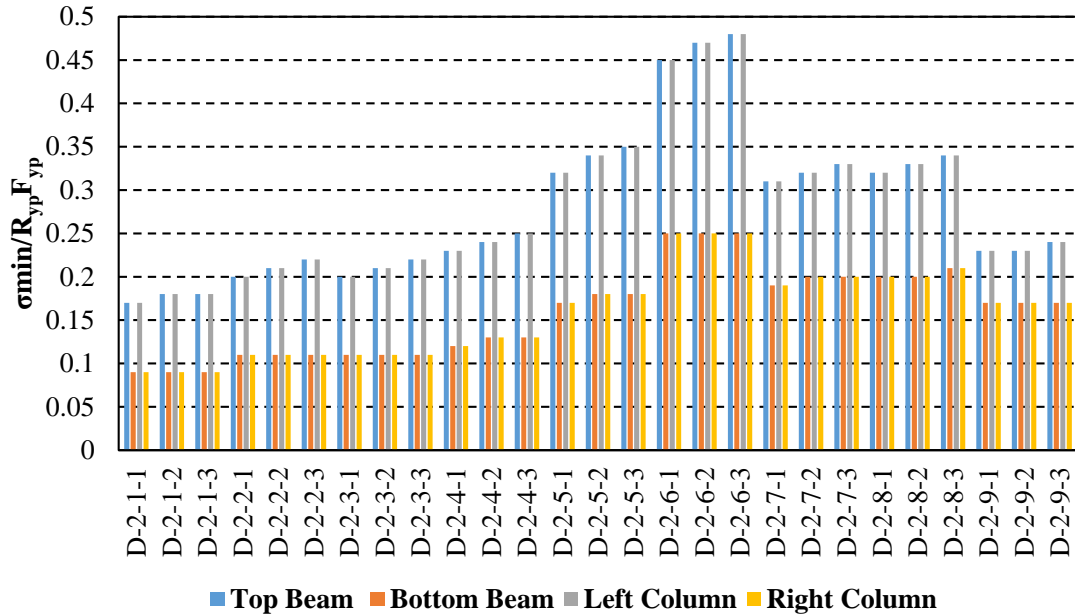
Figure 5.19. Normalized σmin of all 50 strips in SPSWs with L/H=1.5
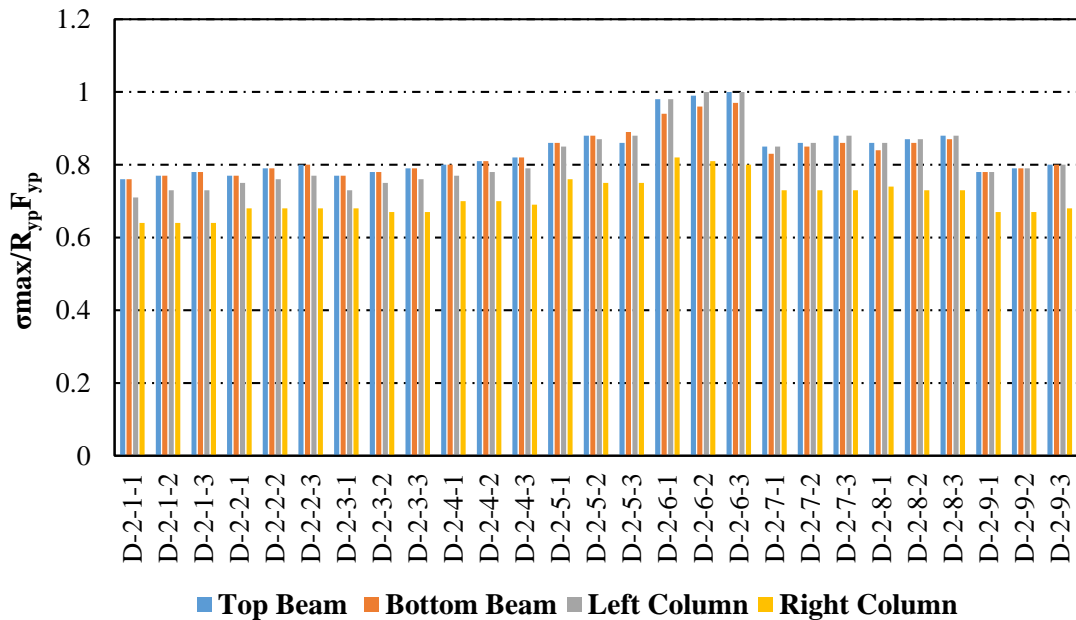
Figure 5.20. Normalized σmax of all 50 strips in SPSWs with L/H=1.5
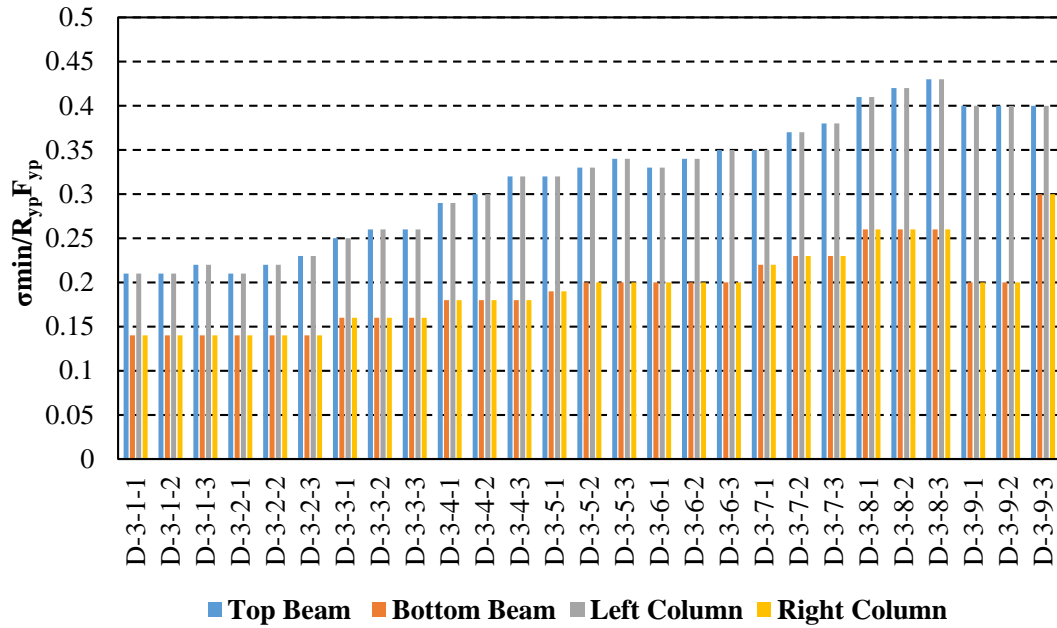
Figure 5.21. Normalized σ_{min} of all 50 strips in SPSWs with L/H=2
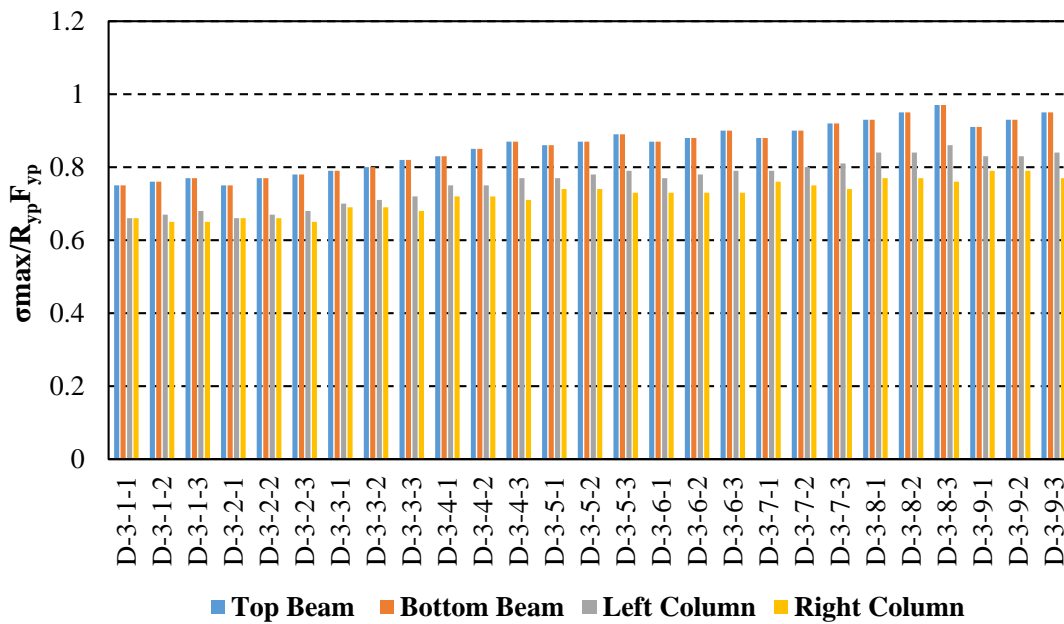
Figure 5.22. Normalized σ_{max} of all 50 strips in SPSWs with L/H=2

It can be noted that the maximum stress occurs closer to the right end of the beam and the left end of the beam in the top beam and the bottom beam (from figures 5.15 and 5.17) which implies to the fact that the strips connected to the top beam in one end and to the bottom beam on the other end resist higher tensile stresses and strips connected to the

65

columns in one end and to the beams on the other end resist lower tensile stresses. Figure 5.23 schematically depicted the strips with maximum stress in SPSWs with aspect ratio equal to 1.5 and 2.
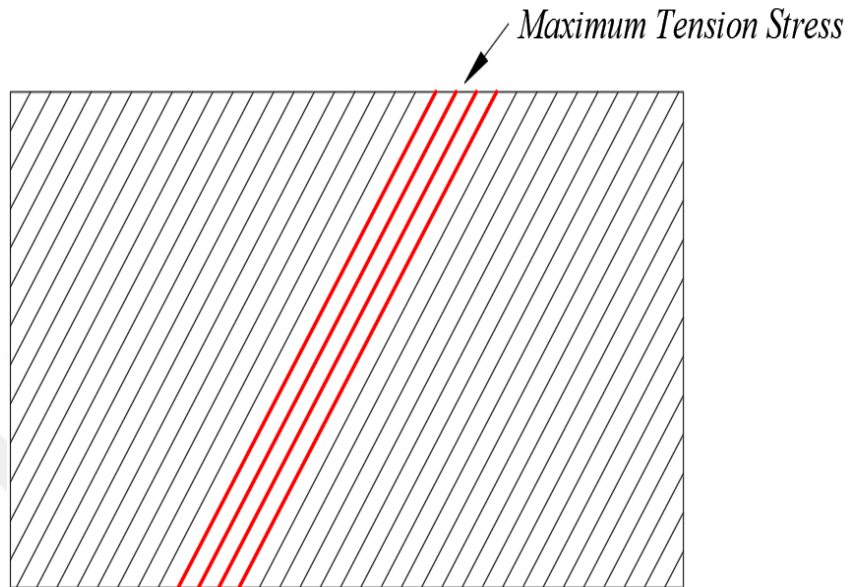
Figure 5.23. Schematic location of maximum stress in the strips in SPSWs with

L/H=1.5 and L/H=2

According to the web plate stress distribution in figures 5.24 and 5.25 and related σ_{avg} values in figures 5.26 and 5.27 it can be easily seen that in either SPSWs with aspect ratio of 1.5 and 2, all of the strips yield at 2% drift and column stiffness do not have any effect on the web plate stress distribution. It is worth to mention that, after yielding of the entire web plate bottom beam remain elastic while the hinges form at both bottom and top beams ends and left and right columns bases.

In advance, it should be stated that the rest of the σ_{avg} of strips, normalized σ_{min} and σ_{max} for all SPSWs are tabulated in appendix A.
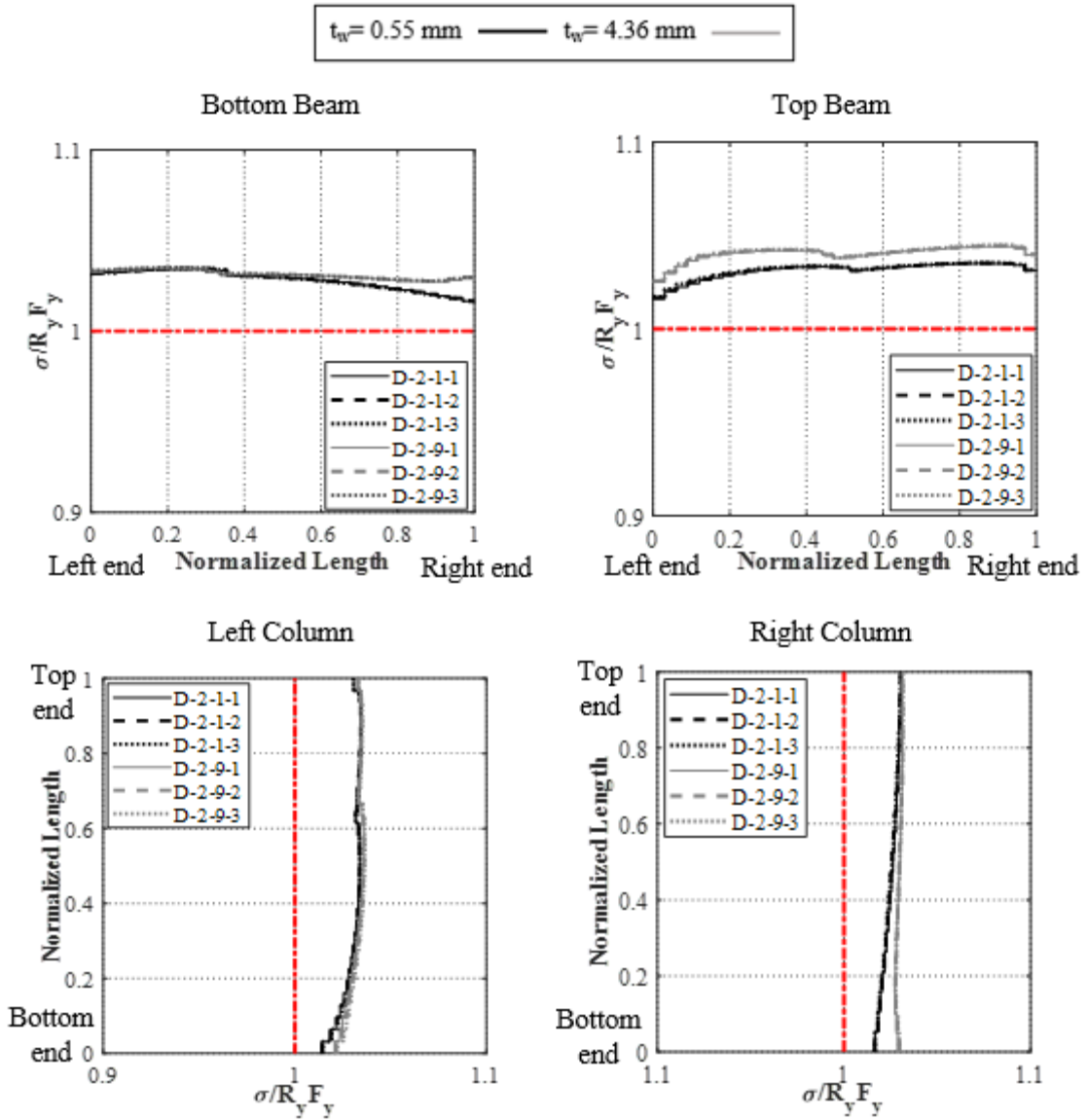
Figure 5.24. Web plate stress distribution along the boundary frame at 2% drift with
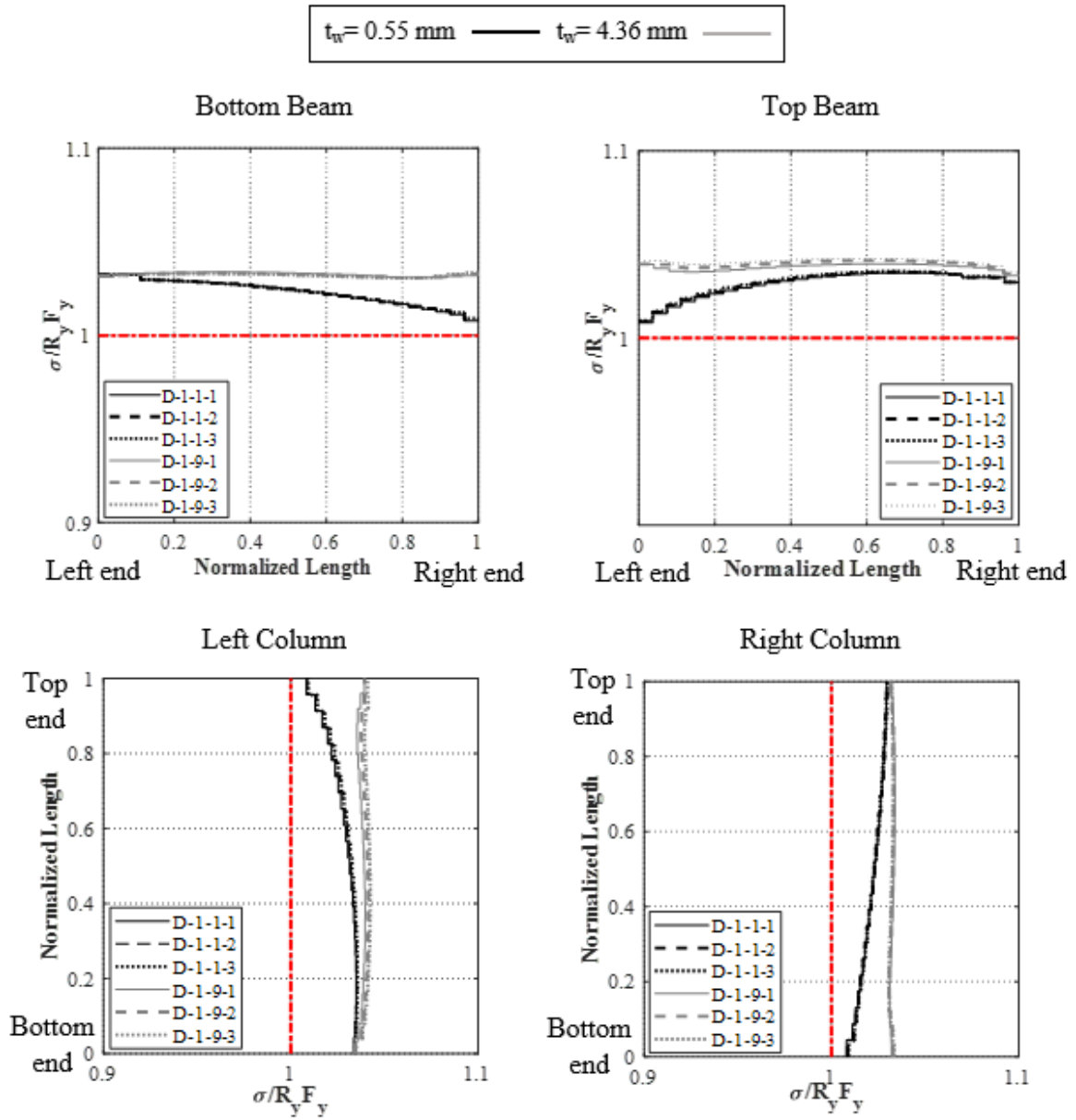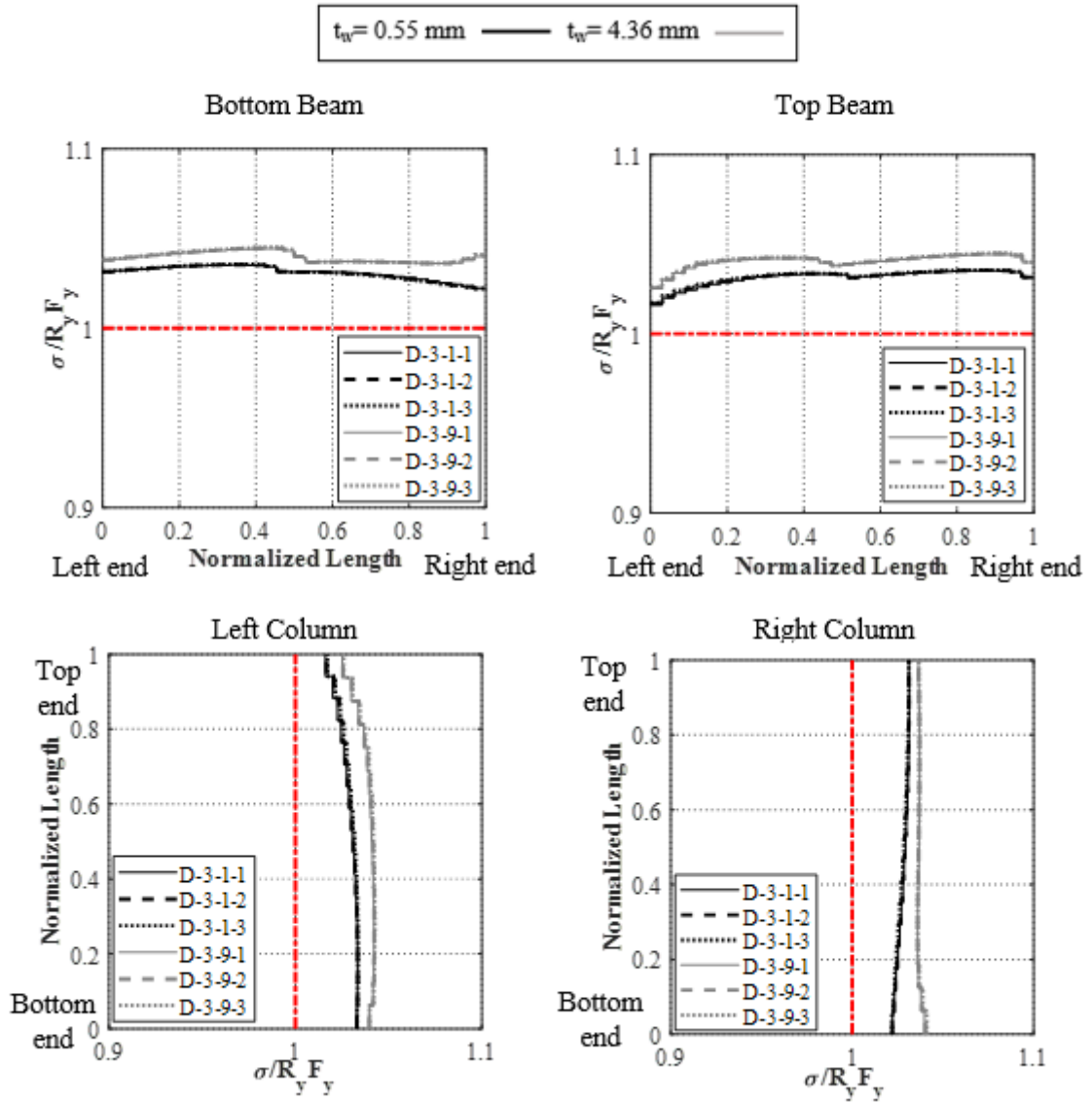
L/H=1.5

Figure 5.25. Web plate stress distribution along the boundary frame at 2% drift with
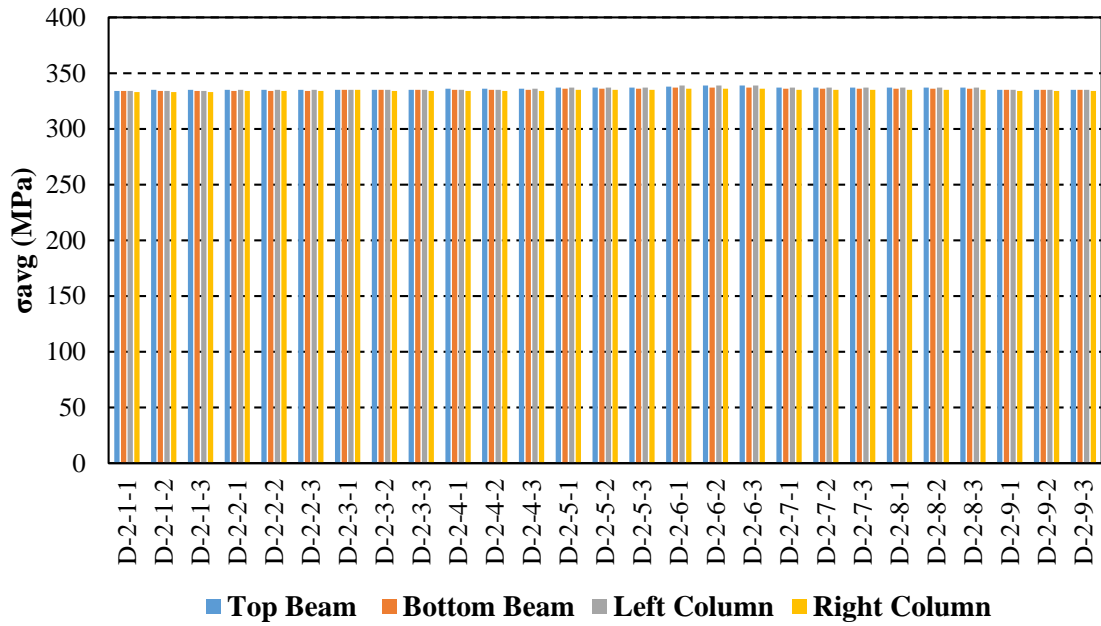
L/H=2

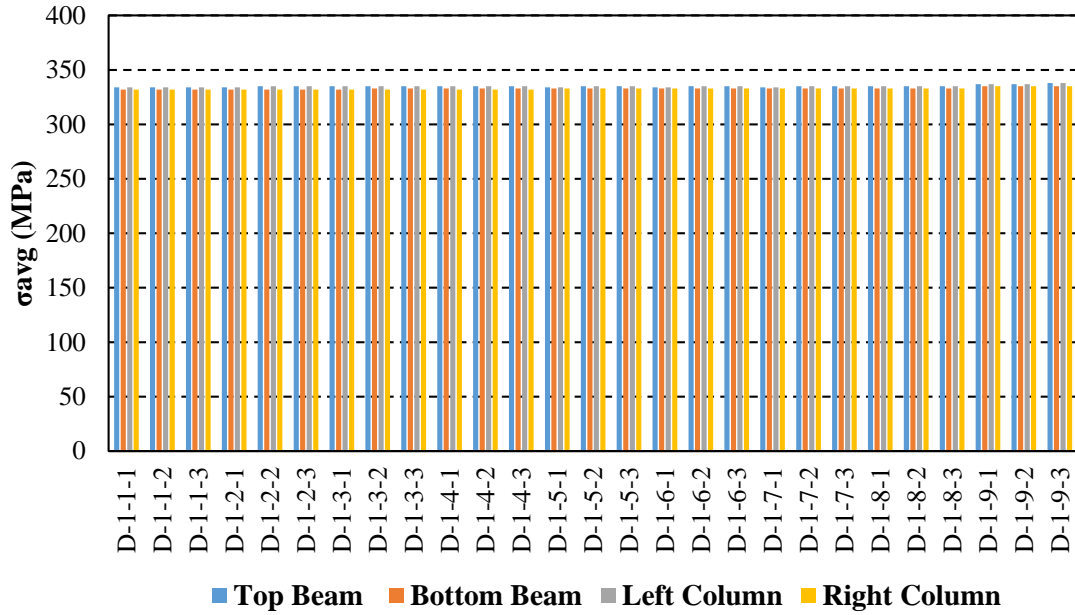**Figure 5.26.** σ_{avg} of the strips connected to the surrounding boundary frame elements for all designs at 2% drift with L/H=1.5
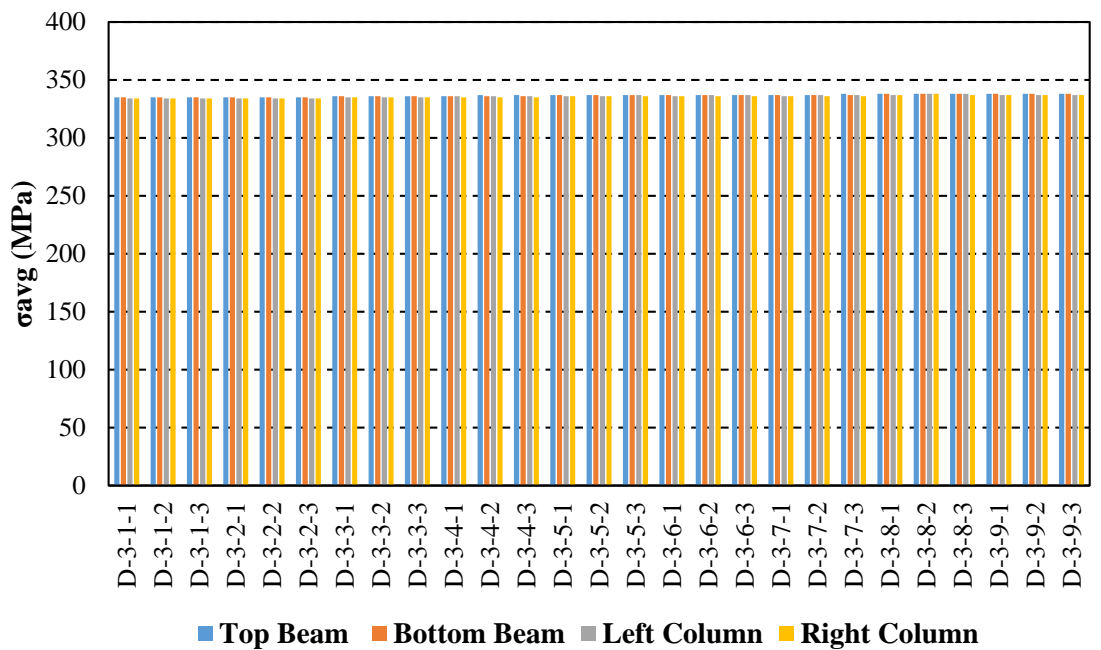
Figure 5.27. σ_{avg} of the strips connected to the surrounding boundary frame elements for all designs at 2% drift with L/H=2

5.3.3. Relationship between Flexibility Factor and Stress Variation in the Web Plate

Kuhn et al. (1952) expressed the stress amplification factor C_2 as shown in equation 5.1 and used the equation for the analysis of curved shear webs working in the diagonal tension. To characterize the uniformity of the elastic web tension field stress in the strips, amplification factor, C_2 is employed to capture the differences between the maximum and mean stresses. In this study, σ_{max} and σ_{mean} of 50 strips are considered. Large value of C_2 shows the difference between the σ_{max} and σ_{mean} which is indicating the less uniform web tension field.

$$C_2 = \frac{\sigma_{max}}{\sigma_{mean}} - 1 \qquad\qquad \text{Eq (5.1)}$$

Demanding minimum flexural stiffness of VBE and HBE to ensure the uniformity of elastic infill tension in the web plate and avoid undesirable VBE and HBE behaviors, normalized VBE flexibility limit with respect to HBE flexibility limit is given in equation 5.2.

$$\omega_{tnorm} = \frac{h}{L} \sqrt[4]{\frac{I_b h}{I_c L}} \qquad\qquad \text{Eq (5.2)}$$

Figure 5.28 shows the relationship between stress amplification factor and normalized flexibility factor (ω_{tnorm}) in five different drifts such as 0.2%, 0.3%, 0.6%, 1% and 2%. As seen in figure 5.28, at drift ratio such as 0.2%, difference between σ_{max} and σ_{mean} (C_2) are higher. In other words, at these drift ratio distribution of the stresses in strips are less uniform. As drift levels of SPSWs progressively increase, web plates develop uniform tension fields (region that strips are yielded) and the difference between the σ_{max} and σ_{mean} decreased.
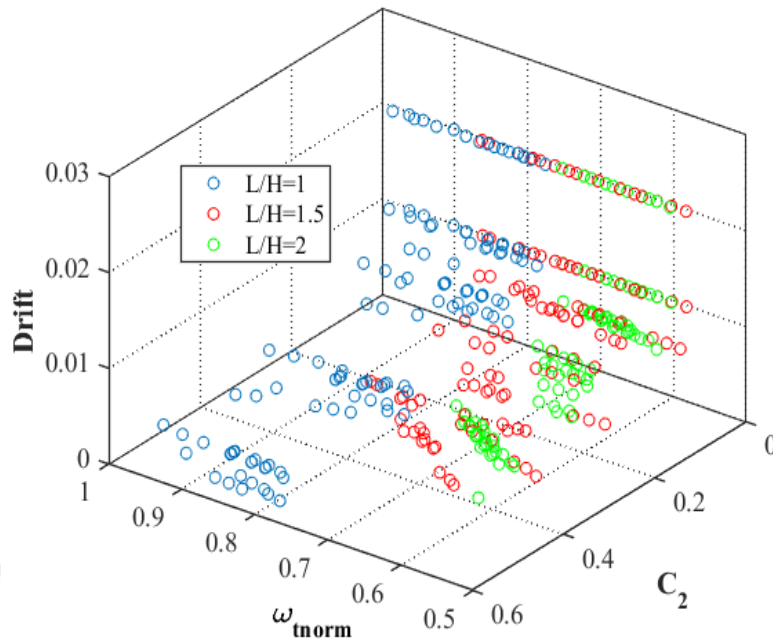
Figure 5.28. Relationship between normalized flexibility factor, C2 and drift

In the following, using surface fitting in MATLAB® (Moore, 2017), we propose a closed-form expression for C_2 which is an explicit function of ω_{tnorm}, drift and aspect ratio. In figure 5.29, we present the data of C_2 versus ω_{tnorm} and drift at the aspect ratio of 1, 1.5 and 2. Based on curve fitting in MATLAB®, C_2 can be approximated as

$$C_2 = 0.788 \times 10^{-7} (\omega_{tnorm})^{-1.037} \times (Drift)^{-2.013} \times (AspectRatio)^{0.112} \qquad \text{Eq (5.3)}$$

In figure 5.29, fitted curves are presented for aspect ratios of 1, 1.5 and 2. From figures, it can be verified that the proposed expression provides an acceptable fit for all obtained data through pushover analyses in different scenarios under considerations.
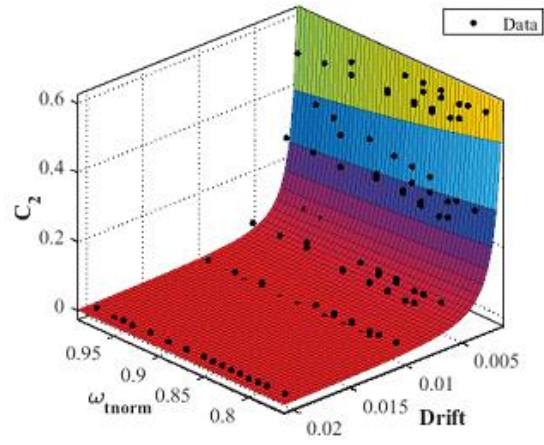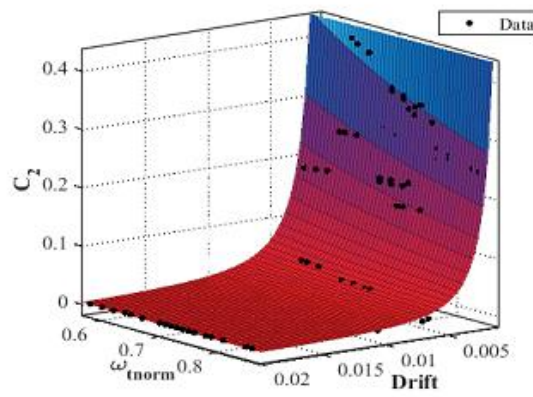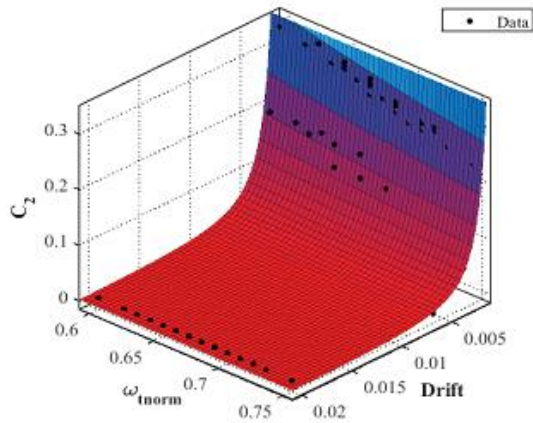
Figure 5.29. Surface fitting for (a) L/H=1 (b) L/H=1.5 (c) L/H=2

CHAPTER VI

SUMMARY AND CONCLUSION

6.1.   Summary

As a lateral load resisting system in high seismic regions, steel plate shear walls are preferred due to their high strength and stiffness. AISC341-16 presents the stiffness limits for beams and columns of the steel plate shear walls to ensure that the web plate entirely yield in tension prior to the yielding of the beams and columns. In this thesis a parametric study has been conducted to investigate the influence of boundary frame stiffness on the variation of stresses in the web plate of steel plate shear walls.

In this study a simplified model known as the strip model which includes series of evenly spaced tension-only inclined truss elements connected to the beams and columns is employed to simulate the tension field behavior of the web plate under lateral loading. Cyclic quasi-static analysis of one-bay one-story SPSW tested by Lubell et al. (2000) is conducted in OpenSEES to validate the strip model against the experimental work. Results from OpenSEES and experimental work were in a good agreement.

Capacity design of the beams and columns have been presented based on the design procedure suggested by Sabelli and Bruneau (2007). In this study single story SPSWs with moment resisting beam to column connections were considered. Bottom beam not anchored to the ground while column bases were assumed to be fixed. As a result, 27 sets of SPSWs were designed in a such a way that each includes two more designs with stiffer columns while the beam sections remain the same. 9 different plate

thickness and 3 different aspect ratios were considered in these designs. Finally, numerical parametric study has been undertaken on mentioned 81 SPSWs in OpenSEES.

6.2. Conclusions

The following conclusions were drawn based on the results of the study:

- Conducted nonlinear pushover analysis results reveal that the column stiffness does not have a significant impact on the distribution of the tension field forces acting on the boundary frame (SPSWs are loaded laterally from left side to the right). In SPSWs with aspect ratio of 1, at lower drifts maximum stresses occurred in strips connected to the top beam in one end and the left column in the other end. However, in SPSWs with aspect ratios of 1.5, for the web plates thinner than 1.98 mm maximum stresses occurred in the strips connected to the top and bottom beam at both ends while in the web plates thicker than this value maximum stresses were in the strips connected to the left column in one end and to the top beam at the other end. For SPSWs with aspect ratio of 2, maximum stress occurs in the strips connected to the bottom beam at the one end and the top beam at the other end. At a higher drift such as 2%, all of strips yielded in tension.

- In this study, suggested plastic section modulus limit by AISC341-16 for horizontal boundary elements is critical for SPSWs with aspect ratio of 1 and plates thinner than 1.3 mm. For the rest of the SPSWs with the aspect ratio of 1 and plates thicker than 1.3 mm and aspect ratio of 1.5 and 2 that have plates with thickness of 0.55 mm to 4.36 mm, plastic section modulus limit does not govern

since the W-shaped steel sections selected based on the force demands have higher value of plastic section modulus.

- In this case of study, given stiffness limits for the boundary frames of SPSWs makes it unattainable to capacity design the beams and columns that have aspect ratios more than 2 with available W-shaped steel sections. On the other hand, capacity designing of SPSWs showed that in SPSWs with aspect ratios of 1, 1.5 and 2, PM interaction in columns is dominated.

- As explained in chapter 4, the required strength equations provided by Sabelli and Bruneau (2007) were Adopted for SPSW designs. The required shear strength in the VBEs extracted from the structural analysis doubles the required shear strength determined per Sabelli and Bruneau (2007). In other words, the closed-form equations provided in the Design Guide, significantly underestimates the shear force demands in VBEs. With regards to HBEs, the closed-form equations overestimate the required shear strength about 20% for SPSWs with an aspect ratio of 1 while underestimates it about 10% for SPSWs with aspect ratios of 1.5 and 2. This results stems from the fact that the closed-form equations do not consider the depth of the boundary frame elements; however, the horizontal component of the web plate stress acting along the boundary frame elements due to the offset from the centerline of the boundary frame elements. As the aspect ratio increases, deeper beams are needed; consequently, these secondary forces become prominent. It is recommended the boundary frame depth be considered in design, especially for high aspect ratio SPSWs. In some designs, these issues might be critical and require an overview in design of HBE.

- The closed-form expression for uniformity of tension stresses in web plate is also obtained with respect to flexibility of beams and columns, aspect ratio and drift (equation 5.3). The proposed expression is a function of aforementioned variables which provides an acceptable fit with the data from pushover analysis.

6.3. *Future Work*

In the literature, although distribution of the stresses in the web plate has been studied, the study regarding to this issue is limited. To further expand the understanding of variation of stress distribution in the web plate of SPSWs, future research studies should focus on the following topics:

- Parametric study on multistory steel plate shear walls with considering varying plate thickness in each story or considering the same plate thickness in all stories is recommended to provide better information about the stress distribution in the web plate. Also considering more plate thickness could be much more beneficial.

- In this study W-shaped section for beam and columns from AISC Shape Database were selected. Wide range of different shapes can be used to design the boundary elements and evaluate the distribution of the stress in the web plate. This can provide more alternatives for aspect ratio and plate thickness.

- The loading condition in this parametric study was static loading. However, steel plate shear walls used for the structures exposed to dynamic loads such

as earthquake. Influence of the boundary frame stiffness on variation of the stresses in the webplate should be investigated under dynamic loading.

- In this study, for the design of beam to column connections any specifications were not considered. In the next studies this issue should not be ignored.

APPENDIX A
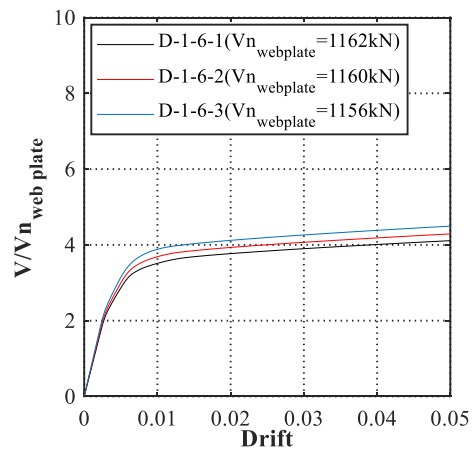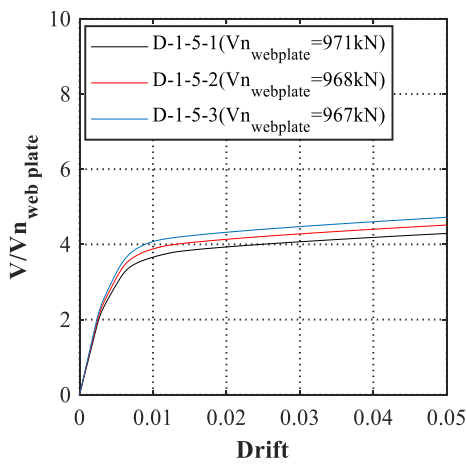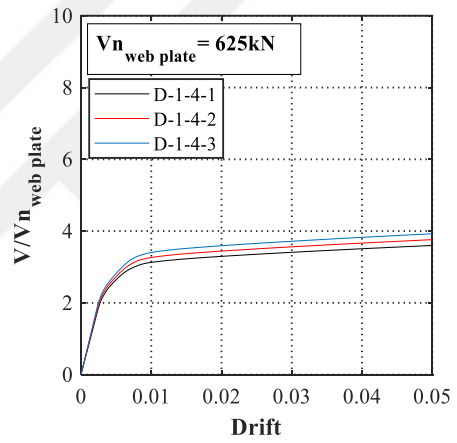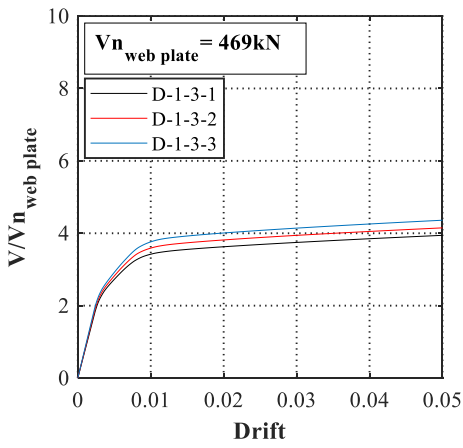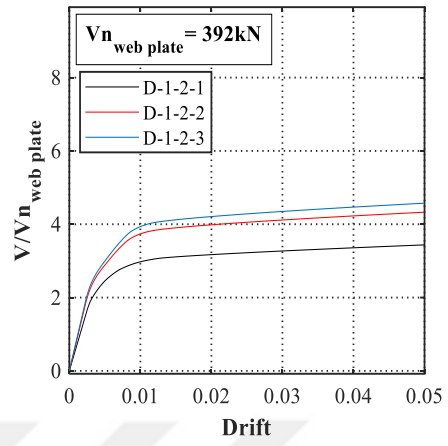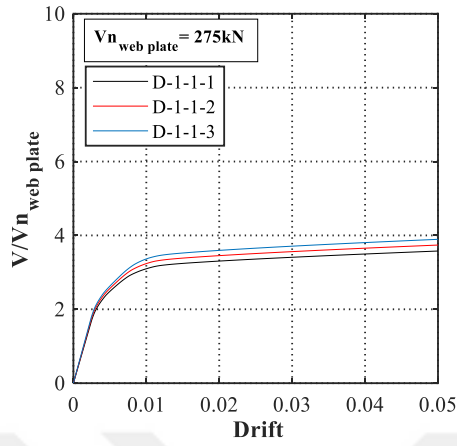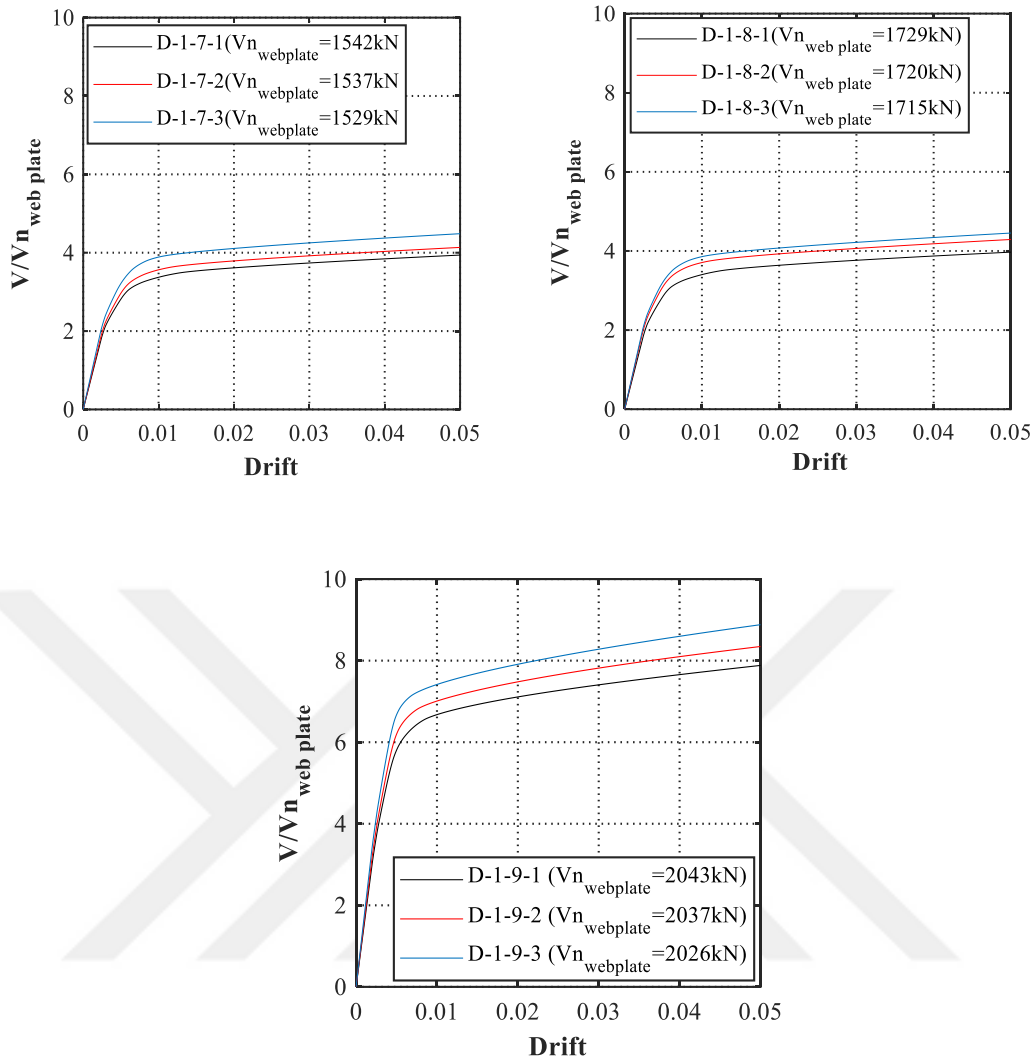
Figure A.1. Normalized base shear versus drift of SPSWs with aspect ratio of 1
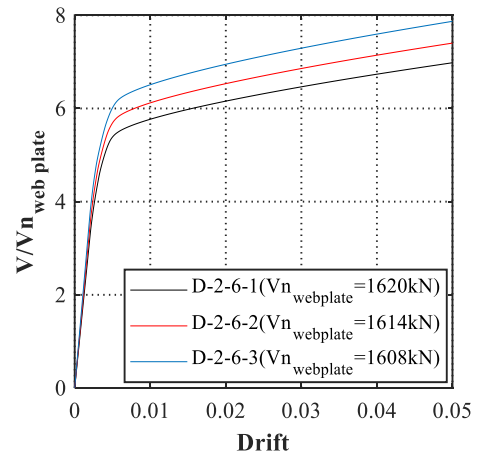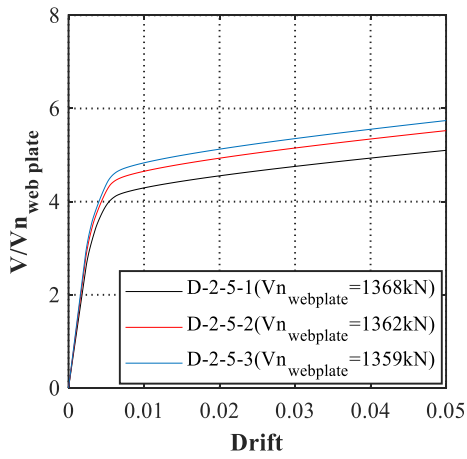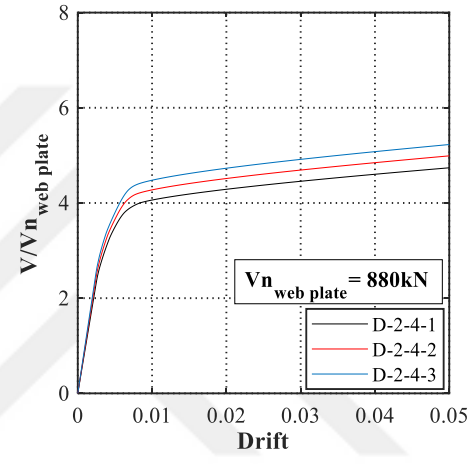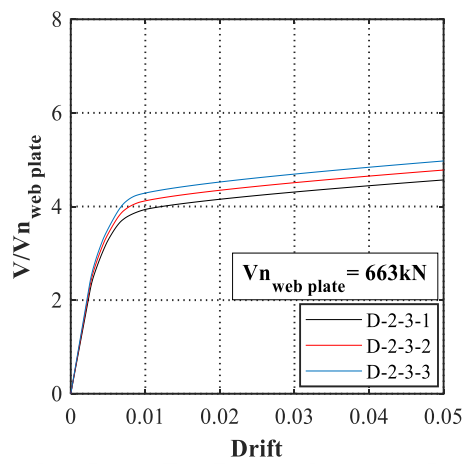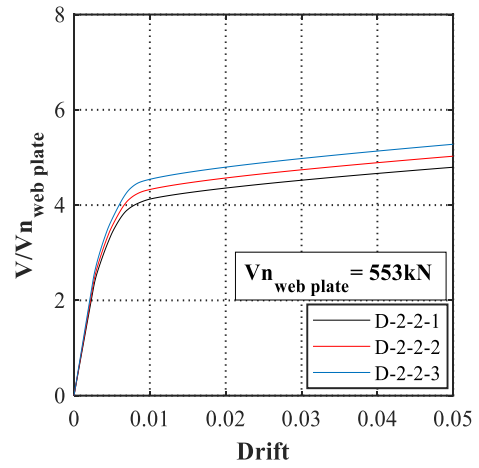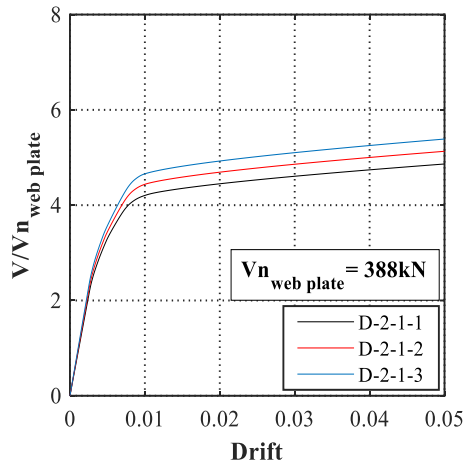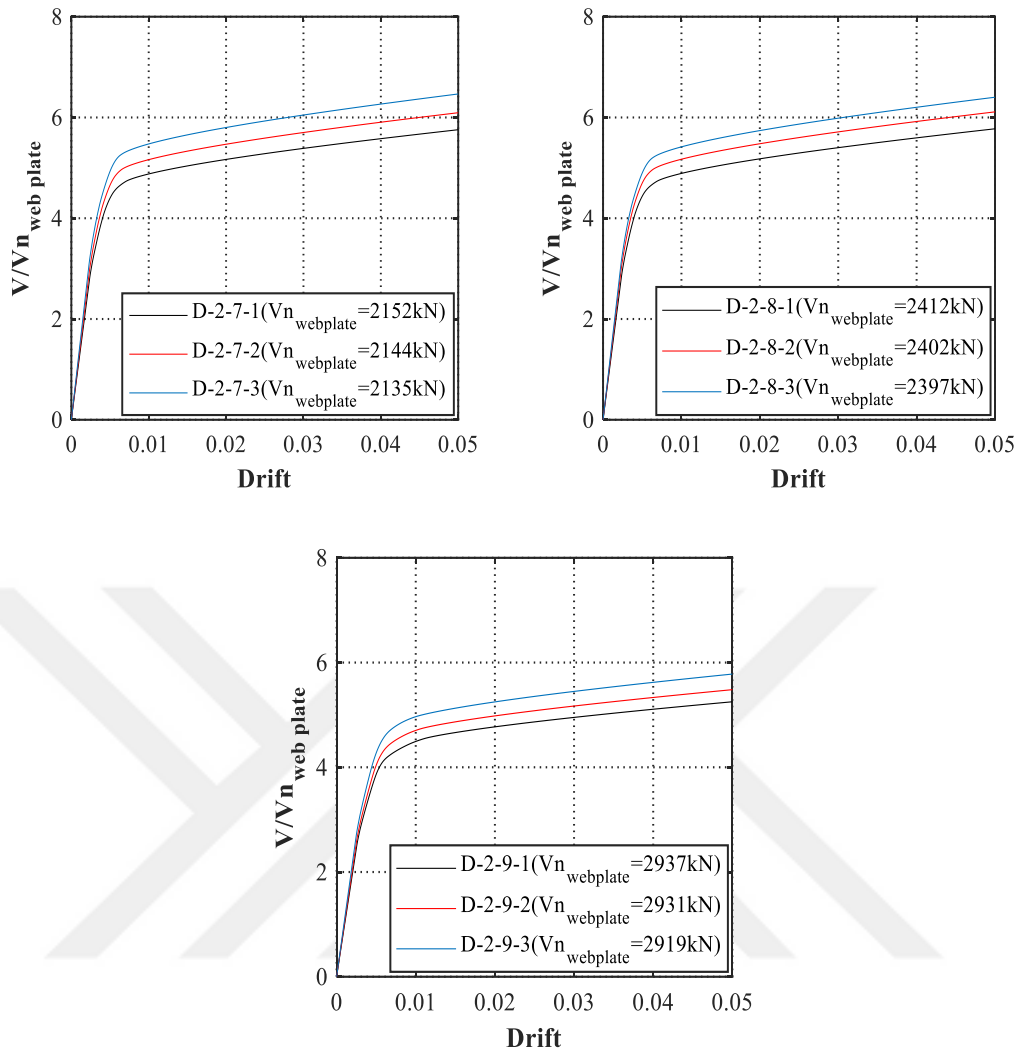
Figure A.2. Normalized base shear versus drift of SPSWs with aspect ratio of 1.5
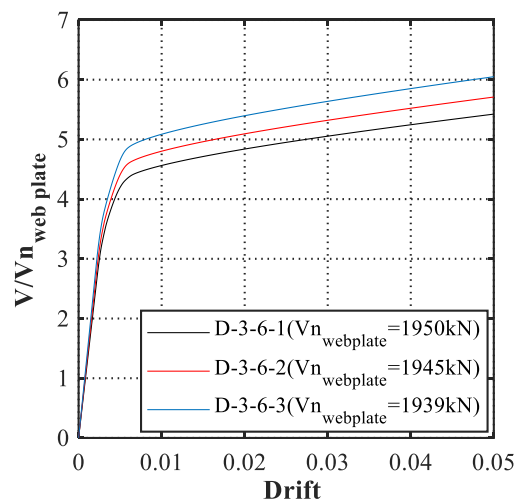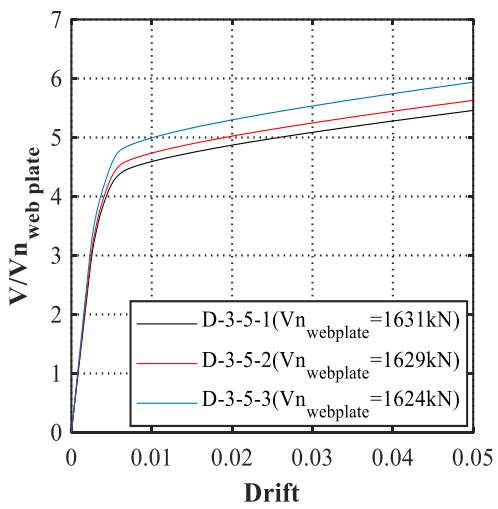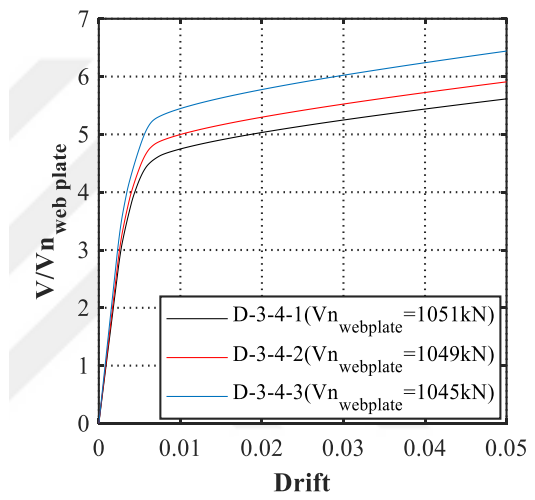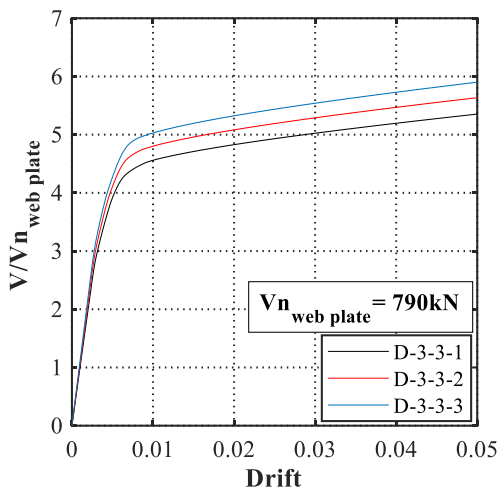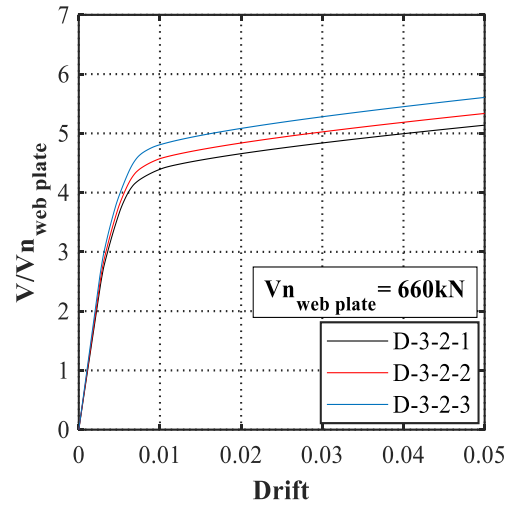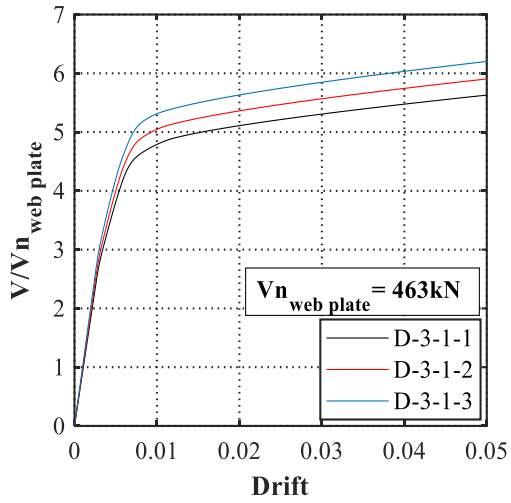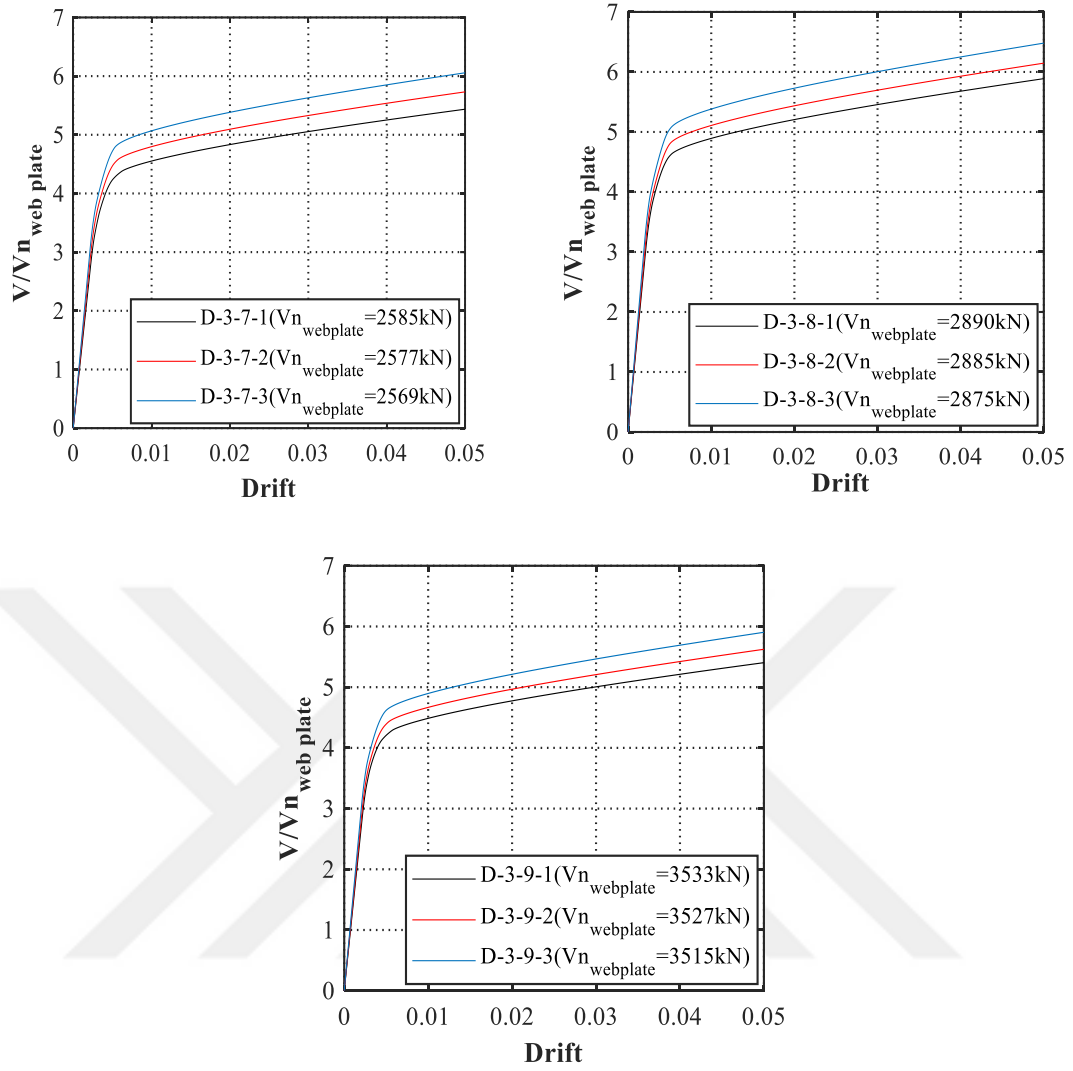
Figure A.3. Normalized base shear versus drift of SPSWs with aspect ratio of 2

Table A.1 Tension field stress acting on the boundary frame at 0.2% drift with L/H=1 and t_w=0.55

Name	Member	σ_{avg}	$\sigma_{min}/R_{yp}F_{yp}$	$\sigma_{max}/R_{yp}F_{yp}$
D-1-1-1	Top Beam	190	0.11	0.80
	Bottom Beam	149	0.03	0.72
	Left Column	183	0.11	0.80
	Right Column	136	0.03	0.67
D-1-1-2	Top Beam	194	0.12	0.82
	Bottom Beam	150	0.04	0.73
	Left Column	187	0.12	0.82
	Right Column	136	0.04	0.67
D-1-1-3	Top Beam	197	0.12	0.83
	Bottom Beam	150	0.04	0.73
	Left Column	191	0.12	0.83
	Right Column	136	0.04	0.68

Table A.2 Tension field stress acting on the boundary frame at 2% drift with L/H=1 and t_w=0.55

Name	Member	σ_{avg}	$\sigma_{min}/R_{yp}F_{yp}$	$\sigma_{max}/R_{yp}F_{yp}$
D-1-1-1	Top Beam	334	1.00	1.03
	Bottom Beam	332	1.00	1.03
	Left Column	334	1.00	1.03
	Right Column	332	1.00	1.03
D-1-1-2	Top Beam	334	1.00	1.03
	Bottom Beam	332	1.00	1.03
	Left Column	334	1.00	1.03
	Right Column	332	1.00	1.03
D-1-1-3	Top Beam	334	1.00	1.03
	Bottom Beam	332	1.00	1.03
	Left Column	334	1.00	1.03
	Right Column	332	1.00	1.03

Table A.3 Tension field stress action on the boundary frame at 0.2% drift with L/H=1 and t_w=0.79

Name	Member	σ_{avg} (MPa)	$\sigma_{min}/R_{yp}F_{yp}$	$\sigma_{max}/R_{yp}F_{yp}$
D-1-2-1	Top Beam	187	0.11	0.74
	Bottom Beam	153	0.04	0.71
	Left Column	181	0.11	0.79
	Right Column	140	0.04	0.67
D-1-2-2	Top Beam	206	0.15	0.85
	Bottom Beam	149	0.05	0.74
	Left Column	203	0.15	0.85
	Right Column	142	0.05	0.68
D-1-2-3	Top Beam	210	0.16	0.86
	Bottom Beam	149	0.05	0.74
	Left Column	207	0.16	0.88
	Right Column	142	0.05	0.69

Table A.4 Tension field stress action on the boundary frame at 2% drift with L/H=1 and t_w=0.79

Name	Member	σ_{avg} (MPa)	$\sigma_{min}/R_{yp}F_{yp}$	$\sigma_{max}/R_{yp}F_{yp}$
D-1-2-1	Top Beam	334	1.01	1.03
	Bottom Beam	332	1.01	1.03
	Left Column	334	1.01	1.03
	Right Column	332	1.01	1.03
D-1-2-2	Top Beam	335	1.01	1.03
	Bottom Beam	332	1.01	1.03
	Left Column	335	1.01	1.03
	Right Column	332	1.01	1.03
D-1-2-3	Top Beam	335	1.01	1.03
	Bottom Beam	332	1.01	1.03
	Left Column	335	1.01	1.03
	Right Column	332	1.01	1.03

Table A.5 Tension field stress action on the boundary frame at 0.2% drift with L/H=1 and t_w=0.95

Name	Member	σ_{avg} (MPa)	$\sigma_{min}/R_{yp}F_{yp}$	$\sigma_{max}/R_{yp}F_{yp}$
D-1-3-1	Top Beam	206	0.15	0.85
	Bottom Beam	156	0.04	0.75
	Left Column	200	0.15	0.85
	Right Column	142	0.04	0.69
D-1-3-2	Top Beam	209	0.16	0.86
	Bottom Beam	156	0.05	0.76
	Left Column	204	0.16	0.86
	Right Column	241	0.05	0.69
D-1-3-3	Top Beam	213	0.16	0.87
	Bottom Beam	156	0.05	0.76
	Left Column	208	0.16	0.87
	Right Column	141	0.05	0.69

Table A.6 Tension field stress action on the boundary frame at 2% drift with L/H=1 and t_w=0.95

Name	Member	σ_{avg} (MPa)	$\sigma_{min}/R_{yp}F_{yp}$	$\sigma_{max}/R_{yp}F_{yp}$
D-1-3-1	Top Beam	335	1.01	1.03
	Bottom Beam	332	1.01	1.03
	Left Column	335	1.01	1.03
	Right Column	332	1.01	1.03
D-1-3-2	Top Beam	335	1.01	1.03
	Bottom Beam	333	1.01	1.03
	Left Column	335	1.01	1.03
	Right Column	332	1.01	1.03
D-1-3-3	Top Beam	335	1.01	1.03
	Bottom Beam	333	1.01	1.03
	Left Column	335	1.01	1.03
	Right Column	332	1.01	1.03

Table A.7 Tension field stress action on the boundary frame at 0.2% drift with L/H=1 and t_w=1.27

Name	Member	σ_{avg} (MPa)	$\sigma_{min}/R_{yp}F_{yp}$	$\sigma_{max}/R_{yp}F_{yp}$
D-1-4-1	Top Beam	206	0.16	0.84
	Bottom Beam	164	0.05	0.75
	Left Column	201	0.16	0.84
	Right Column	152	0.05	0.75
D-1-4-2	Top Beam	211	0.17	0.85
	Bottom Beam	165	0.06	0.76
	Left Column	205	0.17	0.85
	Right Column	151	0.06	0.76
D-1-4-3	Top Beam	215	0.18	0.87
	Bottom Beam	165	0.06	0.77
	Left Column	210	0.18	0.87
	Right Column	152	0.06	0.77

Table A.8 Tension field stress action on the boundary frame at 2% drift with L/H=1 and t_w=1.27

Name	Member	σ_{avg} (MPa)	$\sigma_{min}/R_{yp}F_{yp}$	$\sigma_{max}/R_{yp}F_{yp}$
D-1-4-1	Top Beam	335	1.01	1.03
	Bottom Beam	333	1.01	1.03
	Left Column	335	1.01	1.03
	Right Column	332	1.01	1.03
D-1-4-2	Top Beam	335	1.01	1.03
	Bottom Beam	333	1.01	1.03
	Left Column	335	1.01	1.03
	Right Column	332	1.01	1.03
D-1-4-3	Top Beam	335	1.01	1.03
	Bottom Beam	333	1.01	1.03
	Left Column	335	1.01	1.03
	Right Column	332	1.01	1.03

Table A.9 Tension field stress action on the boundary frame at 0.2% drift with L/H=1 and t_w=1.98

Name	Member	σ_{avg} (MPa)	$\sigma_{min}/R_{yp}F_{yp}$	$\sigma_{max}/R_{yp}F_{yp}$
D-1-5-1	Top Beam	203	0.16	0.83
	Bottom Beam	158	0.08	0.70
	Left Column	201	0.16	0.83
	Right Column	152	0.08	0.69
D-1-5-2	Top Beam	208	0.17	0.84
	Bottom Beam	158	0.09	0.70
	Left Column	207	0.17	0.85
	Right Column	153	0.09	0.70
D-1-5-3	Top Beam	212	0.18	0.86
	Bottom Beam	159	0.09	0.70
	Left Column	211	0.18	0.86
	Right Column	153	0.09	0.69

Table A.10 Tension field stress action on the boundary frame at 2% drift with L/H=1 and t_w=1.98

Name	Member	σ_{avg} (MPa)	$\sigma_{min}/R_{yp}F_{yp}$	$\sigma_{max}/R_{yp}F_{yp}$
D-1-5-1	Top Beam	334	1.01	1.03
	Bottom Beam	333	1.01	1.03
	Left Column	334	1.01	1.03
	Right Column	333	1.01	1.03
D-1-5-2	Top Beam	335	1.01	1.03
	Bottom Beam	333	1.01	1.03
	Left Column	335	1.01	1.03
	Right Column	333	1.01	1.03
D-1-5-3	Top Beam	335	1.02	1.03
	Bottom Beam	333	1.01	1.03
	Left Column	335	1.02	1.03
	Right Column	333	1.01	1.03

Table A.11 Tension field stress action on the boundary frame at 0.2% drift with L/H=1 and tw=2.38

Name	Member	σ_{avg} (MPa)	$\sigma_{min}/R_{yp}F_{yp}$	$\sigma_{max}/R_{yp}F_{yp}$
D-1-6-1	Top Beam	201	0.16	0.83
	Bottom Beam	157	0.08	0.70
	Left Column	199	0.16	0.83
	Right Column	151	0.08	0.69
D-1-6-2	Top Beam	206	0.17	0.84
	Bottom Beam	157	0.08	0.70
	Left Column	204	0.17	0.84
	Right Column	152	0.08	0.69
D-1-6-3	Top Beam	210	0.18	0.86
	Bottom Beam	158	0.09	0.71
	Left Column	209	0.18	0.86
	Right Column	152	0.09	0.69

Table A.12 Tension field stress action on the boundary frame at 2% drift with L/H=1 and t_w=2.38

Name	Member	σ_{avg} (MPa)	$\sigma_{min}/R_{yp}F_{yp}$	$\sigma_{max}/R_{yp}F_{yp}$
D-1-6-1	Top Beam	334	1.01	1.03
	Bottom Beam	333	1.01	1.03
	Left Column	334	1.01	1.03
	Right Column	333	1.01	1.03
D-1-6-2	Top Beam	335	1.01	1.03
	Bottom Beam	333	1.01	1.03
	Left Column	335	1.01	1.03
	Right Column	333	1.01	1.03
D-1-6-3	Top Beam	335	1.01	1.03
	Bottom Beam	333	1.01	1.03
	Left Column	335	1.01	1.03
	Right Column	333	1.01	1.03

Table A.13 Tension field stress action on the boundary frame at 0.2% drift with L/H=1 and t_w=3.17

Name	Member	σ_{avg} (MPa)	$\sigma_{min}/R_{yp}F_{yp}$	$\sigma_{max}/R_{yp}F_{yp}$
D-1-7-1	Top Beam	201	0.15	0.83
	Bottom Beam	157	0.08	0.70
	Left Column	199	0.15	0.83
	Right Column	151	0.08	0.69
D-1-7-2	Top Beam	206	0.17	0.84
	Bottom Beam	158	0.08	0.70
	Left Column	205	0.17	0.84
	Right Column	152	0.08	0.69
D-1-7-3	Top Beam	215	0.19	0.87
	Bottom Beam	159	0.09	0.71
	Left Column	214	0.19	0.87
	Right Column	153	0.09	0.70

Table A.14 Tension field stress action on the boundary frame at 2% drift with L/H=1 and t_w=3.17

Name	Member	σ_{avg} (MPa)	$\sigma_{min}/R_{yp}F_{yp}$	$\sigma_{max}/R_{yp}F_{yp}$
D-1-7-1	Top Beam	334	1.01	1.03
	Bottom Beam	333	1.01	1.03
	Left Column	334	1.01	1.03
	Right Column	333	1.01	1.03
D-1-7-2	Top Beam	335	1.01	1.03
	Bottom Beam	333	1.01	1.03
	Left Column	335	1.01	1.03
	Right Column	333	1.01	1.03
D-1-7-3	Top Beam	335	1.02	1.03
	Bottom Beam	333	1.01	1.03
	Left Column	335	1.02	1.03
	Right Column	333	1.01	1.03

Table A.15 Tension field stress action on the boundary frame at 0.2% drift with L/H=1 and t_w=3.57

Name	Member	σ_{avg} (MPa)	$\sigma_{min}/R_{yp}F_{yp}$	$\sigma_{max}/R_{yp}F_{yp}$
D-1-8-1	Top Beam	203	0.16	0.83
	Bottom Beam	159	0.08	0.70
	Left Column	202	0.16	0.83
	Right Column	153	0.08	0.70
D-1-8-2	Top Beam	212	0.18	0.86
	Bottom Beam	160	0.09	0.71
	Left Column	211	0.18	0.86
	Right Column	155	0.09	0.70
D-1-8-3	Top Beam	217	0.19	0.88
	Bottom Beam	161	0.10	0.71
	Left Column	216	0.19	0.88
	Right Column	155	0.10	0.71

Table A.16 Tension field stress action on the boundary frame at 2% drift with L/H=1 and t_w=3.57

Name	Member	σ_{avg} (MPa)	$\sigma_{min}/R_{yp}F_{yp}$	$\sigma_{max}/R_{yp}F_{yp}$
D-1-8-1	Top Beam	335	1.01	1.03
	Bottom Beam	333	1.01	1.03
	Left Column	335	1.01	1.03
	Right Column	333	1.01	1.03
D-1-8-2	Top Beam	335	1.02	1.03
	Bottom Beam	333	1.01	1.03
	Left Column	335	1.02	1.03
	Right Column	333	1.01	1.03
D-1-8-3	Top Beam	335	1.02	1.03
	Bottom Beam	333	1.01	1.03
	Left Column	335	1.02	1.03
	Right Column	333	1.01	1.03

Table A.17 Tension field stress acting on the boundary frame at 0.2% drift with L/H=1 and tw=4.36

Name	Member	σ_{avg}	$\sigma_{min}/R_{yp}F_{yp}$	$\sigma_{max}/R_{yp}F_{yp}$
D-1-9-1	Top Beam	269	0.4	1.00
	Bottom Beam	199	0.2	0.77
	Left Column	269	0.4	1.00
	Right Column	199	0.2	0.77
D-1-9-2	Top Beam	273	0.4	1.00
	Bottom Beam	200	0.2	0.78
	Left Column	273	0.4	1.00
	Right Column	200	0.2	0.78
D-1-9-3	Top Beam	278	0.4	1.00
	Bottom Beam	200	0.2	0.78
	Left Column	278	0.4	1.00
	Right Column	200	0.2	0.78

Table A.18 Tension field stress acting on the boundary frame at 2% drift with L/H=1 and tw=4.36

Name	Member	σ_{avg}	$\sigma_{min}/R_{yp}F_{yp}$	$\sigma_{max}/R_{yp}F_{yp}$
D-1-9-1	Top Beam	337	1.03	1.04
	Bottom Beam	335	1.03	1.03
	Left Column	337	1.03	1.04
	Right Column	335	1.03	1.03
D-1-9-2	Top Beam	337	1.03	1.04
	Bottom Beam	335	1.03	1.03
	Left Column	337	1.03	1.04
	Right Column	335	1.03	1.03
D-1-9-3	Top Beam	338	1.03	1.04
	Bottom Beam	335	1.03	1.03
	Left Column	338	1.03	1.04
	Right Column	335	1.03	1.03

Table A.19 Tension field stress acting on the boundary frame at 0.2% drift with L/H=1.5 and tw=0.55

Name	Member	σ_{avg} (MPa)	$\sigma_{min}/R_{yp}F_{yp}$	$\sigma_{max}/R_{yp}F_{yp}$
D-2-1-1	Top Beam	198	0.17	0.76
	Bottom Beam	179	0.09	0.76
	Left Column	174	0.17	0.71
	Right Column	143	0.09	0.64
D-2-1-2	Top Beam	200	0.18	0.77
	Bottom Beam	179	0.09	0.77
	Left Column	176	0.18	0.73
	Right Column	142	0.09	0.64
D-2-1-3	Top Beam	203	0.18	0.78
	Bottom Beam	180	0.09	0.78
	Left Column	179	0.18	0.73
	Right Column	141	0.09	0.64

Table A.20 Tension field stress acting on the boundary frame at 2% drift with L/H=1.5 and tw=0.55

Name	Member	σ_{avg} (MPa)	$\sigma_{min}/R_{yp}F_{yp}$	$\sigma_{max}/R_{yp}F_{yp}$
D-2-1-1	Top Beam	334	1.01	1.03
	Bottom Beam	334	1.01	1.03
	Left Column	334	1.01	1.03
	Right Column	333	1.01	1.03
D-2-1-2	Top Beam	335	1.01	1.03
	Bottom Beam	334	1.01	1.03
	Left Column	334	1.01	1.03
	Right Column	333	1.01	1.03
D-2-1-3	Top Beam	335	1.01	1.03
	Bottom Beam	334	1.01	1.03
	Left Column	334	1.01	1.03
	Right Column	333	1.01	1.03

Table A.21 Tension field stress action on the boundary frame at 0.2% drift with
L/H=1.5 and t_w=0.79

Name	Member	σ_{avg} (MPa)	$\sigma_{min}/R_{yp}F_{yp}$	$\sigma_{max}/R_{yp}F_{yp}$
D-2-2-1	Top Beam	208	0.20	0.77
	Bottom Beam	192	0.11	0.77
	Left Column	186	0.20	0.75
	Right Column	160	0.11	0.68
D-2-2-2	Top Beam	211	0.21	0.79
	Bottom Beam	192	0.11	0.79
	Left Column	190	0.21	0.76
	Right Column	159	0.11	0.68
D-2-2-3	Top Beam	214	0.22	0.80
	Bottom Beam	193	0.11	0.80
	Left Column	193	0.22	0.77
	Right Column	178	0.11	0.68

Table A.22 Tension field stress action on the boundary frame at 2% drift with L/H=1.5
and t_w=0.79

Name	Member	σ_{avg} (MPa)	$\sigma_{min}/R_{yp}F_{yp}$	$\sigma_{max}/R_{yp}F_{yp}$
D-2-2-1	Top Beam	335	1.01	1.03
	Bottom Beam	334	1.02	1.03
	Left Column	335	1.01	1.03
	Right Column	334	1.02	1.03
D-2-2-2	Top Beam	335	1.02	1.03
	Bottom Beam	334	1.02	1.03
	Left Column	335	1.02	1.03
	Right Column	334	1.02	1.03
D-2-2-3	Top Beam	335	1.01	1.03
	Bottom Beam	334	1.02	1.03
	Left Column	335	1.01	1.03
	Right Column	334	1.02	1.03

Table A.23 Tension field stress action on the boundary frame at 0.2% drift with L/H=1.5 and t_w=0.95

Name	Member	σ_{avg} (MPa)	$\sigma_{min}/R_{yp}F_{yp}$	$\sigma_{max}/R_{yp}F_{yp}$
D-2-3-1	Top Beam	205	0.20	0.77
	Bottom Beam	190	0.11	0.77
	Left Column	183	0.20	0.73
	Right Column	159	0.11	0.68
D-2-3-2	Top Beam	208	0.21	0.78
	Bottom Beam	191	0.11	0.78
	Left Column	186	0.21	0.75
	Right Column	158	0.11	0.67
D-2-3-3	Top Beam	211	0.21	0.79
	Bottom Beam	191	0.11	0.79
	Left Column	189	0.21	0.76
	Right Column	157	0.11	0.67

Table A.24 Tension field stress action on the boundary frame at 2% drift with L/H=1.5 and t_w=0.95

Name	Member	σ_{avg} (MPa)	$\sigma_{min}/R_{yp}F_{yp}$	$\sigma_{max}/R_{yp}F_{yp}$
D-2-3-1	Top Beam	335	1.01	1.03
	Bottom Beam	335	1.02	1.03
	Left Column	335	1.01	1.03
	Right Column	335	1.02	1.03
D-2-3-2	Top Beam	335	1.01	1.03
	Bottom Beam	335	1.02	1.03
	Left Column	335	1.01	1.03
	Right Column	334	1.02	1.03
D-2-3-3	Top Beam	335	1.01	1.03
	Bottom Beam	335	1.02	1.03
	Left Column	335	1.01	1.03
	Right Column	334	1.02	1.03

Table A.25 Tension field stress action on the boundary frame at 0.2% drift with L/H=1.5 and t_w=1.27

Name	Member	σ_{avg} (MPa)	$\sigma_{min}/R_{yp}F_{yp}$	$\sigma_{max}/R_{yp}F_{yp}$
D-2-4-1	Top Beam	217	0.23	0.80
	Bottom Beam	200	0.12	0.80
	Left Column	196	0.23	0.77
	Right Column	169	0.12	0.70
D-2-4-2	Top Beam	221	0.24	0.81
	Bottom Beam	201	0.13	0.81
	Left Column	201	0.24	0.78
	Right Column	168	0.13	0.70
D-2-4-3	Top Beam	224	0.25	0.82
	Bottom Beam	201	0.13	0.82
	Left Column	204	0.25	0.79
	Right Column	167	0.13	0.69

Table A.26 Tension field stress action on the boundary frame at 2% drift with L/H=1.5 and t_w=1.27

Name	Member	σ_{avg} (MPa)	$\sigma_{min}/R_{yp}F_{yp}$	$\sigma_{max}/R_{yp}F_{yp}$
D-2-4-1	Top Beam	336	1.02	1.03
	Bottom Beam	335	1.02	1.03
	Left Column	335	1.02	1.03
	Right Column	334	1.02	1.03
D-2-4-2	Top Beam	336	1.02	1.04
	Bottom Beam	335	1.02	1.04
	Left Column	335	1.02	1.04
	Right Column	334	1.02	1.03
D-2-4-3	Top Beam	336	1.02	1.04
	Bottom Beam	335	1.02	1.04
	Left Column	336	1.02	1.04
	Right Column	334	1.02	1.03

Table A.27 Tension field stress action on the boundary frame at 0.2% drift with
L/H=1.5 and t_w=1.98

Name	Member	σ_{avg} (MPa)	$\sigma_{min}/R_{yp}F_{yp}$	$\sigma_{max}/R_{yp}F_{yp}$
D-2-5-1	Top Beam	244	0.32	0.86
	Bottom Beam	223	0.17	0.86
	Left Column	226	0.32	0.85
	Right Column	190	0.17	0.76
D-2-5-2	Top Beam	250	0.34	0.88
	Bottom Beam	225	0.18	0.88
	Left Column	233	0.34	0.87
	Right Column	187	0.18	0.75
D-2-5-3	Top Beam	253	0.35	0.86
	Bottom Beam	225	0.18	0.89
	Left Column	236	0.35	0.88
	Right Column	186	0.18	0.75

Table A.28 Tension field stress action on the boundary frame at 2% drift with L/H=1.5
and t_w=1.98

Name	Member	σ_{avg} (MPa)	$\sigma_{min}/R_{yp}F_{yp}$	$\sigma_{max}/R_{yp}F_{yp}$
D-2-5-1	Top Beam	337	1.02	1.04
	Bottom Beam	336	1.02	1.04
	Left Column	337	1.02	1.04
	Right Column	335	1.02	1.03
D-2-5-2	Top Beam	337	1.02	1.04
	Bottom Beam	336	1.03	1.04
	Left Column	337	1.02	1.04
	Right Column	335	1.03	1.03
D-2-5-3	Top Beam	337	1.02	1.04
	Bottom Beam	336	1.03	1.04
	Left Column	337	1.02	1.04
	Right Column	335	1.03	1.03

Table A.29 Tension field stress action on the boundary frame at 0.2% drift with L/H=1.5 and t_w=2.38

Name	Member	σ_{avg} (MPa)	$\sigma_{min}/R_{yp}F_{yp}$	$\sigma_{max}/R_{yp}F_{yp}$
D-2-6-1	Top Beam	280	0.45	0.98
	Bottom Beam	246	0.25	0.94
	Left Column	270	0.45	0.98
	Right Column	211	0.25	0.82
D-2-6-2	Top Beam	284	0.47	0.99
	Bottom Beam	247	0.25	0.96
	Left Column	275	0.47	1.0
	Right Column	209	0.25	0.81
D-2-6-3	Top Beam	288	0.48	1.0
	Bottom Beam	248	0.25	0.97
	Left Column	280	0.48	1.0
	Right Column	208	0.25	0.80

Table A.30 Tension field stress action on the boundary frame at 2% drift with L/H=1.5 and t_w=2.38

Name	Member	σ_{avg} (MPa)	$\sigma_{min}/R_{yp}F_{yp}$	$\sigma_{max}/R_{yp}F_{yp}$
D-2-6-1	Top Beam	338	1.03	1.04
	Bottom Beam	337	1.03	1.04
	Left Column	339	1.03	1.04
	Right Column	336	1.03	1.03
D-2-6-2	Top Beam	339	1.03	1.04
	Bottom Beam	337	1.03	1.04
	Left Column	339	1.03	1.04
	Right Column	336	1.03	1.03
D-2-6-3	Top Beam	339	1.03	1.04
	Bottom Beam	337	1.03	1.04
	Left Column	339	1.03	1.04
	Right Column	336	1.03	1.03

Table A.31 Tension field stress action on the boundary frame at 0.2% drift with L/H=1.5 and t_w=3.17

Name	Member	σ_{avg} (MPa)	$\sigma_{min}/R_{yp}F_{yp}$	$\sigma_{max}/R_{yp}F_{yp}$
D-2-7-1	Top Beam	238	0.31	0.85
	Bottom Beam	213	0.19	0.83
	Left Column	224	0.31	0.85
	Right Column	183	0.19	0.73
D-2-7-2	Top Beam	242	0.32	0.86
	Bottom Beam	214	0.20	0.85
	Left Column	230	0.32	0.86
	Right Column	182	0.20	0.73
D-2-7-3	Top Beam	247	0.33	0.88
	Bottom Beam	215	0.20	0.86
	Left Column	234	0.33	0.88
	Right Column	182	0.20	0.73

Table A.32 Tension field stress action on the boundary frame at 2% drift with L/H=1.5 and t_w=3.17

Name	Member	σ_{avg} (MPa)	$\sigma_{min}/R_{yp}F_{yp}$	$\sigma_{max}/R_{yp}F_{yp}$
D-2-7-1	Top Beam	337	1.02	1.04
	Bottom Beam	336	1.03	1.04
	Left Column	337	1.02	1.04
	Right Column	335	1.03	1.03
D-2-7-2	Top Beam	337	1.02	1.04
	Bottom Beam	336	1.03	1.04
	Left Column	337	1.02	1.04
	Right Column	335	1.03	1.03
D-2-7-3	Top Beam	337	1.02	1.04
	Bottom Beam	336	1.03	1.04
	Left Column	337	1.02	1.04
	Right Column	335	1.03	1.03

Table A.33 Tension field stress action on the boundary frame at 0.2% drift with
L/H=1.5 and t$_w$=3.57

Name	Member	σ_{avg} (MPa)	$\sigma_{min}/R_{yp}F_{yp}$	$\sigma_{max}/R_{yp}F_{yp}$
D-2-8-1	Top Beam	241	0.32	0.86
	Bottom Beam	214	0.20	0.84
	Left Column	227	0.32	0.86
	Right Column	184	0.20	0.74
D-2-8-2	Top Beam	245	0.33	0.87
	Bottom Beam	215	0.20	0.86
	Left Column	232	0.33	0.87
	Right Column	184	0.20	0.73
D-2-8-3	Top Beam	248	0.34	0.88
	Bottom Beam	216	0.21	0.87
	Left Column	235	0.34	0.88
	Right Column	183	0.21	0.73

Table A.34 Tension field stress action on the boundary frame at 2% drift with L/H=1.5
and t$_w$=3.57

Name	Member	σ_{avg} (MPa)	$\sigma_{min}/R_{yp}F_{yp}$	$\sigma_{max}/R_{yp}F_{yp}$
D-2-8-1	Top Beam	337	1.02	1.04
	Bottom Beam	336	1.03	1.04
	Left Column	337	1.02	1.04
	Right Column	335	1.03	1.03
D-2-8-2	Top Beam	337	1.02	1.04
	Bottom Beam	336	1.03	1.04
	Left Column	337	1.02	1.04
	Right Column	335	1.03	1.03
D-2-8-3	Top Beam	337	1.02	1.04
	Bottom Beam	336	1.03	1.04
	Left Column	337	1.02	1.04
	Right Column	335	1.03	1.03

Table A.35 Tension field stress acting on the boundary frame at 0.2% drift with L/H=1.5 and tw=4.36

Name	Member	σ_{avg} (MPa)	$\sigma_{min}/R_{yp}F_{yp}$	$\sigma_{max}/R_{yp}F_{yp}$
D-2-9-1	Top Beam	212	0.23	0.78
	Bottom Beam	190	0.17	0.78
	Left Column	196	0.23	0.78
	Right Column	163	0.17	0.67
D-2-9-2	Top Beam	215	0.23	0.79
	Bottom Beam	190	0.17	0.79
	Left Column	200	0.23	0.79
	Right Column	162	0.17	0.67
D-2-9-3	Top Beam	219	0.24	0.80
	Bottom Beam	191	0.17	0.80
	Left Column	204	0.24	0.80
	Right Column	162	0.17	0.68

Table A.36 Tension field stress acting on the boundary frame at 2% drift with L/H=1.5 and tw=4.36

Name	Member	σ_{avg} (MPa)	$\sigma_{min}/R_{yp}F_{yp}$	$\sigma_{max}/R_{yp}F_{yp}$
D-2-9-1	Top Beam	335	1.02	1.03
	Bottom Beam	335	1.02	1.03
	Left Column	335	1.02	1.03
	Right Column	334	1.02	1.03
D-2-9-2	Top Beam	335	1.02	1.03
	Bottom Beam	335	1.02	1.03
	Left Column	335	1.02	1.03
	Right Column	334	1.02	1.03
D-2-9-3	Top Beam	335	1.02	1.03
	Bottom Beam	335	1.02	1.03
	Left Column	335	1.02	1.03
	Right Column	334	1.02	1.03

Table A.37 Tension field stress action on the boundary frame at 0.2% drift with L/H=2.0 and t_w=0.55

Name	Member	σ_{avg} (MPa)	$\sigma_{min}/R_{yp}F_{yp}$	$\sigma_{max}/R_{yp}F_{yp}$
D-3-1-1	Top Beam	199	0.21	0.75
	Bottom Beam	193	0.14	0.75
	Left Column	170	0.21	0.66
	Right Column	160	0.14	0.66
D-3-1-2	Top Beam	201	0.21	0.76
	Bottom Beam	194	0.14	0.76
	Left Column	172	0.21	0.67
	Right Column	158	0.14	0.65
D-3-1-3	Top Beam	204	0.22	0.77
	Bottom Beam	195	0.14	0.77
	Left Column	175	0.22	0.68
	Right Column	156	0.14	0.65

Table A.38 Tension field stress action on the boundary frame at 2% drift with L/H=2.0 and t_w=0.55

Name	Member	σ_{avg} (MPa)	$\sigma_{min}/R_{yp}F_{yp}$	$\sigma_{max}/R_{yp}F_{yp}$
D-3-1-1	Top Beam	333	1.01	1.03
	Bottom Beam	334	1.01	1.03
	Left Column	332	1.01	1.03
	Right Column	333	1.01	1.03
D-3-1-2	Top Beam	336	1.01	1.03
	Bottom Beam	334	1.01	1.03
	Left Column	332	1.01	1.03
	Right Column	332	1.01	1.03
D-3-1-3	Top Beam	334	1.01	1.03
	Bottom Beam	334	1.01	1.03
	Left Column	332	1.01	1.03
	Right Column	332	1.01	1.03

Table A.39 Tension field stress action on the boundary frame at 0.2% drift with L/H=2.0 and t_w=0.79

Name	Member	σ_{avg} (MPa)	$\sigma_{min}/R_{yp}F_{yp}$	$\sigma_{max}/R_{yp}F_{yp}$
D-3-2-1	Top Beam	200	0.21	0.75
	Bottom Beam	196	0.14	0.75
	Left Column	170	0.21	0.66
	Right Column	162	0.14	0.66
D-3-2-2	Top Beam	203	0.22	0.77
	Bottom Beam	197	0.14	0.77
	Left Column	172	0.22	0.67
	Right Column	161	0.14	0.66
D-3-2-3	Top Beam	206	0.23	0.78
	Bottom Beam	198	0.14	0.78
	Left Column	175	0.23	0.68
	Right Column	159	0.14	0.65

Table A.40 Tension field stress action on the boundary frame at 2% drift with L/H=2.0 and t_w=0.79

Name	Member	σ_{avg} (MPa)	$\sigma_{min}/R_{yp}F_{yp}$	$\sigma_{max}/R_{yp}F_{yp}$
D-3-2-1	Top Beam	335	1.01	1.04
	Bottom Beam	335	1.02	1.04
	Left Column	334	1.01	1.03
	Right Column	334	1.02	1.03
D-3-2-2	Top Beam	335	1.01	1.04
	Bottom Beam	335	1.02	1.04
	Left Column	334	1.01	1.03
	Right Column	334	1.02	1.03
D-3-2-3	Top Beam	335	1.01	1.04
	Bottom Beam	335	1.02	1.04
	Left Column	334	1.01	1.03
	Right Column	334	1.02	1.03

Table A.41 Tension field stress action on the boundary frame at 0.2% drift with L/H=2.0 and t_w=0.95

Name	Member	σ_{avg} (MPa)	$\sigma_{min}/R_{yp}F_{yp}$	$\sigma_{max}/R_{yp}F_{yp}$
D-3-3-1	Top Beam	213	0.25	0.79
	Bottom Beam	207	0.16	0.79
	Left Column	184	0.25	0.70
	Right Column	173	0.16	0.69
D-3-3-2	Top Beam	216	0.26	0.80
	Bottom Beam	208	0.16	0.80
	Left Column	187	0.26	0.71
	Right Column	171	0.16	0.69
D-3-3-3	Top Beam	219	0.26	0.82
	Bottom Beam	209	0.16	0.82
	Left Column	189	0.26	0.72
	Right Column	169	0.16	0.68

Table A.42 Tension field stress action on the boundary frame at 2% drift with L/H=2.0 and t_w=0.95

Name	Member	σ_{avg} (MPa)	$\sigma_{min}/R_{yp}F_{yp}$	$\sigma_{max}/R_{yp}F_{yp}$
D-3-3-1	Top Beam	336	1.02	1.04
	Bottom Beam	336	1.02	1.04
	Left Column	335	1.02	1.04
	Right Column	335	1.02	1.03
D-3-3-2	Top Beam	336	1.02	1.04
	Bottom Beam	336	1.02	1.04
	Left Column	335	1.02	1.04
	Right Column	335	1.02	1.03
D-3-3-3	Top Beam	336	1.02	1.04
	Bottom Beam	336	1.02	1.04
	Left Column	335	1.02	1.03
	Right Column	335	1.02	1.03

Table A.43 Tension field stress action on the boundary frame at 0.2% drift with L/H=2.0 and t_w=1.27

Name	Member	σ_{avg} (MPa)	$\sigma_{min}/R_{yp}F_{yp}$	$\sigma_{max}/R_{yp}F_{yp}$
D-3-4-1	Top Beam	227	0.29	0.83
	Bottom Beam	219	0.18	0.83
	Left Column	200	0.29	0.75
	Right Column	181	0.18	0.72
D-3-4-2	Top Beam	231	0.30	0.85
	Bottom Beam	220	0.18	0.85
	Left Column	201	0.30	0.75
	Right Column	179	0.18	0.72
D-3-4-3	Top Beam	237	0.32	0.87
	Bottom Beam	222	0.18	0.87
	Left Column	208	0.32	0.77
	Right Column	178	0.18	0.71

Table A.44 Tension field stress action on the boundary frame at 2% drift with L/H=2.0 and t_w=1.27

Name	Member	σ_{avg} (MPa)	$\sigma_{min}/R_{yp}F_{yp}$	$\sigma_{max}/R_{yp}F_{yp}$
D-3-4-1	Top Beam	336	1.02	1.04
	Bottom Beam	336	1.03	1.04
	Left Column	336	1.02	1.04
	Right Column	335	1.03	1.03
D-3-4-2	Top Beam	337	1.02	1.04
	Bottom Beam	336	1.03	1.04
	Left Column	336	1.02	1.04
	Right Column	335	1.03	1.03
D-3-4-3	Top Beam	337	1.02	1.04
	Bottom Beam	336	1.03	1.04
	Left Column	336	1.02	1.04
	Right Column	335	1.03	1.03

Table A.45 Tension field stress action on the boundary frame at 0.2% drift with L/H=2.0 and t_w=1.98

Name	Member	σ_{avg} (MPa)	$\sigma_{min}/R_{yp}F_{yp}$	$\sigma_{max}/R_{yp}F_{yp}$
D-3-5-1	Top Beam	237	0.32	0.86
	Bottom Beam	228	0.19	0.86
	Left Column	209	0.32	0.77
	Right Column	189	0.19	0.74
D-3-5-2	Top Beam	240	0.33	0.87
	Bottom Beam	229	0.20	0.87
	Left Column	211	0.33	0.78
	Right Column	187	0.20	0.74
D-3-5-3	Top Beam	243	0.34	0.89
	Bottom Beam	230	0.20	0.89
	Left Column	214	0.34	0.79
	Right Column	185	0.20	0.73

Table A.46 Tension field stress action on the boundary frame at 2% drift with L/H=2.0 and t_w=1.98

Name	Member	σ_{avg} (MPa)	$\sigma_{min}/R_{yp}F_{yp}$	$\sigma_{max}/R_{yp}F_{yp}$
D-3-5-1	Top Beam	337	1.02	1.04
	Bottom Beam	337	1.03	1.04
	Left Column	336	1.02	1.04
	Right Column	336	1.03	1.03
D-3-5-2	Top Beam	337	1.02	1.04
	Bottom Beam	337	1.03	1.04
	Left Column	336	1.02	1.04
	Right Column	336	1.03	1.03
D-3-5-3	Top Beam	337	1.02	1.04
	Bottom Beam	337	1.03	1.04
	Left Column	337	1.02	1.04
	Right Column	336	1.03	1.03

Table A.47 Tension field stress action on the boundary frame at 0.2% drift with L/H=2.0 and t_w=2.38

Name	Member	σ_{avg} (MPa)	$\sigma_{min}/R_{yp}F_{yp}$	$\sigma_{max}/R_{yp}F_{yp}$
D-3-6-1	Top Beam	238	0.33	0.87
	Bottom Beam	228	0.20	0.87
	Left Column	210	0.33	0.77
	Right Column	188	0.20	0.73
D-3-6-2	Top Beam	242	0.34	0.88
	Bottom Beam	230	0.20	0.88
	Left Column	213	0.34	0.78
	Right Column	186	0.20	0.73
D-3-6-3	Top Beam	246	0.35	0.90
	Bottom Beam	231	0.20	0.90
	Left Column	216	0.35	0.79
	Right Column	184	0.20	0.73

Table A.48 Tension field stress action on the boundary frame at 2% drift with L/H=2.0 and t_w=2.38

Name	Member	σ_{avg} (MPa)	$\sigma_{min}/R_{yp}F_{yp}$	$\sigma_{max}/R_{yp}F_{yp}$
D-3-6-1	Top Beam	337	1.02	1.04
	Bottom Beam	337	1.03	1.04
	Left Column	336	1.02	1.04
	Right Column	336	1.03	1.03
D-3-6-2	Top Beam	337	1.02	1.04
	Bottom Beam	337	1.03	1.04
	Left Column	337	1.02	1.04
	Right Column	336	1.03	1.03
D-3-6-3	Top Beam	337	1.02	1.04
	Bottom Beam	337	1.03	1.04
	Left Column	337	1.02	1.04
	Right Column	336	1.03	1.03

Table A.49 Tension field stress action on the boundary frame at 0.2% drift with
L/H=2.0 and t$_w$=3.17

Name	Member	σ_{avg} (MPa)	$\sigma_{min}/R_{yp}F_{yp}$	$\sigma_{max}/R_{yp}F_{yp}$
D-3-7-1	Top Beam	244	0.35	0.88
	Bottom Beam	234	0.22	0.88
	Left Column	217	0.35	0.79
	Right Column	196	0.22	0.76
D-3-7-2	Top Beam	248	0.37	0.90
	Bottom Beam	235	0.23	0.90
	Left Column	221	0.37	0.80
	Right Column	194	0.23	0.75
D-3-7-3	Top Beam	252	0.38	0.92
	Bottom Beam	237	0.23	0.92
	Left Column	224	0.38	0.81
	Right Column	192	0.23	0.74

Table A.50 Tension field stress action on the boundary frame at 2% drift with L/H=2.0
and t$_w$=3.17

Name	Member	σ_{avg} (MPa)	$\sigma_{min}/R_{yp}F_{yp}$	$\sigma_{max}/R_{yp}F_{yp}$
D-3-7-1	Top Beam	337	1.02	1.04
	Bottom Beam	337	1.03	1.04
	Left Column	336	1.02	1.04
	Right Column	336	1.03	1.03
D-3-7-2	Top Beam	337	1.02	1.04
	Bottom Beam	337	1.03	1.04
	Left Column	337	1.02	1.04
	Right Column	336	1.03	1.03
D-3-7-3	Top Beam	338	1.02	1.04
	Bottom Beam	337	1.03	1.04
	Left Column	337	1.02	1.04
	Right Column	336	1.03	1.04

Table A.51 Tension field stress action on the boundary frame at 0.2% drift with L/H=2.0 and t_w=3.57

Name	Member	σ_{avg} (MPa)	$\sigma_{min}/R_{yp}F_{yp}$	$\sigma_{max}/R_{yp}F_{yp}$
D-3-8-1	Top Beam	259	0.41	0.93
	Bottom Beam	242	0.26	0.93
	Left Column	232	0.41	0.84
	Right Column	203	0.26	0.77
D-3-8-2	Top Beam	262	0.42	0.95
	Bottom Beam	246	0.26	0.95
	Left Column	235	0.42	0.84
	Right Column	201	0.26	0.77
D-3-8-3	Top Beam	267	0.43	0.97
	Bottom Beam	248	0.26	0.97
	Left Column	239	0.43	0.86
	Right Column	199	0.26	0.76

Table A.52 Tension field stress action on the boundary frame at 2% drift with L/H=2.0 and t_w=3.57

Name	Member	σ_{avg} (MPa)	$\sigma_{min}/R_{yp}F_{yp}$	$\sigma_{max}/R_{yp}F_{yp}$
D-3-8-1	Top Beam	338	1.02	1.04
	Bottom Beam	338	1.03	1.04
	Left Column	337	1.02	1.04
	Right Column	337	1.03	1.04
D-3-8-2	Top Beam	338	1.02	1.04
	Bottom Beam	338	1.03	1.04
	Left Column	338	1.02	1.04
	Right Column	338	1.03	1.04
D-3-8-3	Top Beam	338	1.03	1.04
	Bottom Beam	338	1.03	1.04
	Left Column	338	1.03	1.04
	Right Column	337	1.03	1.04

Table A.53 Tension field stress action on the boundary frame at 0.2% drift with
L/H=2.0 and t_w=4.36

Name	Member	σ_{avg} (MPa)	$\sigma_{min}/R_{yp}F_{yp}$	$\sigma_{max}/R_{yp}F_{yp}$
D-3-9-1	Top Beam	255	0.4	0.91
	Bottom Beam	245	0.2	0.91
	Left Column	230	0.4	0.83
	Right Column	208	0.2	0.79
D-3-9-2	Top Beam	258	0.4	0.93
	Bottom Beam	246	0.2	0.93
	Left Column	232	0.4	0.83
	Right Column	206	0.2	0.79
D-3-9-3	Top Beam	263	0.4	0.95
	Bottom Beam	248	0.3	0.95
	Left Column	236	0.4	0.84
	Right Column	204	0.3	0.77

Table A.54 Tension field stress action on the boundary frame at 2% drift with L/H=2.0
and t_w=4.36

Name	Member	σ_{avg} (MPa)	$\sigma_{min}/R_{yp}F_{yp}$	$\sigma_{max}/R_{yp}F_{yp}$
D-3-9-1	Top Beam	338	1.02	1.04
	Bottom Beam	338	1.03	1.04
	Left Column	337	1.02	1.04
	Right Column	337	1.03	1.04
D-3-9-2	Top Beam	338	1.02	1.04
	Bottom Beam	338	1.03	1.04
	Left Column	337	1.02	1.04
	Right Column	337	1.03	1.04
D-3-9-3	Top Beam	338	1.02	1.04
	Bottom Beam	338	1.03	1.04
	Left Column	337	1.02	1.04
	Right Column	337	1.03	1.04

BIBLIOGRAPHY

[1]   AISC. (2005). ANSI/AISC 341-05 ''Seismic provisions for structural steel buildings.''. American Institute of Steel Construction Inc, American Institute of Steel Construction, Chicago, IL.

[2]   AISC. (2015). Steel Construction Manual, 15th Ed. American Institute of Steel Construction. Chicago, IL.

[3]   AISC. (2016a). ANSI/AISC 341-16. Seismic Provisions for Structural Steel Buildings. American Institute of Steel Construction, America.

[4]   AISC. (2016b). ANSI/AISC 358-16, Prequalified Connections for Special and Intermediate Steel Moment Frames for Seismic Applications. American Institute of Steel Construction, America.

[5]   AISC. (2016c). ANSI/AISC 360-16. Specification for structural steel buildings. American Institute of Steel Construction, America.

[6]   Alavi, E., & Nateghi, F. (2013). Experimental study on diagonally stiffened steel plate shear walls with central perforation. Journal of Constructional Steel Research, 89, 9-20.

[7]   ASCE. (2005). SEI/ASCE 7-05. Minimum Design Loads for Buildings and Other Structures (including Supplement No. 1). American Society of Civil Engineers, Reston, VA.

[8]   ATC-24. (1992). Guidelines for Cyclic Seismic Testing of Components of Steel Structures. Redwood City, Report prepared for the Applied Technology Council.

[9]   Basler. (1961). Strength of plate girders in shear. Journal of the Structural Division, 87(7), 151-180.

[10]   Berman, & Bruneau. (2003). Plastic analysis and design of steel plate shear walls. Journal of Structural Engineering, 129(11), 1448-1456.

[11]   Berman, & Bruneau. (2004). Steel plate shear walls are not plate girders. Engineering Journal-American Institute of Steel Construction, 41, 95-106.

[12]   Berman, & Bruneau. (2008). Capacity design of vertical boundary elements in steel plate shear walls. Engineering Journal (AISC), 15.

[13]   Caccese, V., Elgaaly, M., & Chen, R. (1993). Experimental study of thin steel-plate shear walls under cyclic load. Journal of Structural Engineering, 119(2), 573-587.

[14]   Driver, R. G., & University of Alberta. Dept. of Civil and Environmental Engineering. (1997). Seismic behaviour of steel plate shear walls (Doctoral dissertation, University of Alberta).

[15]   Driver. (1998). Cyclic test of four-story steel plate shear wall. Journal of Structural Engineering, 124(2), 112-120.

[16]   Elgaaly, M. (1998). Thin steel plate shear walls behavior and analysis. Thin-Walled Structures, 32(1-3), 151-180.

[17]   Elgaaly, M., Caccese, V., & Du, C. (1993). Post buckling behavior of steel-plate shear walls under cyclic loads. Journal of Structural Engineering, 119(2), 588-605.

[18]   Ismaeil, & Hassaballa. (2013). Seismic Retrofitting of a RC Building by Adding Steel Plate Shear Walls. IOSR Journal of Mechanical and Civil Engineering (IOSR-JMCE), 7(2), 49-62.

[19]   Kuhn, P., Peterson, J. P., & Levin, L. R. (1952). A summary of diagonal tension Part I: methods of analysis.

[20]   Lopez-Garcia, D., & Bruneau, M. (2006). Seismic behavior of intermediate beams in steel plate shear walls. Paper presented at the Proc., 8th US National Conf. on Earthquake Engineering.

[21]   Lubell, A. S., Prion, H. G. L., Ventura, C. E., & Rezai, M. (2000). Unstiffened Steel Plate Shear Wall Performance under Cyclic Loading. Journal of Structural Engineering, 126(4), 453-460.

[22]   McKenna, F., Fenves, G. L., & Scott, M. H. (2000). Open system for earthquake engineering simulation. University of California, Berkeley, CA.

[23]   Moore, H. (2017). MATLAB for Engineers. Pearson.

[24]   Mörel, O. F. (2004). Earthquake performance of un-stiffened thin steel plate shear walls (Master's thesis).

[25]   Purba, R., & Bruneau, M. (2011). Case study on the impact of horizontal boundary elements design on seismic behavior of steel plate shear walls. Journal of Structural Engineering, 138(5), 645-657.

[26]   Purba, R., & Bruneau, M. (2014). Seismic performance of steel plate shear walls considering two different design philosophies of infill plates. I: Deterioration model development. Journal of Structural Engineering, 141(6), 04014160.

[27]   Qu, B., & Bruneau, M. (2010). Behavior of vertical boundary elements in steel plate shear walls. Engineering Journal, Chicago, 47(2), 109-122.

[28]   Sabelli, R., & Bruneau, M. (2007). Steel plate shear walls (AISC design guide). American Institute of Steel Construction, Inc., Chicago, Illinois.

[29]   Thorburn, L. J., Kulak, G. L., & Montgomery, C. J. (1983). Analysis of steel plate shear walls. Edmonton: Dept. of Civil Engineering, University of Alberta.

[30]   Timler. (1998). Design procedures development, analytical verification, and cost evaluation of steel plate shear wall structures. Earthquake Engineering Research Facility Technical Report (98-01).

[31]   Timler, & Kulak. (1983). Experimental Study of Steel Plate Shear Walls: Department of Civil Engineering, University of Alberta.

[32]   Wagner, H. (1931). "Flat Sheet Metal Girders with Very Thin Metal Web. Part I-General Theories and Assumptions,". Technical Memo. No. 604, National Advisory Committee for Aeronautics.

[33]   Webster. (2013). The inelastic seismic response of steel plate shear walls web plates and their interaction with the vertical boundary members. University of Washington.

VITA

Shaghayegh Sadeghzadeh Benam was born in Iran, Tabriz on 15 April 1993. She completed her high school education in 2012. She received her bachelor's degree in Civil Engineering Department of Payame Noor University, Tabriz, Iran in 2015. She started her master's degree in graduate school of Özyeğin University in September 2017. She conducted her M.Sc. study under supervision of Asst. Prof. Dr. Ahmet Yiğit Özçelik. Her Main research is on parametric study on the influence of boundary frame flexibility on variation of the stresses in steel plate shear walls. During her studies, she also worked as a teaching and research assistant.